Nanomechanics
Herbstsemester 12

Ernst Meyer

Contents

Nanomechanics: Introduction

Cantilever: static and dynamic modes of force measurements
Limits of force measurements

Elastic properties of Nanotubes

Weighing single molecules?

Nanomotors

Nanodroplets and Superhydrophobicity

Small Forces

Dynamic Force Microscopy

Mechanical detection of magnetic resonance

Superlubricity

Youngs modulus E

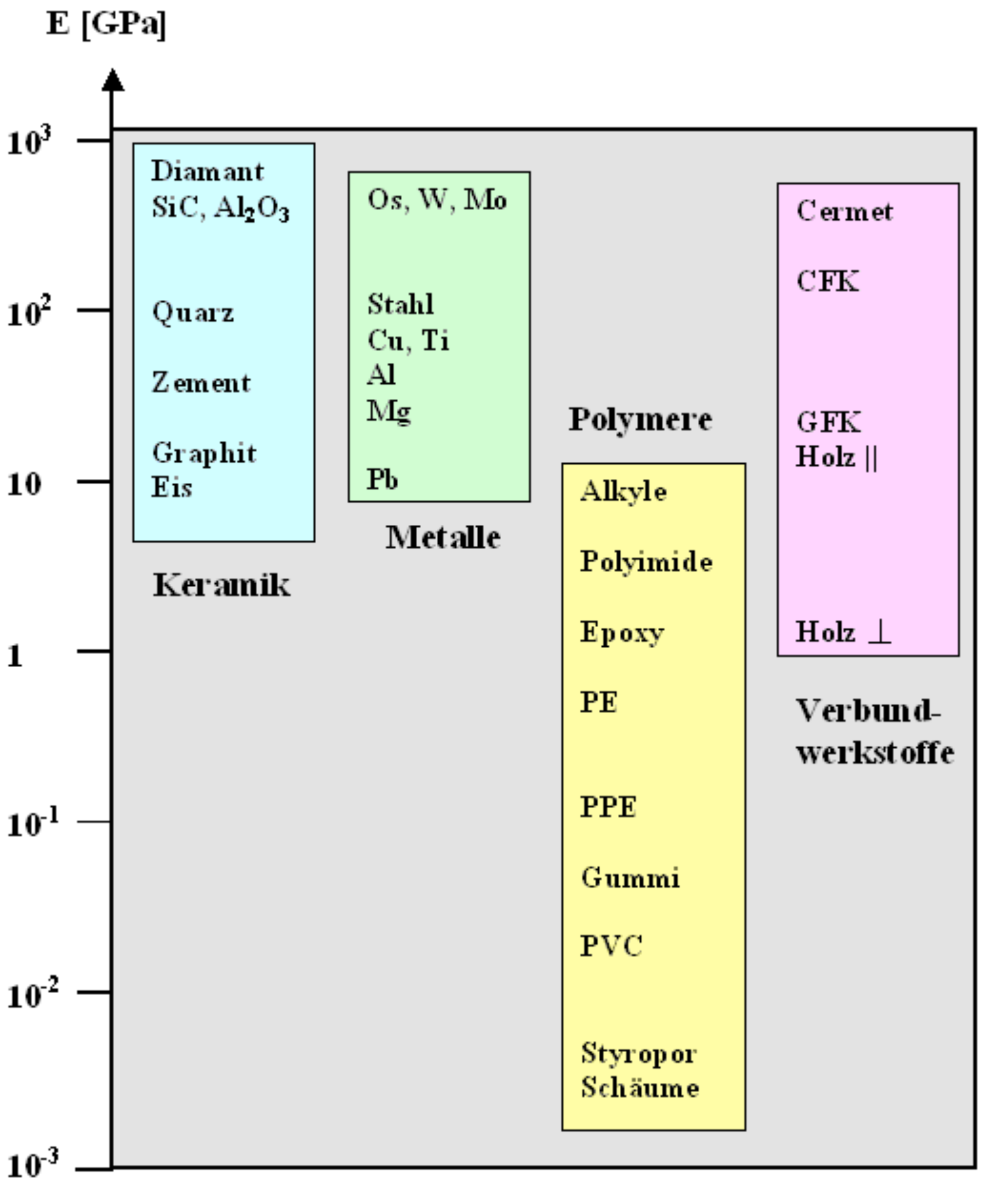

Why NanoMechanics ?

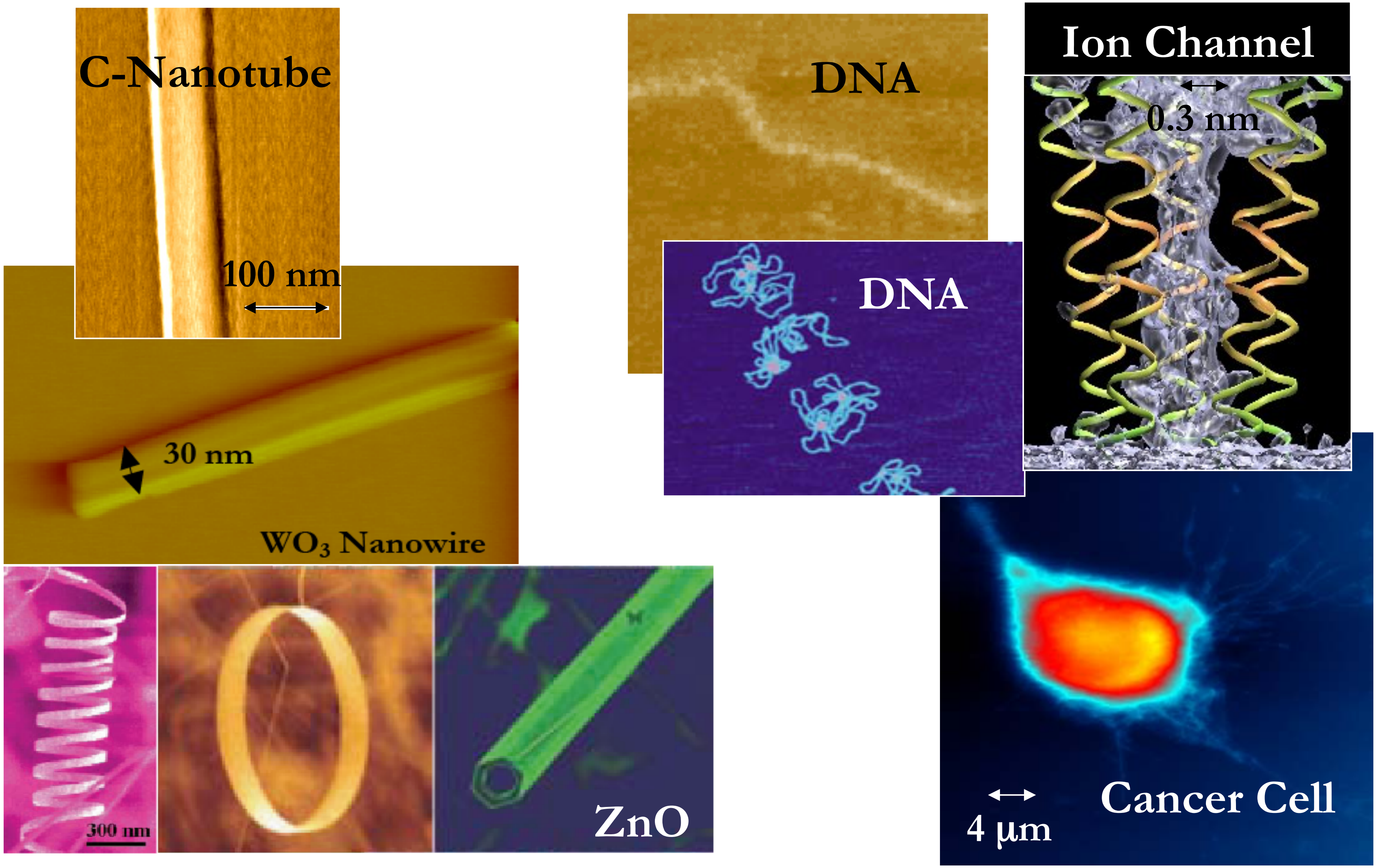

E. Riedo. Georgia Tech

Cantilever

• Cantilever width w, thickness t and length l, tip height: from **SEM pictures**

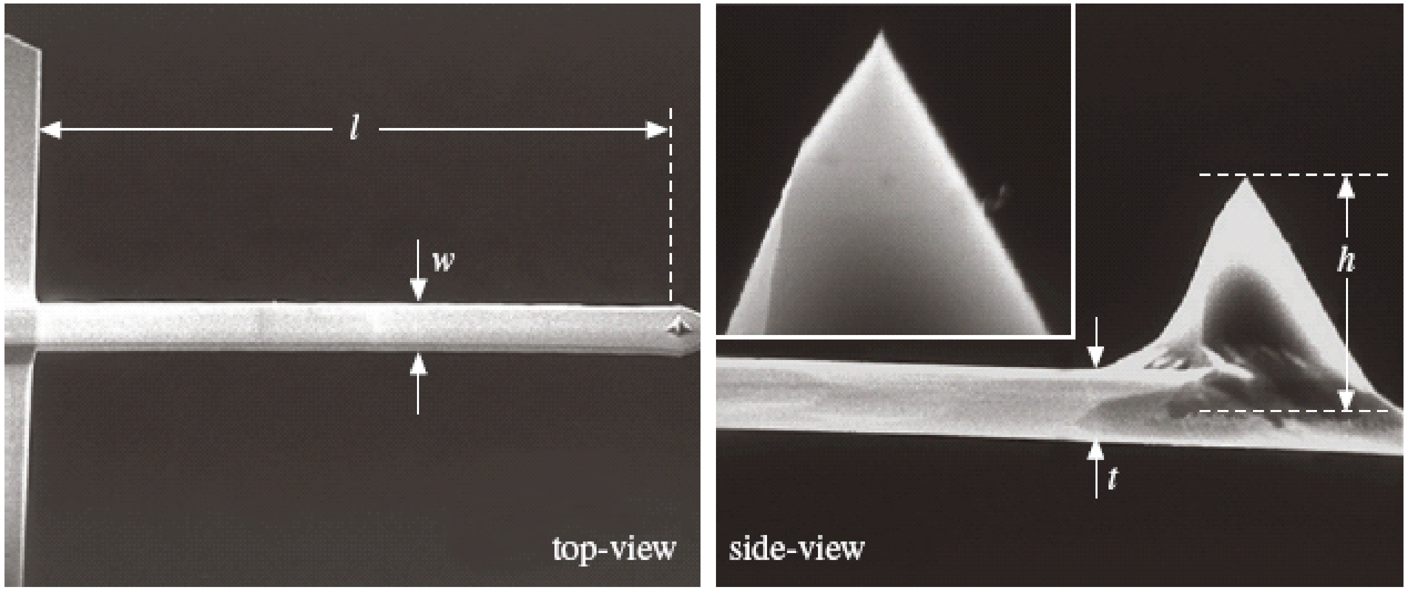

Deformations of beams

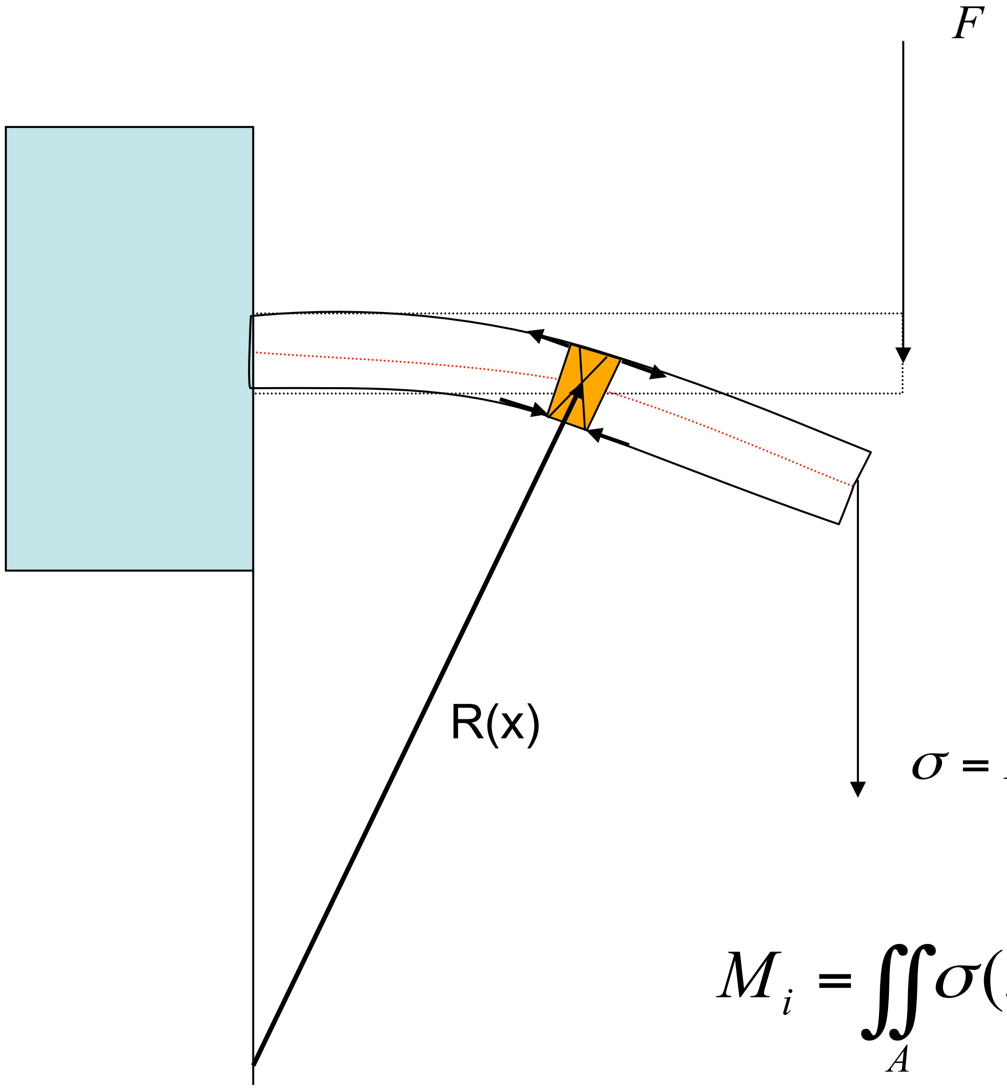

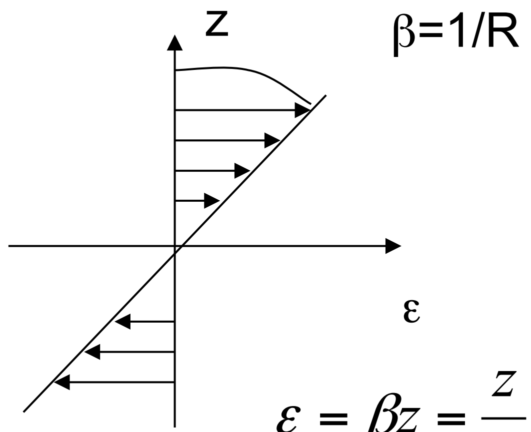

$$\varepsilon = \beta z = \frac{z}{R}$$

$$\sigma = E\varepsilon(z) = E\frac{\Delta l}{l_0} = E\frac{l(z)-l_0}{l_0} = E\frac{z}{R}$$

$$M_i = \iint_A \sigma(x,z)\,z\,dA = \frac{E}{R}\iint_A z^2\,dA = \frac{EI}{R}$$

Deformations of beams

Flexure of Beams (Euler-Bernoulli-Theory)

$$\frac{1}{R} = -\frac{M_o}{EI} \qquad I = \int_A z^2 dA$$

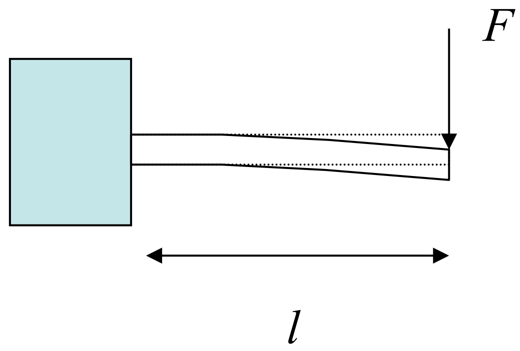

with $\frac{1}{R} \approx \frac{\partial^2 u}{\partial x^2} \quad \Rightarrow \quad \frac{\partial^2 u}{\partial x^2} = -\frac{M_o}{EI}$

with $M_o = F(l-x) \quad \Rightarrow \quad \frac{\partial^2 u}{\partial x^2} = \frac{F}{EI}(l-x)$

R: Radius of curvature
M:Torsional moment
E: Youngs modulus
I: Polar moment of inertia
(Flächenträgheitsmoment)
F: Force

$u(0)=0;\ u'(0)=0: \quad \Rightarrow \quad u(x) = \frac{F}{EI}\left(\frac{lx^2}{2} - \frac{x^3}{6}\right)$

Spring constant of a cantilever

$$k = \frac{F}{u(l)} = \frac{EI}{\left(\frac{l^3}{2} - \frac{l^3}{6}\right)} = \frac{3EI}{l^3}$$

Rectangular cantilever:

$I = wt^3/12$

$$k = \frac{E}{4}\frac{wt^3}{L^3}$$

Cantilever dynamics

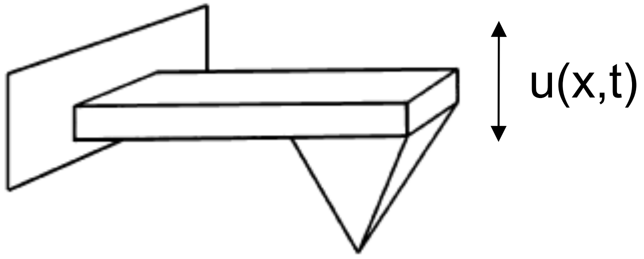

$$EI\frac{\partial^4 u(x,t)}{\partial x^4} + \mu\frac{\partial^2 u}{\partial t^2} = F(x,t)$$

E: Youngs Modulus
I: Moment of Inertia
μ: mass per unit length
F: Force

$$EI\frac{\partial^4 u(x,t)}{\partial x^4} + \mu\frac{\partial^2 u}{\partial t^2} + \gamma\frac{\partial u}{\partial t} = F(x,t)$$

γ: hydrodynamic coefficient

R. Garcia, R. Perez, *Surf. Sci. Rep.* **47**, 197 (2002)

Cantilever dynamics: Free vibrations

$$\omega_i = \alpha_i^2 \sqrt{\frac{EI}{\mu}}$$

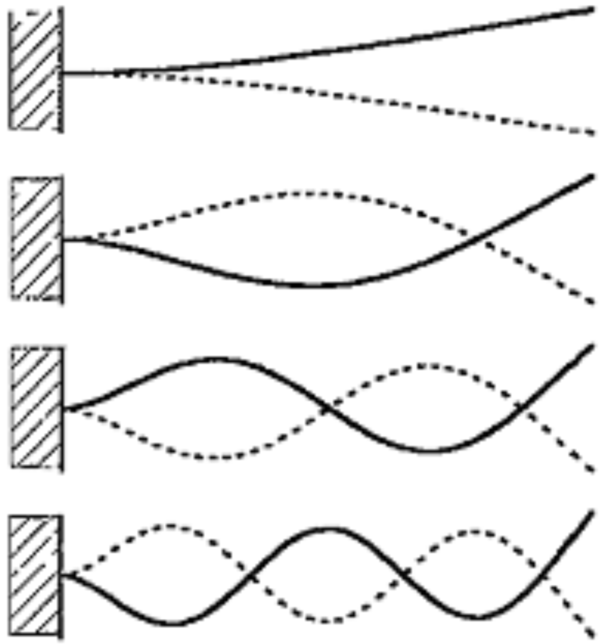

Rectangular cantilever:

$I = wt^3/12$
$\mu = \rho A = \rho w t$

$$\omega_i = \alpha_i^2 t \sqrt{\frac{E}{12\rho}}$$

Silicon:
$E = 1.69E11 N/m2$
$\rho = 2.33e3 kg/m3$

$\alpha_1 l = 1.875$, $\alpha_2 l = 4.694$, $\alpha_3 l = 7.855$, $\alpha_4 l = 10.996$…

Roots of $\cos(\alpha_n l)\cosh(\alpha_n l) + 1 = 0$

Thermal noise spectrum of a free cantilever

1st flexural mode   2nd flexural mode   Torsional mode

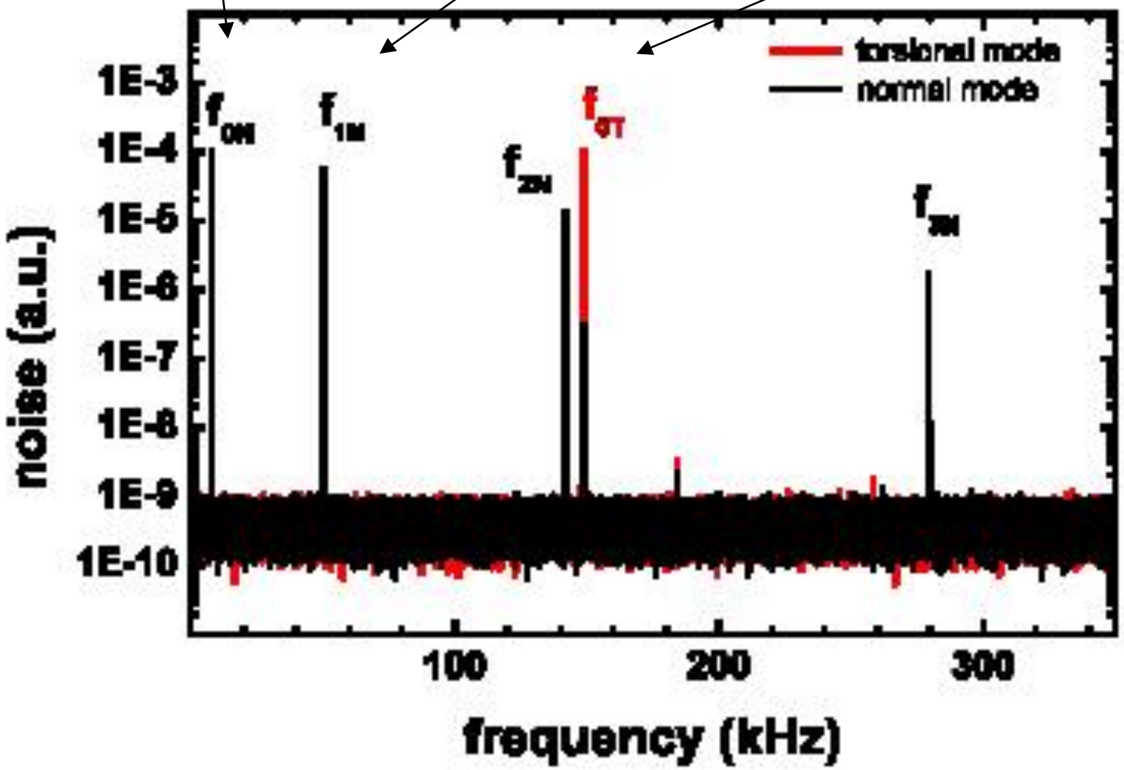

f_N	Exp. (kHz)	Model (kHz)
1st	7.97	
2nd	50.44	49.97
3rd	141.97	139.79
4th	279.62	274.09

The ratio between first and second flexural resonance frequency is about $(\alpha_2/\alpha_1)^2$=6.26 (depends on detailled geometry) Exp: 6-7

Oscillations modes of a free cantilever

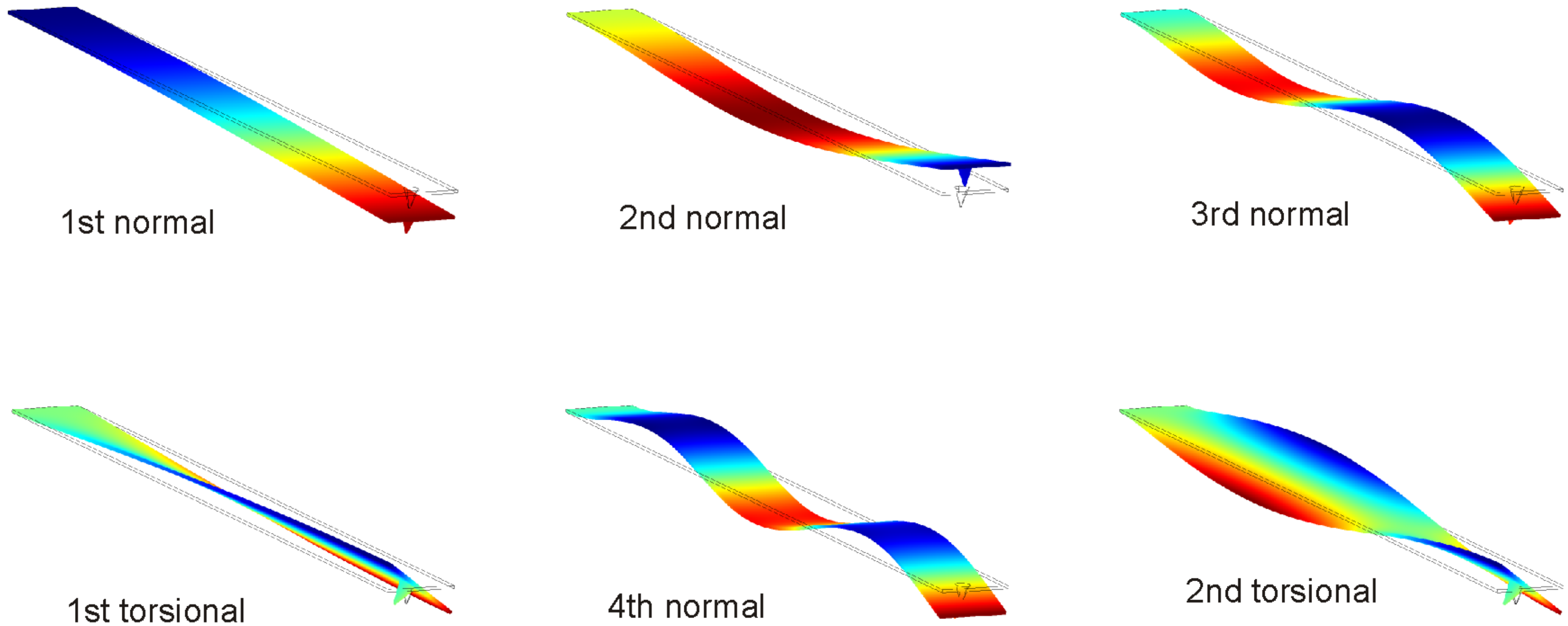

Measure non-linearities by the use of higher harmonic $n\omega_d$

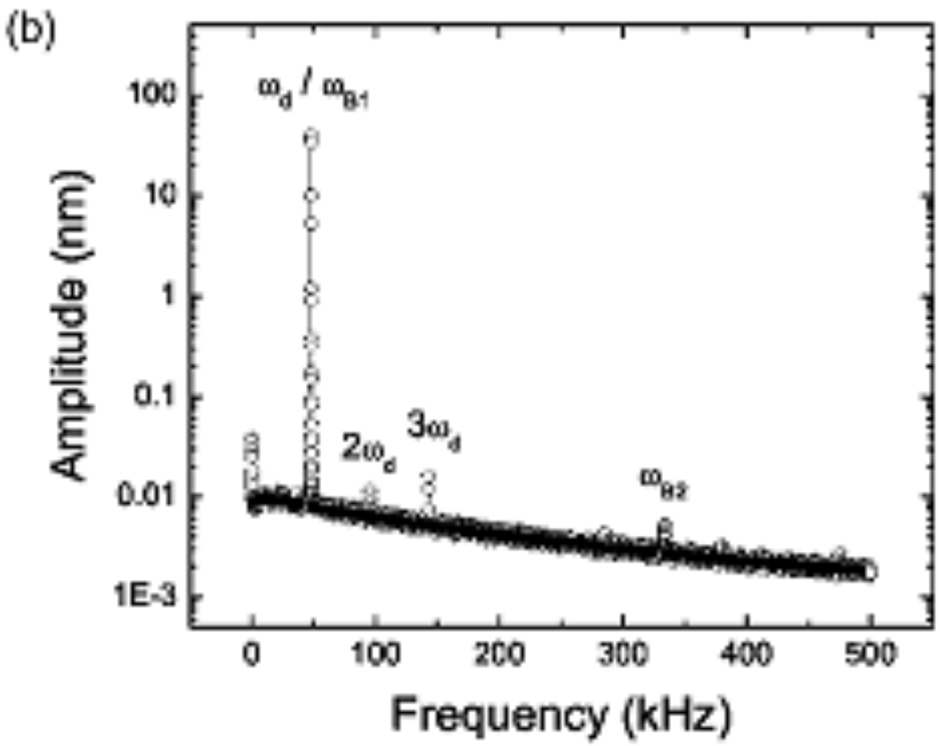

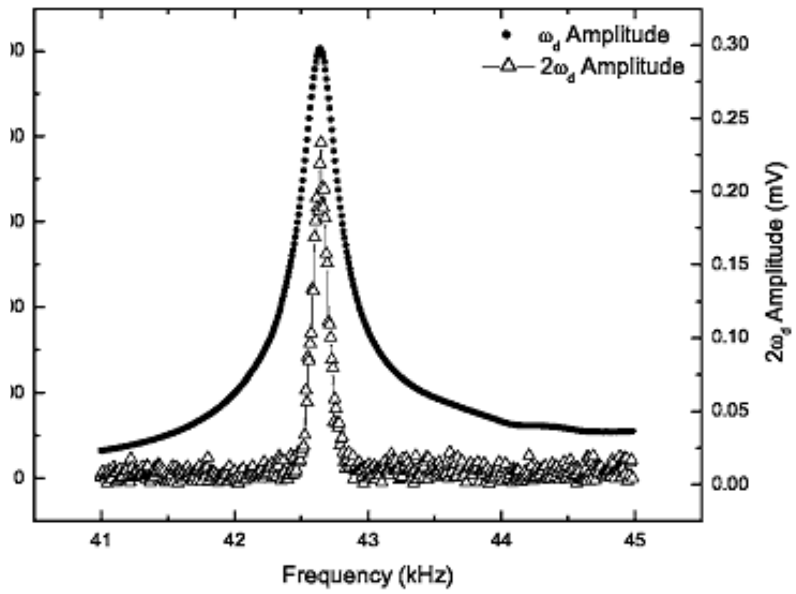

Higher harmonics are sensitive to tip-sample interactions (e.g. van der Waals forces)

S. Crittenden, A. Raman and R. Reifenberger, Phys. Rev. B 72, 235422 (2005)

Enhance non-linearities by coupling higher harmonics to flexural modes

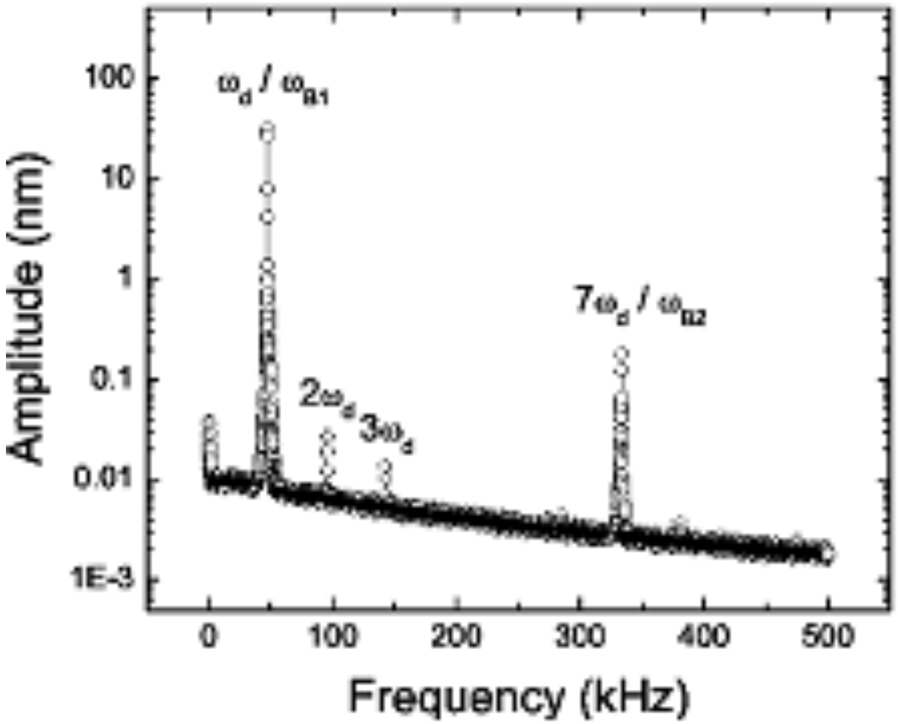

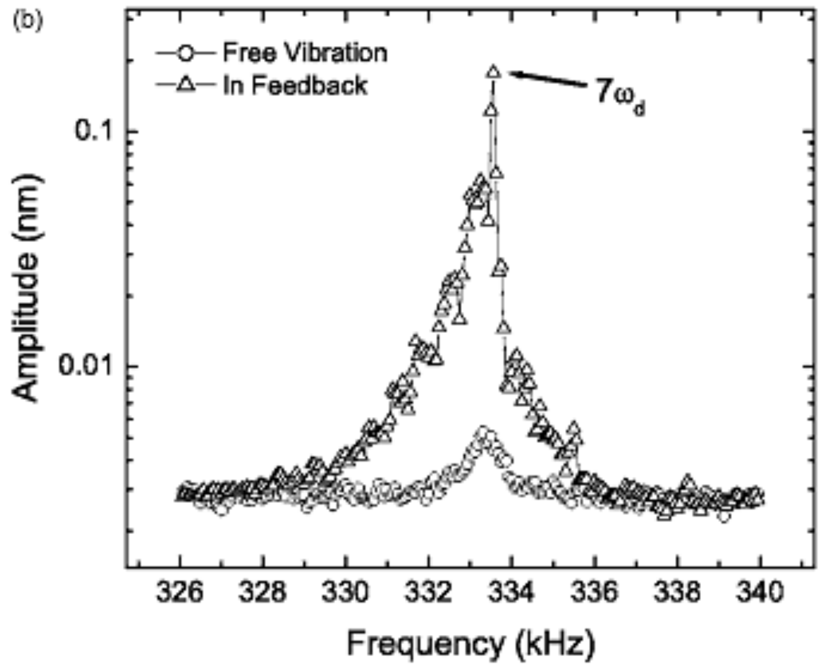

In the case of this cantilever: $7\omega_d \approx \omega_{B2}$; 7th harmonic coincides with 2nd flexural mode

S. Crittenden, A. Raman and R. Reifenberger, Phys. Rev. B 72, 235422 (2005)

Deflection of doubly-clamped beams

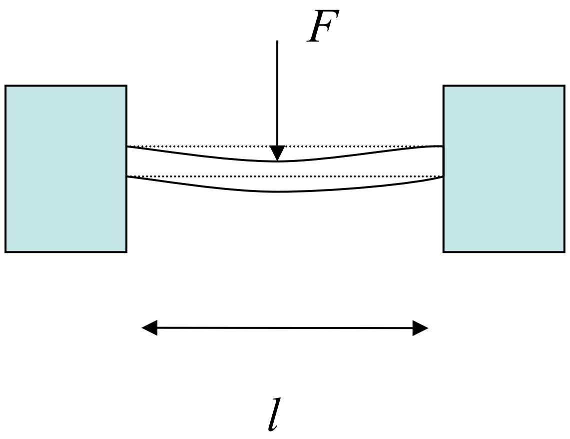

$$\frac{\partial^2 u}{\partial x^2} = \frac{Fl}{2EI}\left(\frac{x}{l} - \frac{1}{4}\right)$$

$$u(x) = \frac{Fl}{2EI}\left(\frac{x^3}{6l} - \frac{x^2}{8}\right)$$

$u(0)=0$; $u'(0)=0$;
$u(l)=0$; $u'(l)=0$;

$$u\left(l/2\right) = -\frac{F}{EI}\frac{l^3}{192}$$

Vibrations of doubly-clamped beam

$$EI\frac{\partial^4 u(x,t)}{\partial x^4} = -\mu\frac{\partial^2 u(x,t)}{\partial t^2}$$

Assuming a harmonic time dependence: $u(x,t)=u(x)e^{i\omega t}$

$$\frac{\partial^4 u(x)}{\partial x^4} = -\frac{\mu}{EI}\omega^2 u(x)$$

Solution: $u(x) = Ae^{i\beta x} + Be^{-i\beta x} + Ce^{\beta x} + De^{-\beta x}$

where $\beta = \left(\frac{\mu}{EI}\right)^{1/4}\omega^{1/2}$

Boundary conditions: u(0)=u(l)=u'(0)=u'(l)=0

$\Rightarrow \cos(\beta_n l)\cosh(\beta_n l)-1=0 \Rightarrow$ $\beta_1 l=4.73$, $\beta_2 l=7.8532$, $\beta_3 l=10.9956$, $\beta_4 l=14.1372$…

Vibrations of doubly-clamped beam

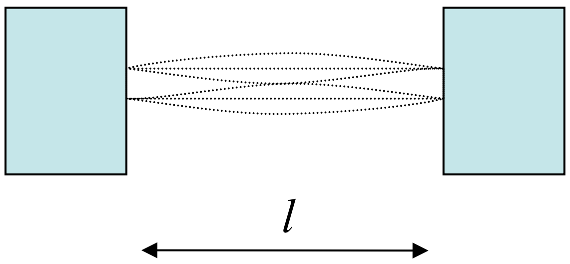

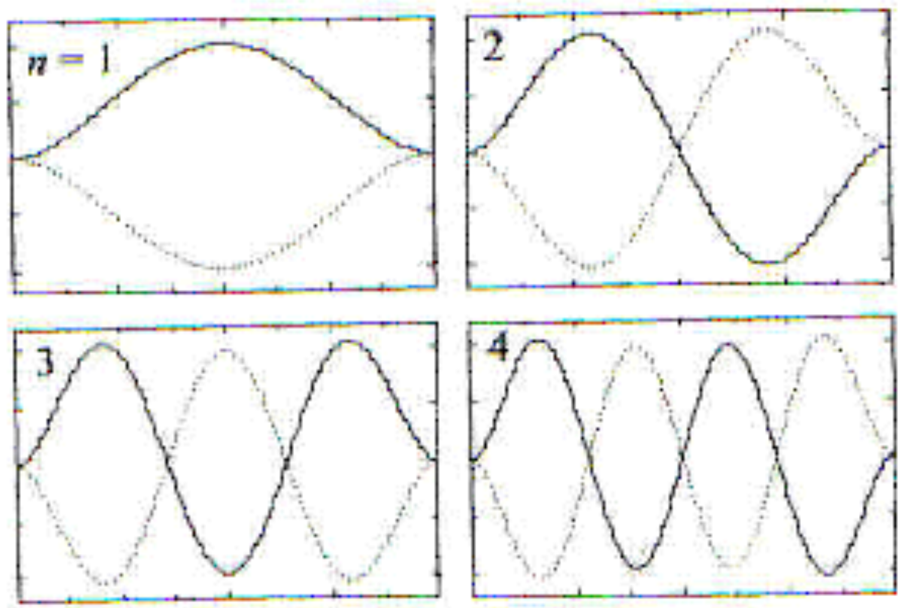

$$\omega_i = \beta_i^2 \sqrt{\frac{EI}{\mu}}$$

$\beta_1 l$=4.73, $\beta_2 l$=7.8532, $\beta_3 l$=10.9956, $\beta_4 l$=14.1372… $\mu=\rho A$

Rectangular cantilever:

$$I = \frac{wt^3}{12}$$

Tube with inner and outer radii:

$$I = \pi \frac{r_2^4 - r_1^4}{4}$$

Short version:

Cantilever: $$f_1 = \frac{1}{2\pi}\left(\frac{1.875}{l}\right)^2 \sqrt{\frac{EI}{\mu}} = \frac{1.875^2}{2\pi\sqrt{12}}\sqrt{\frac{E}{\rho}}\frac{t}{l^2} = 0.162\sqrt{\frac{E}{\rho}}\frac{t}{l^2}$$

Doubly clamped beam:

$$f_1 = \frac{1}{2\pi}\left(\frac{4.73}{l}\right)^2 \sqrt{\frac{EI}{\mu}} = \frac{4.73^2}{2\pi\sqrt{12}}\sqrt{\frac{E}{\rho}}\frac{t}{l^2} = 1.03\sqrt{\frac{E}{\rho}}\frac{t}{l^2}$$

Electromechanical Resonators from Graphene Sheets

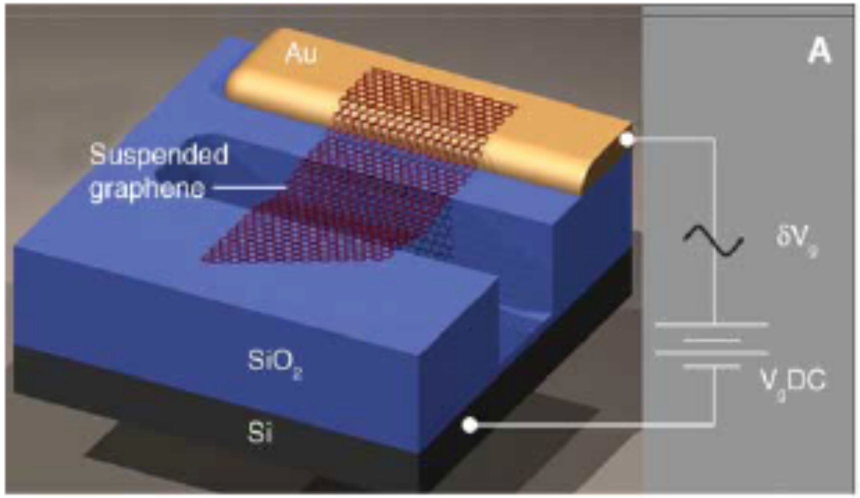

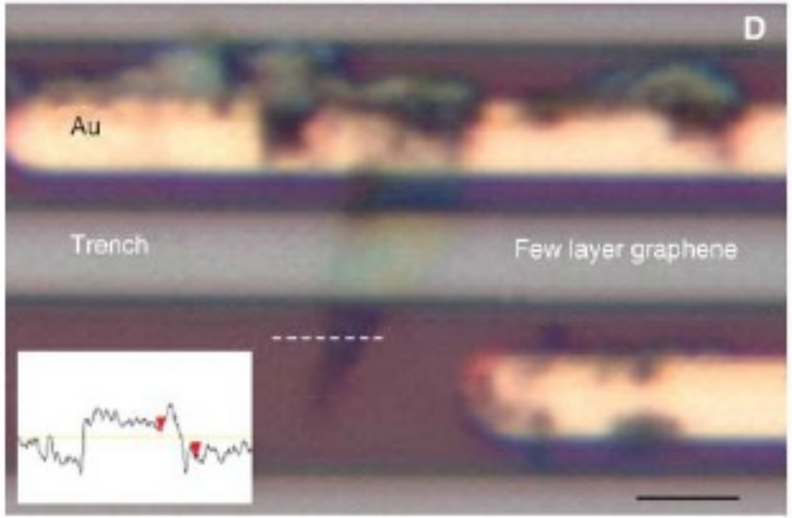

Suited for mass, force and charge sensors

J.S. Bunch, P.L. McEuen, Science 315, 490 (2007)

Electromechanical Resonators from Graphene Sheets

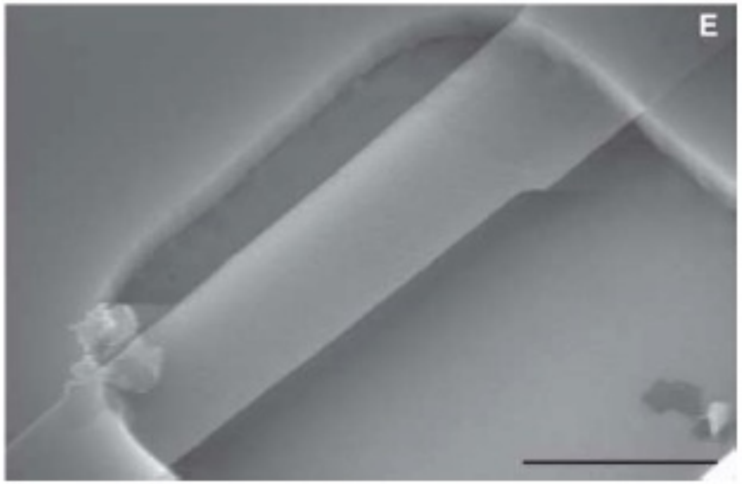

Few (2) layer graphene resonator

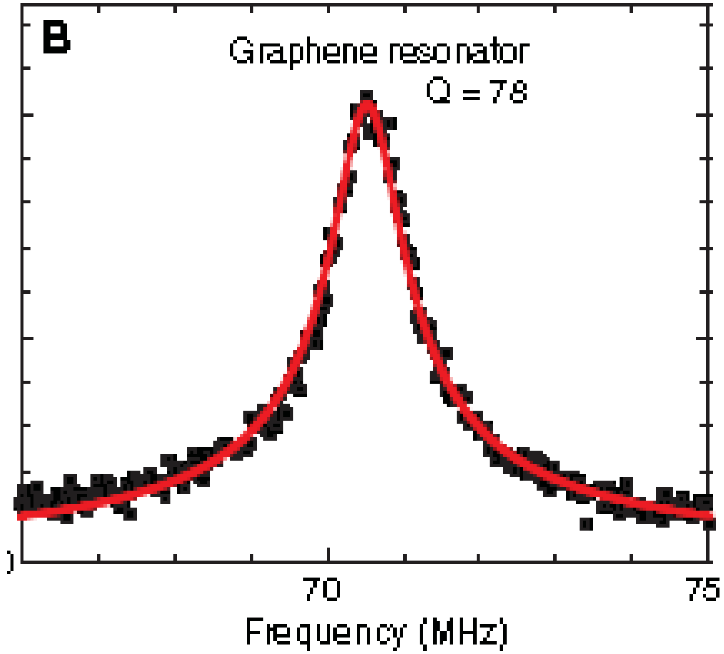

J.S. Bunch, P.L. McEuen, Science 315, 490 (2007)

Electromechanical Resonators from Graphene Sheets

$$f=\left(\left(A\sqrt{\frac{E}{\rho}}\frac{t}{l^2}\right)^2+A^2 0.57\frac{T}{\rho L^2 wt}\right)^{1/2}$$

Cantilever: A=0.162
Doubly clamped beam: A=1.03
T: residual Tension (N)

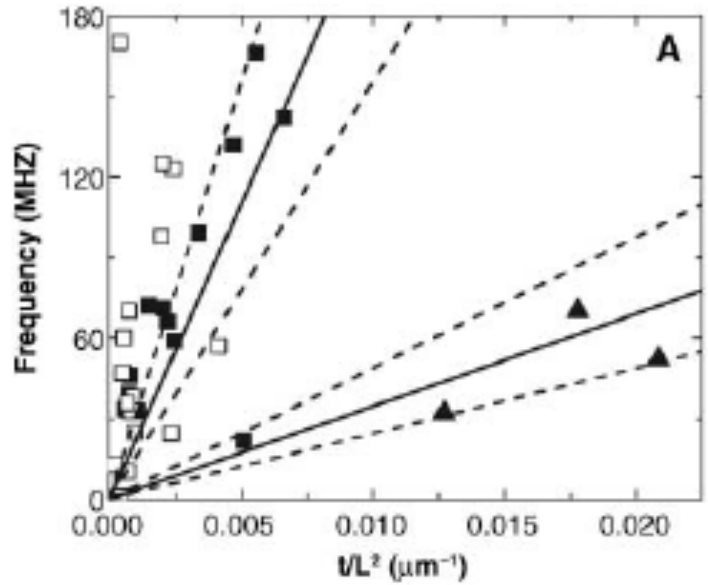

t<0.7nm: higher frequencies due to tension
t>0.7nm: $f \approx t / l^2$
E=1TPa similar to nanotubes

J.S. Bunch, P.L. McEuen, Science 315, 490 (2007)

Bimodal AFM imaging of NEMS oscillations

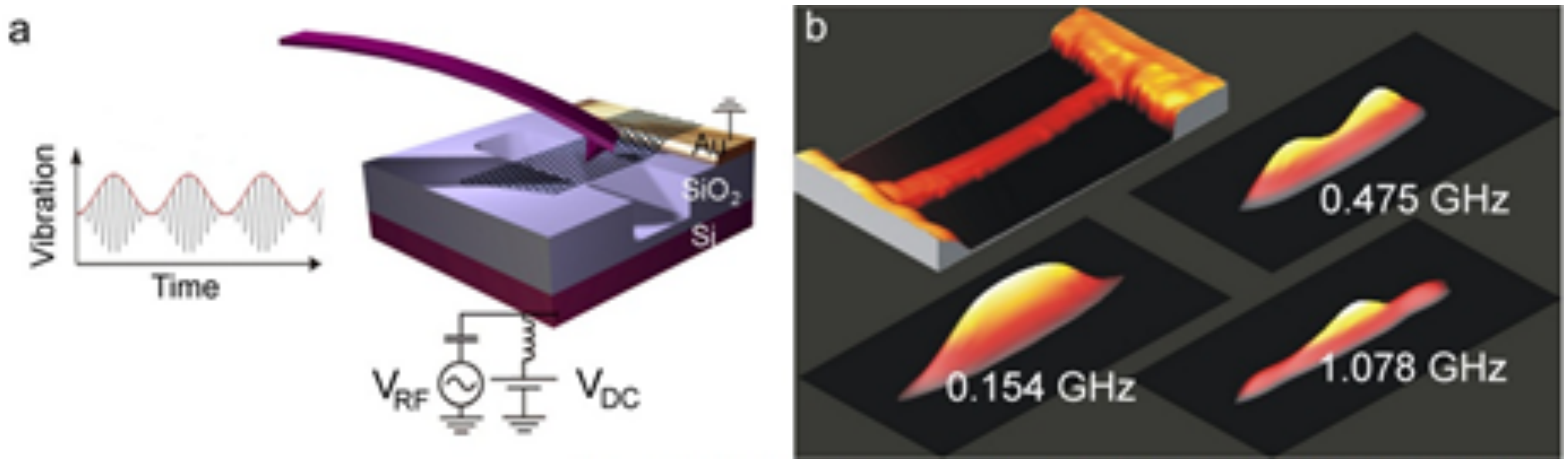

A. San Paulo, A. Bachtold, PRL 99, 085501 (2007); Nano Lett. 8, 1399 (2008).

Swiss Cheese Method: Elasticity of Nanotubes

$$\delta = \delta_B + \delta_S = FL^3/192EI + f_s FL/4GA.$$

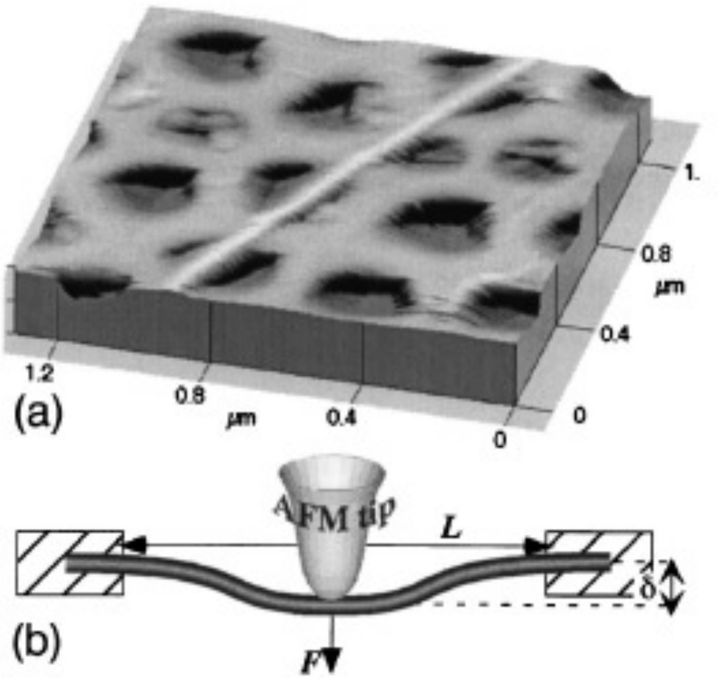

TABLE I. Diameter D, suspended length L, slope of the force-deflection curve $\Delta\delta/\Delta F$, as well as the calculated reduced modulus E_r and shear modulus G for the SWNT ropes studied in this work.

D (nm) ± 0.5 nm	L (nm) $\pm 10\%$	$\Delta\delta/\Delta F$ (m/N)	E_r (GPa) $\pm 50\%$	G (GPa) $\pm 50\%$
3.0	100	1.0	1310	...
3.0	140	4.0	899	...
4.5	285	9.3	642	...
4.5	180	3.0	503	6.5
6.0	200	1.8	369	2.9
6.0	230	3.0	332	1.7
9.0	180	0.5	189	2.3
13.5	360	0.5	298	2.8
13.5	360	1.0	149	0.9
20.0	370	0.5	67	0.7

$\Rightarrow E_{max}$=1310GPa, G=6.5GPa

$\Rightarrow$Bending plus shear of ropes

J.P. Salvetat et al., *Phys. Rev. Lett.* **82**, 944 (1999)

Elasticity of nanowires

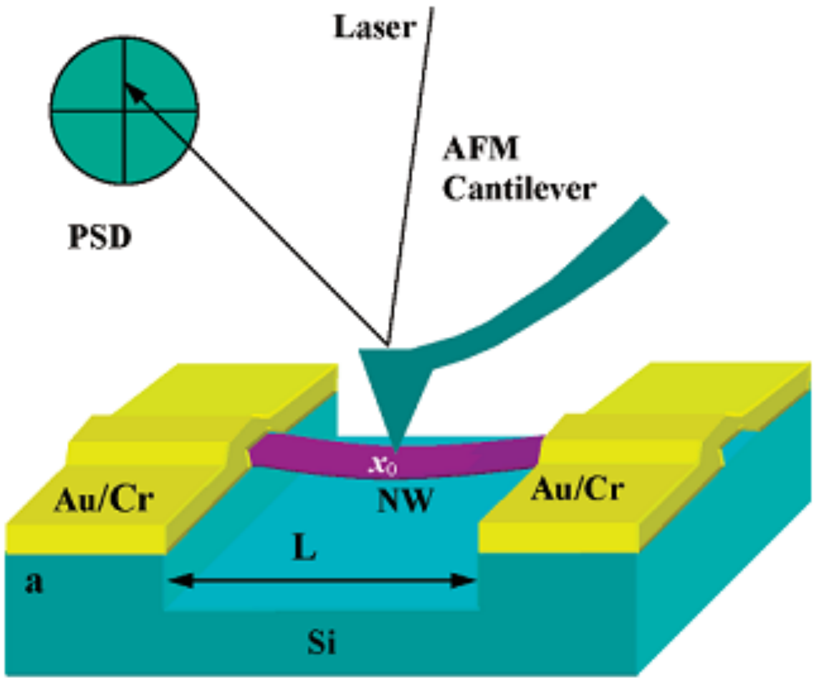

$$E = \frac{f}{\Delta Z}\frac{L^3}{192I}$$

ZnS-Nanowires: E=54GPa

Xiong et la., *Nanoletters* **6**,1904 (2006)

Probing radial elasticity of MWNT

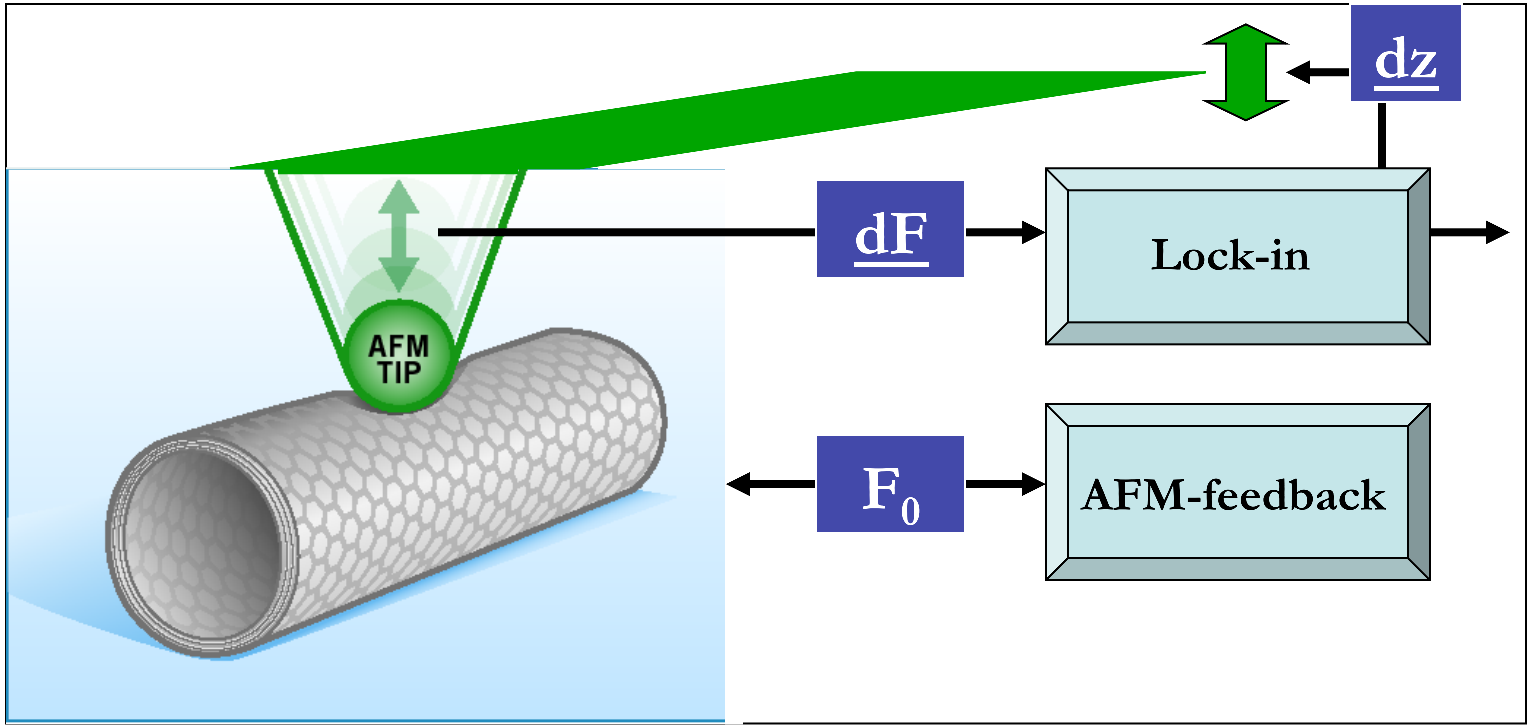

L. Palaci et al., *Phys. Rev. Lett.* **94**, 175502 (05)

Normal contact stiffness

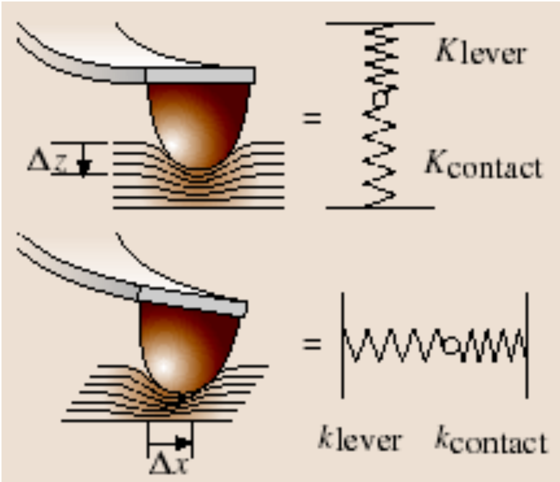

R. W. Carpick, D. F. Ogletree, M. Salmeron,
Appl. Phys. Lett. **70** 1548 (1997)

$$\left(\frac{dF}{d(z_{lever}+z_{indent})}\right)_{F=F_0} = k_{tot}(F_0) = \left(\frac{1}{k_{lever}} + \frac{1}{k_{cont}(F_0)}\right)^{-1}$$

$dF/dz_{tot}(F) \Rightarrow k_{cont}(F)$

$(1/k_{cont}(F))\,dF = dz_{indent}$

where z_{indent} is the indentation of the tip in the NT,

By integration we obtain $F(z_{indent})$ from the experimental $k_{cont}(F)$.

Contact stiffness of multiwalled Carbon nanotubes

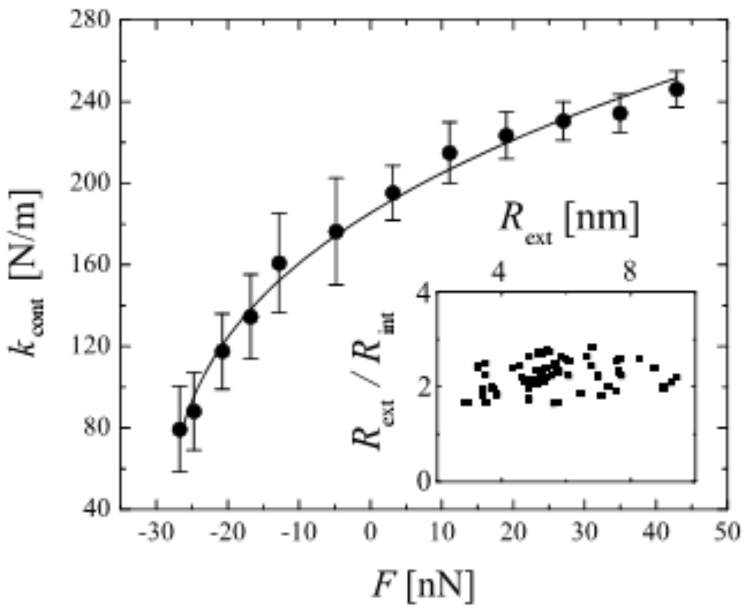

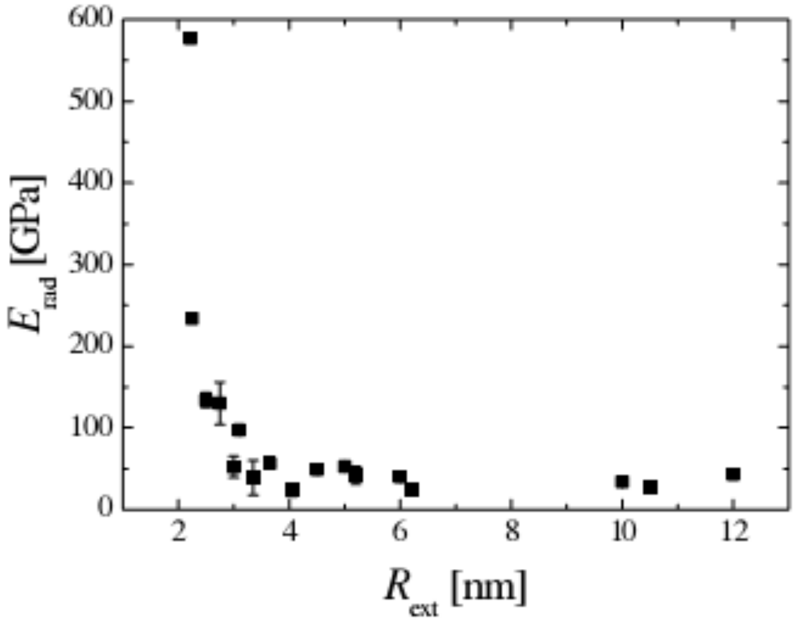

Use of Hertz theory to extract E_{rad}

L. Palaci et al., *Phys. Rev. Lett.* **94**, 175502 (05)

Imaging Graphene Resonators

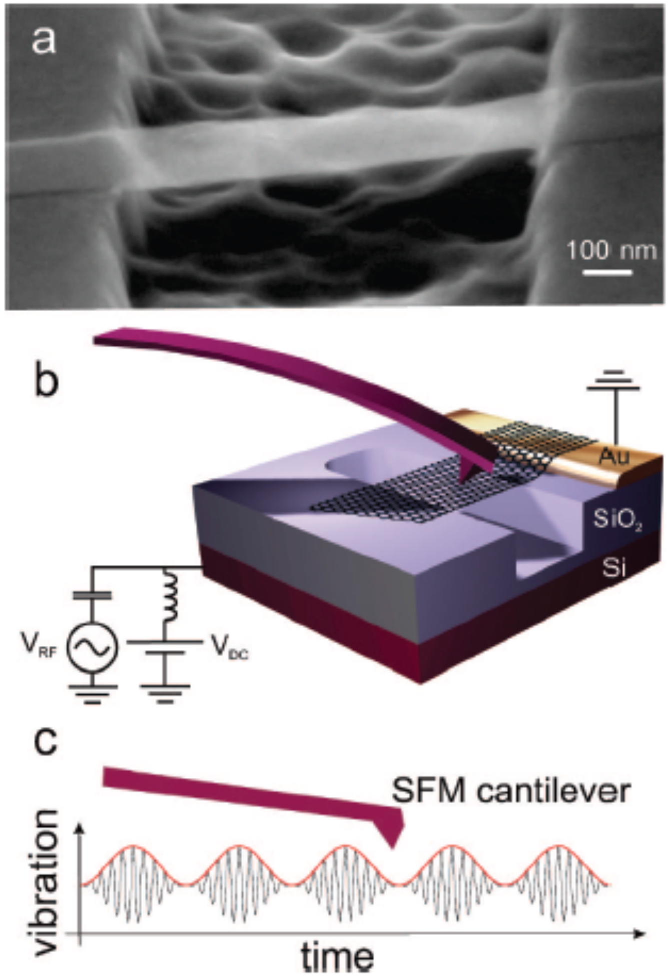

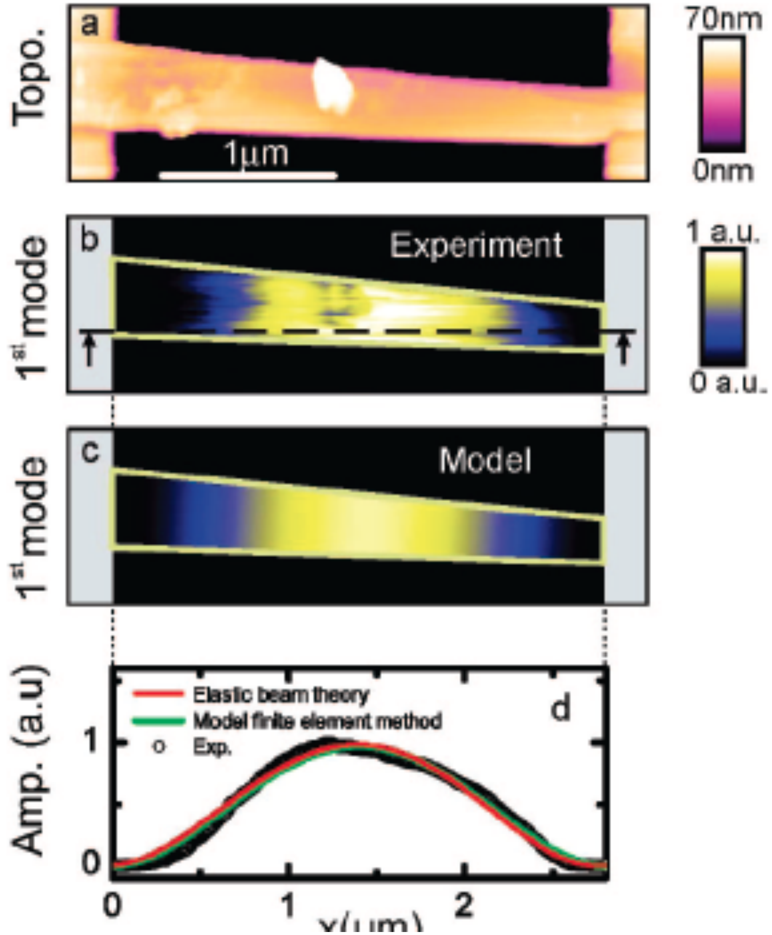

Garcia et al., Nanoletters, 8, 1399 (2008)

Buckling of Graphene resonators

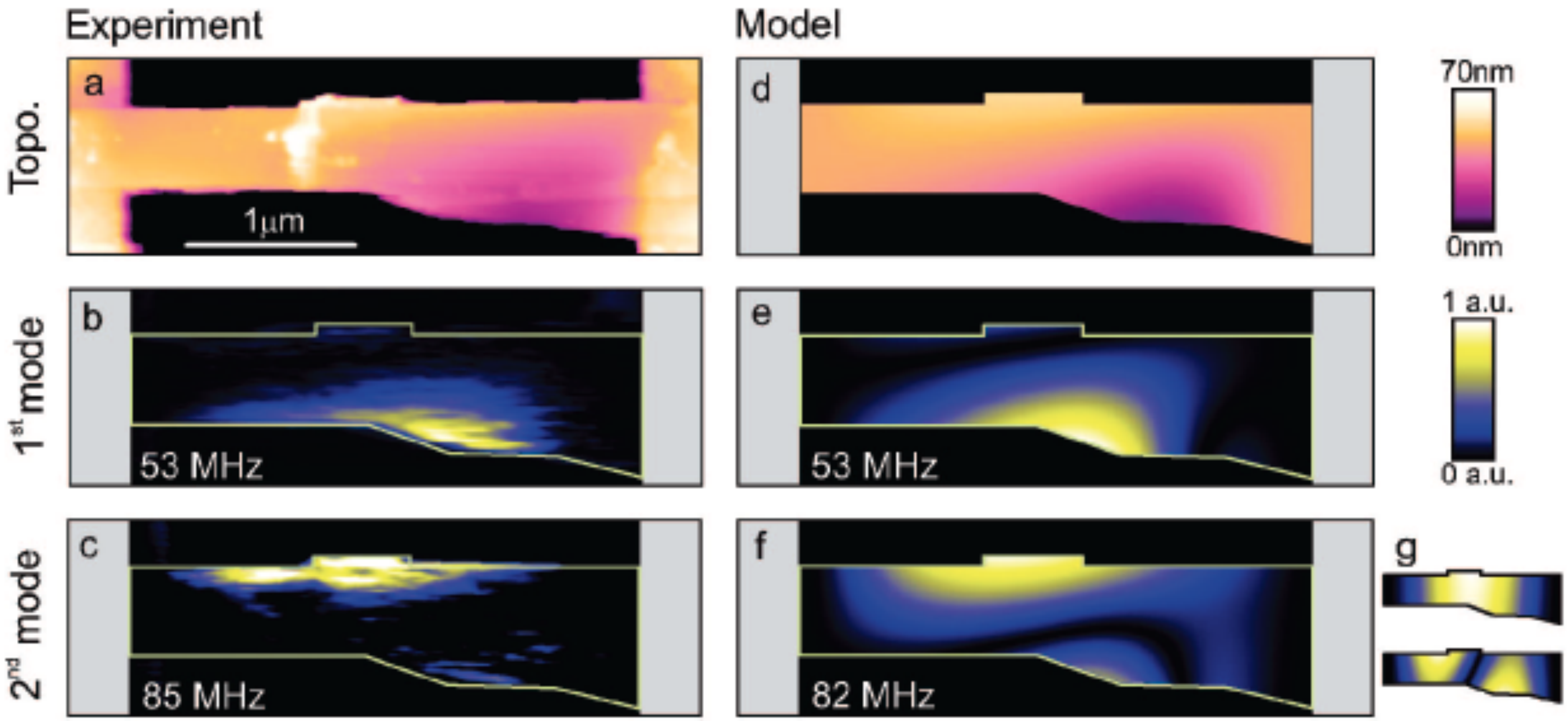

Figure 3. Graphene resonator with local buckling. (a) Measured topography. $t = 6$ nm, $l = 2.8$ μm, $w_{min} = 0.5$ μm, and $w_{max} = 0.8$ μm. The maximum out-of-plane displacement of the buckling is 37 nm. (b−c) Shape of the first and the second eigenmodes (raw data). $V_{DC} - \varphi = 3$ V and $V_{RF} = 40$ mV. The amplitude of vibration is in arbitrary units. (d) Topography obtained using FEM simulations on a stressed graphene sheet. The maximum displacement is 36 nm. See the text for the boundary conditions. (e−f) Shape of the first and the second eigenmodes using FEM simulations. (g) Shape of the two first eigenmodes using FEM simulations without any stress. The resonance frequencies are 17 and 46 MHz.

Local elasticity maps of antigene

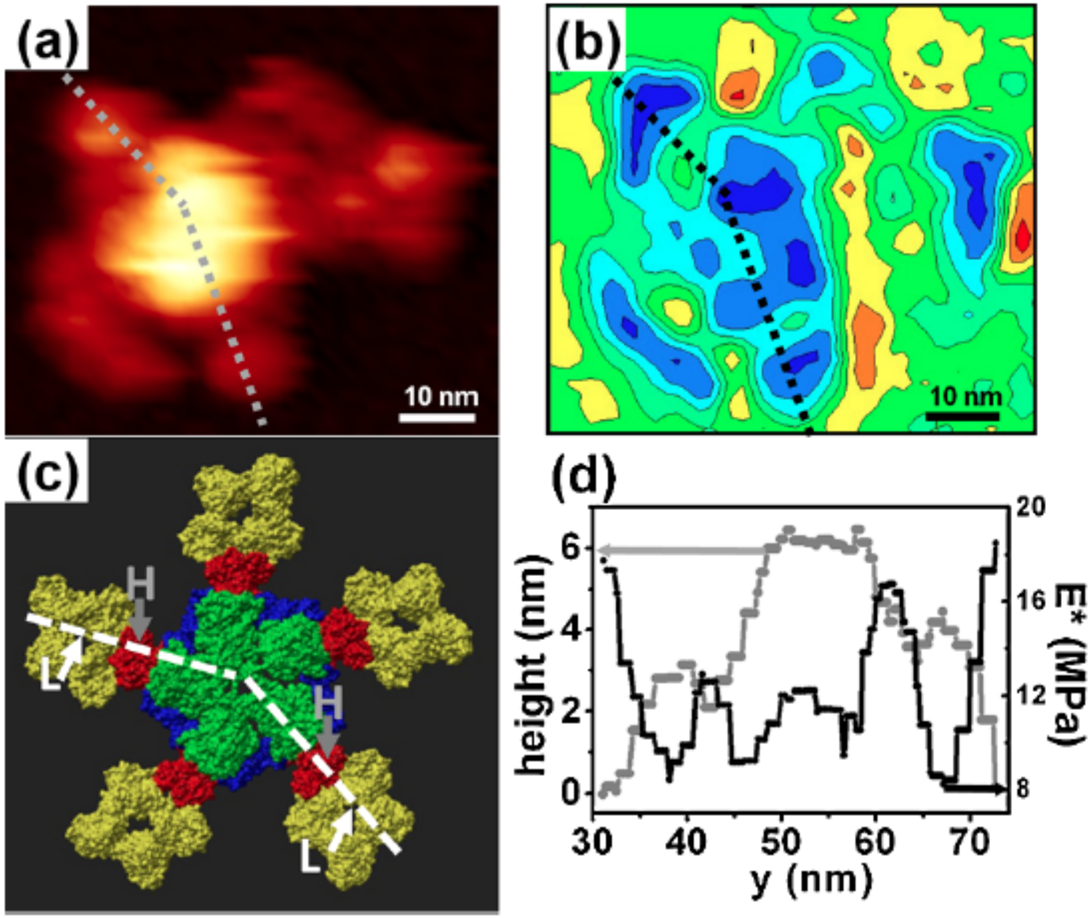

Topography and flexibility map of a single IgM antibody
(a) Bimodal AFM image(b) Flexibility map (c) structure d) profiles
D. Martinez-Martin et al., *Phys.Rev. Lett.* 106, 125208 (2011).

Mass detection by frequency detection

$$f = \frac{1}{2\pi}\sqrt{\frac{k}{m}} \quad \Rightarrow \Delta f = \frac{\partial f}{\partial m}\Delta m = -\frac{1}{2}\frac{\sqrt{k}}{m^{3/2}}\Delta m$$

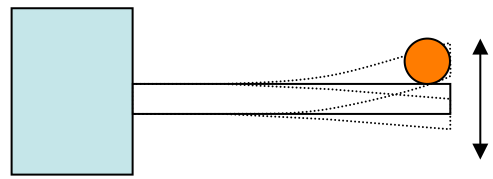

$$\Rightarrow \quad \frac{\Delta f}{f} = -\frac{1}{2}\frac{\sqrt{k}}{m^{3/2}}\frac{\Delta m}{\sqrt{\frac{k}{m}}} = -\frac{1}{2}\frac{\Delta m}{m}$$

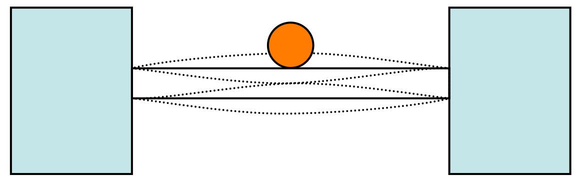

Typical Cantilever (1x10x10μm3)$\Rightarrow$ m= $2\cdot10^{-12}$kg

$\Rightarrow\Delta$m=$4\cdot10^{-12}$kg · Δf/f

$\Rightarrow$with f=137,5kHz; Δf=1mHz$\Rightarrow$ Δm=3 · 10^{-20}kg=3 · 10^{-17}g=30ag

Single virus particle mass detection

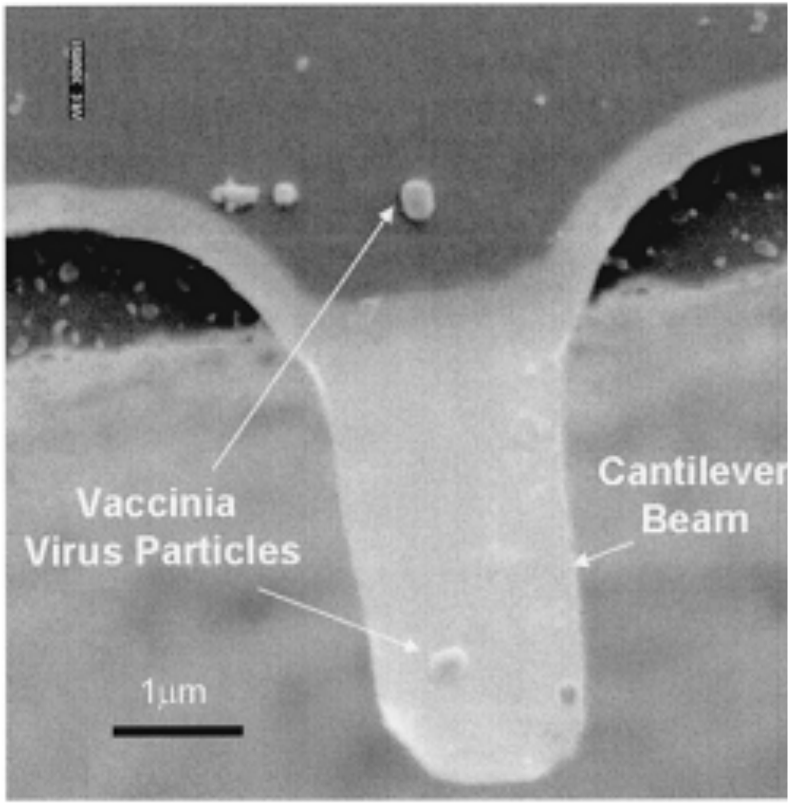

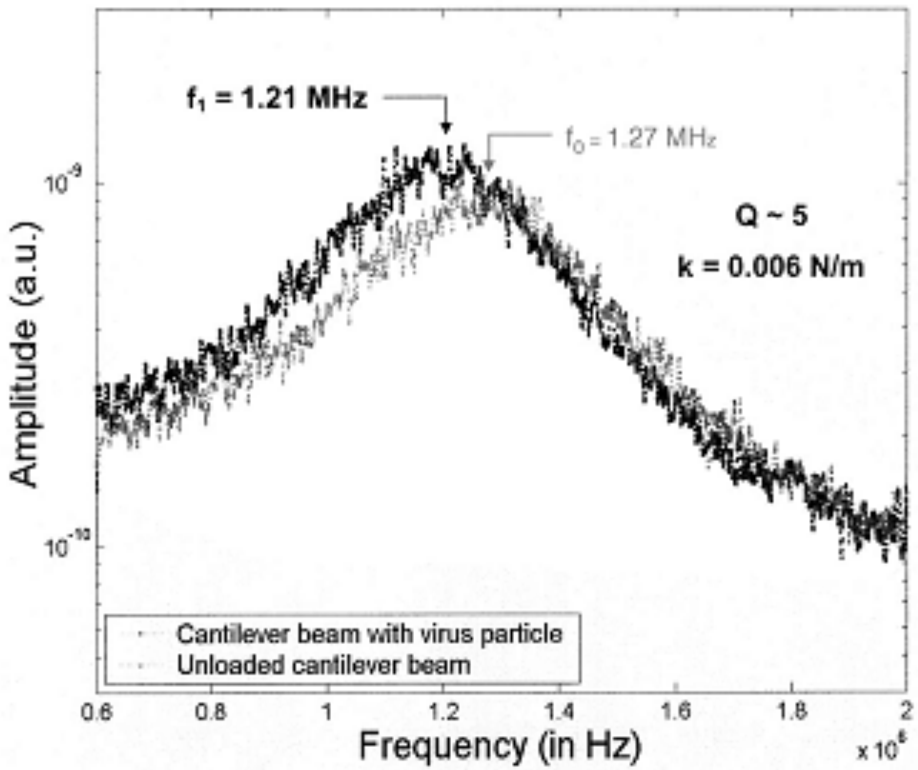

$\Rightarrow$1 virus = 9.5fg

A. Gupta, D. Akin and R. Bashir, *Appl. Phys. Lett.* **84**, 1976 (2004)

Weighing single molecules?

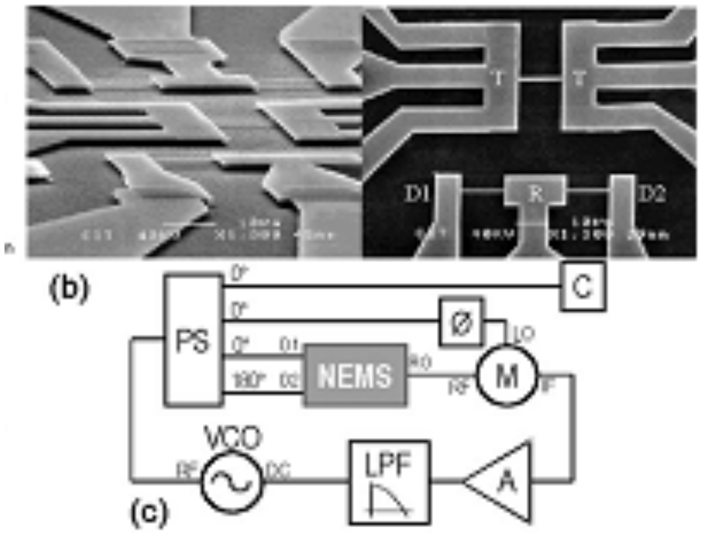

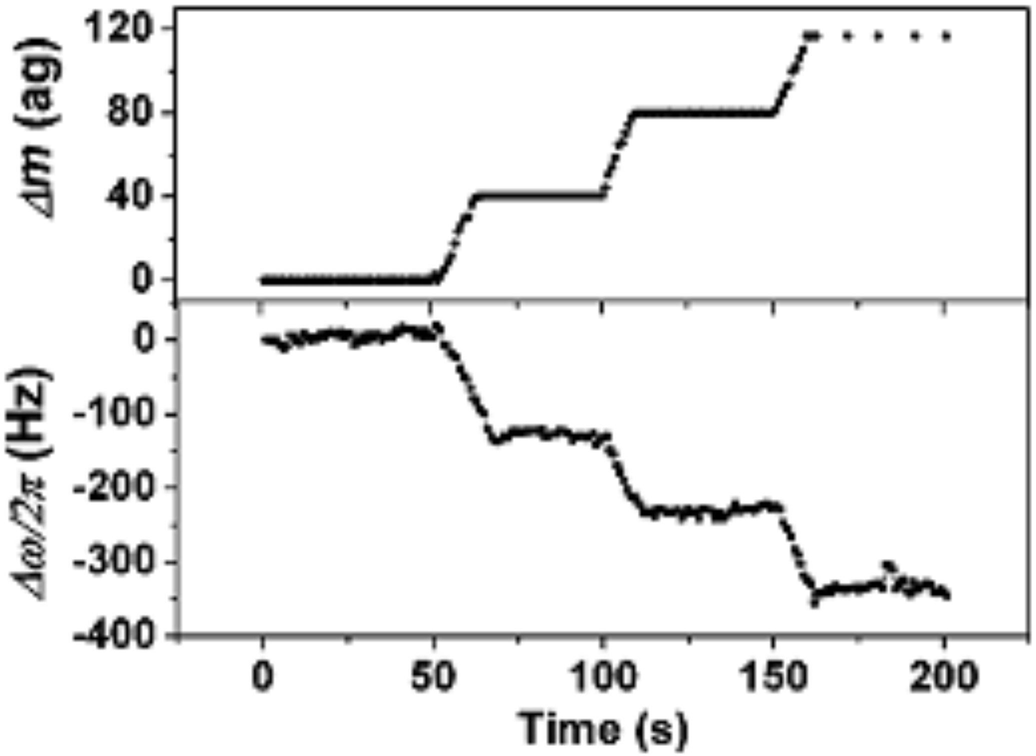

Detection of Attograms; Zeptograms (=10^{-21}g) seems feasable

K.L. Ekinci, X.M.H. Huang and M.L. Roukes, *Appl. Phys. Lett.* **84**, 4469 (2004)

Carbon nanotubes to weigh zeptograms 1.4zg at 4.2K

D=1.9nm
L=900nm

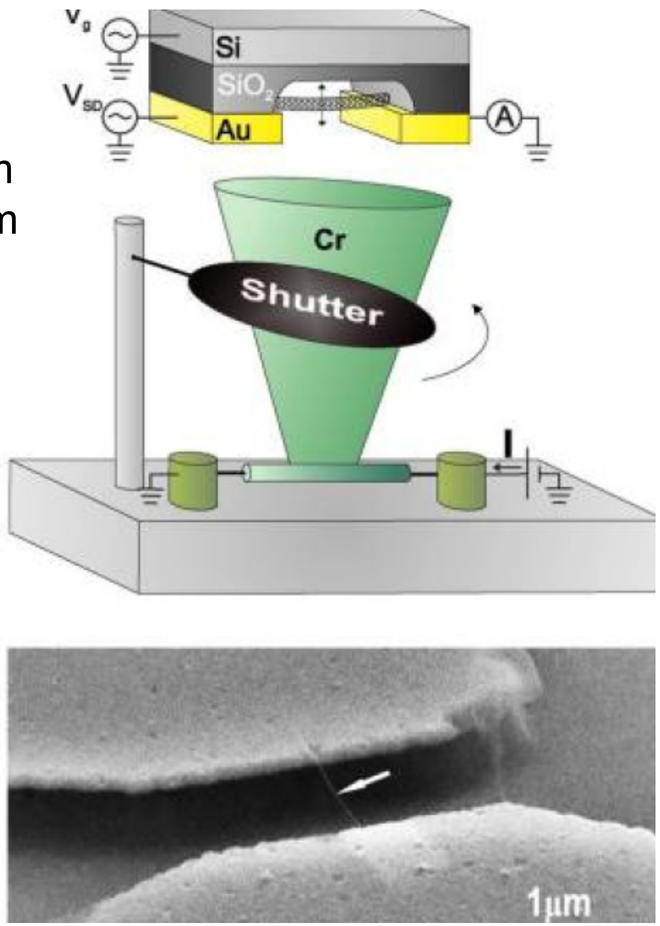

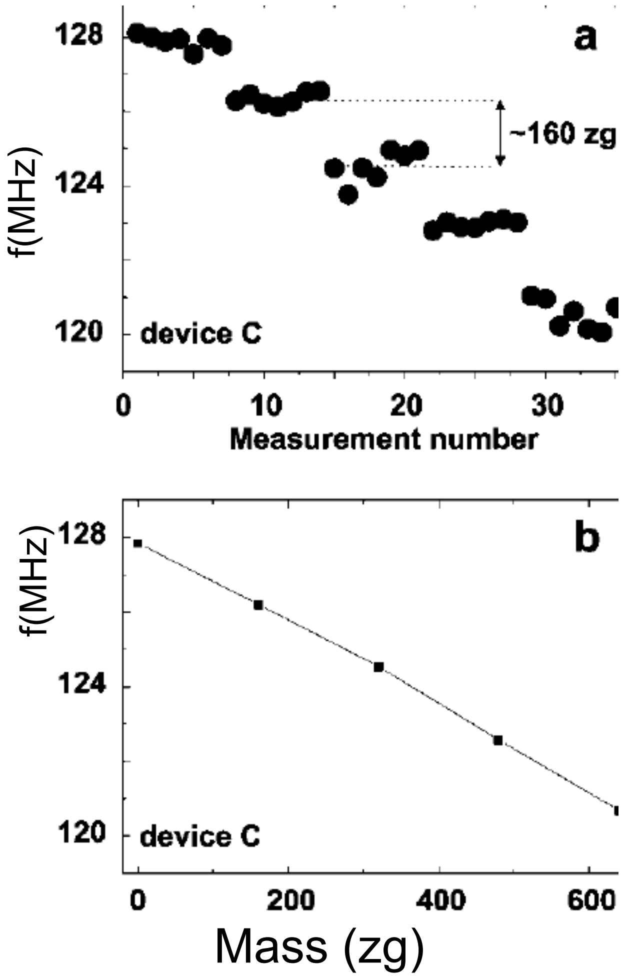

1860Cr atoms

Sensitivity
11Hz/yg

1yg=10^{-24}g

At present 1.4zg
0.1zg=1Cr atom

B. Lassagne et al., *Nanoletters* 8, 3775 (2008).

Mass detection with coupled oscillator

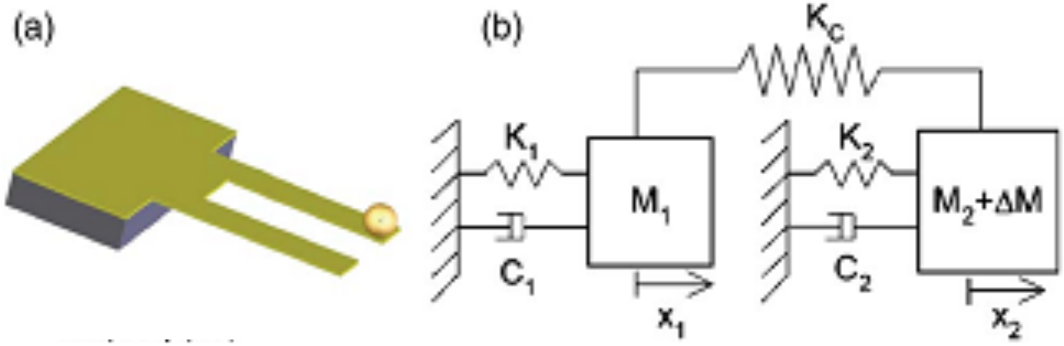

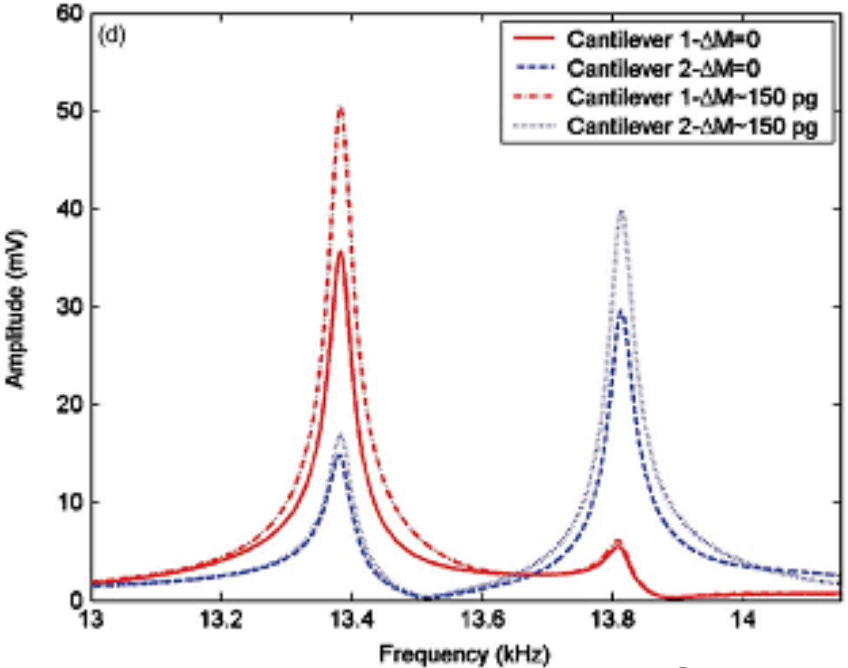

Relative change of amplitude of coupled modes is larger than relative frequency change

M. Spletzer, A. Ravan, A. Wu, X. Xu and R. Reifenberger, Appl. Phys. Lett. 88, 254102 (2006)

Excitation of carbon nanotubes due to rf-excitation

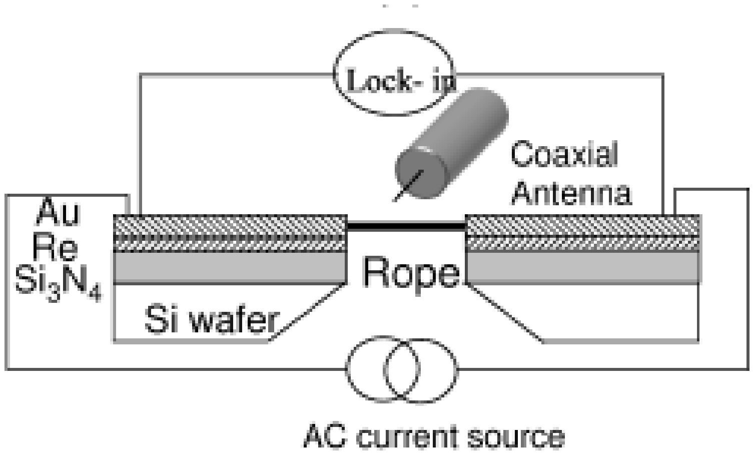

$$f_1 = \frac{22.4}{2\pi} \frac{R}{2L^2} \sqrt{\frac{Y}{\rho}}, \quad f_2=2.7f_1 \; f_3=5.3f_1\ldots$$

But harmonics observed $f_2=2f_1$, $f_3=3f_1$, $f_4=4f_1\ldots$
$\Rightarrow$Tubes under tension

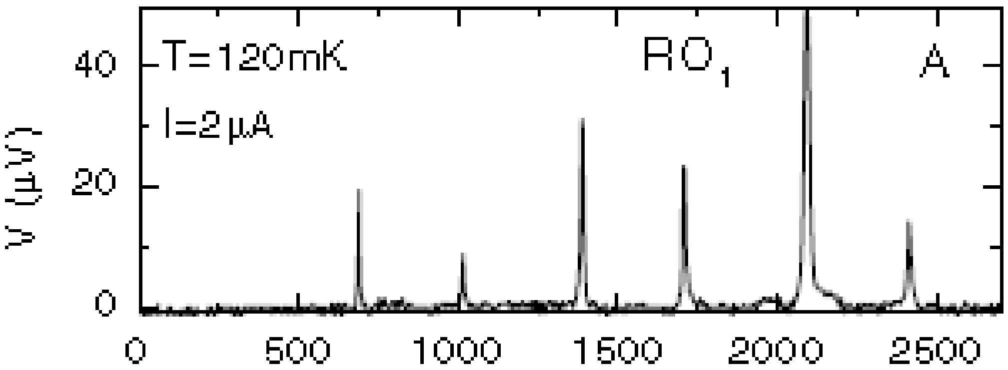

Proximity superconductivity of nanowires (12nmx1.7μm) is lost by heating due to resonant rf-excitation

Electron-sound coupling through two-level systems from adsorbates?

B. Reulet,H. Bouchiat, Phys. Rev. Lett. 85, 2829 (2000)

Nanomotors

Biological motors…

Here: artificial motors

Nanomotor with Multiwalled Carbon Nanotubes: Low friction and negligible wear

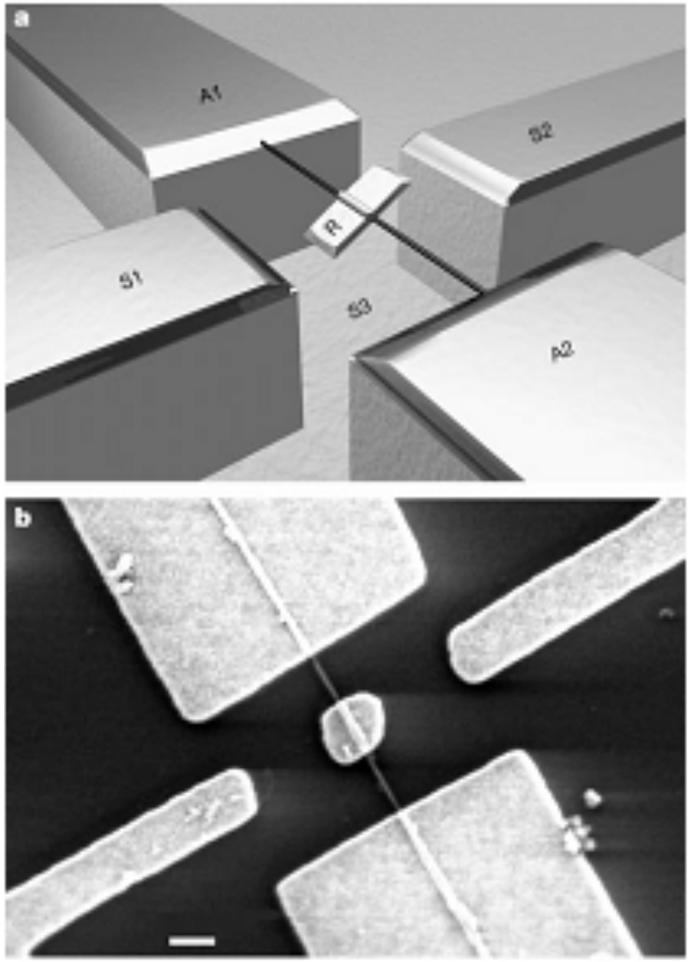

A. Zettl, University of California Berkeley

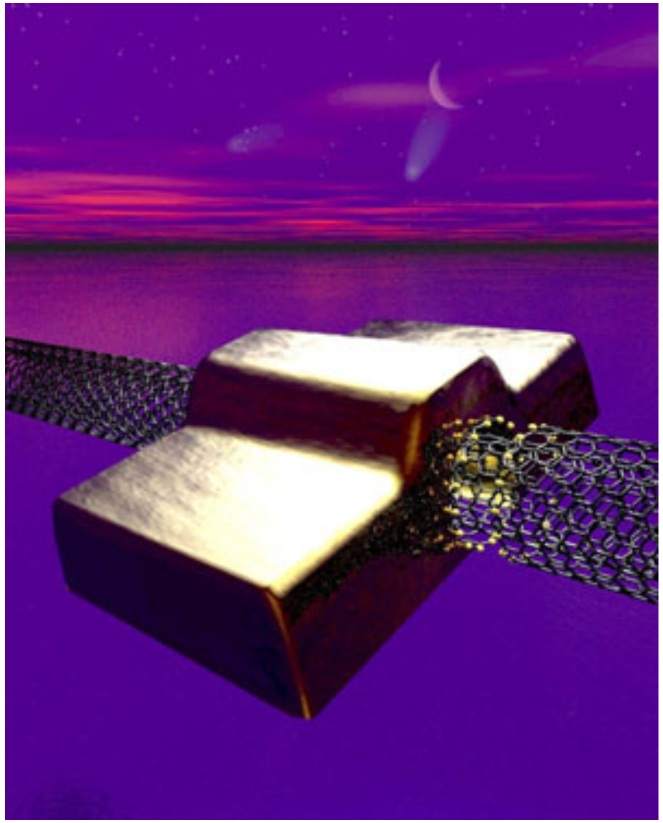

Sliding of incommensurate structures?

A. Fennimoore et al., *Nature* **424**, 408 (2003).

Nano-Motor with CNTs

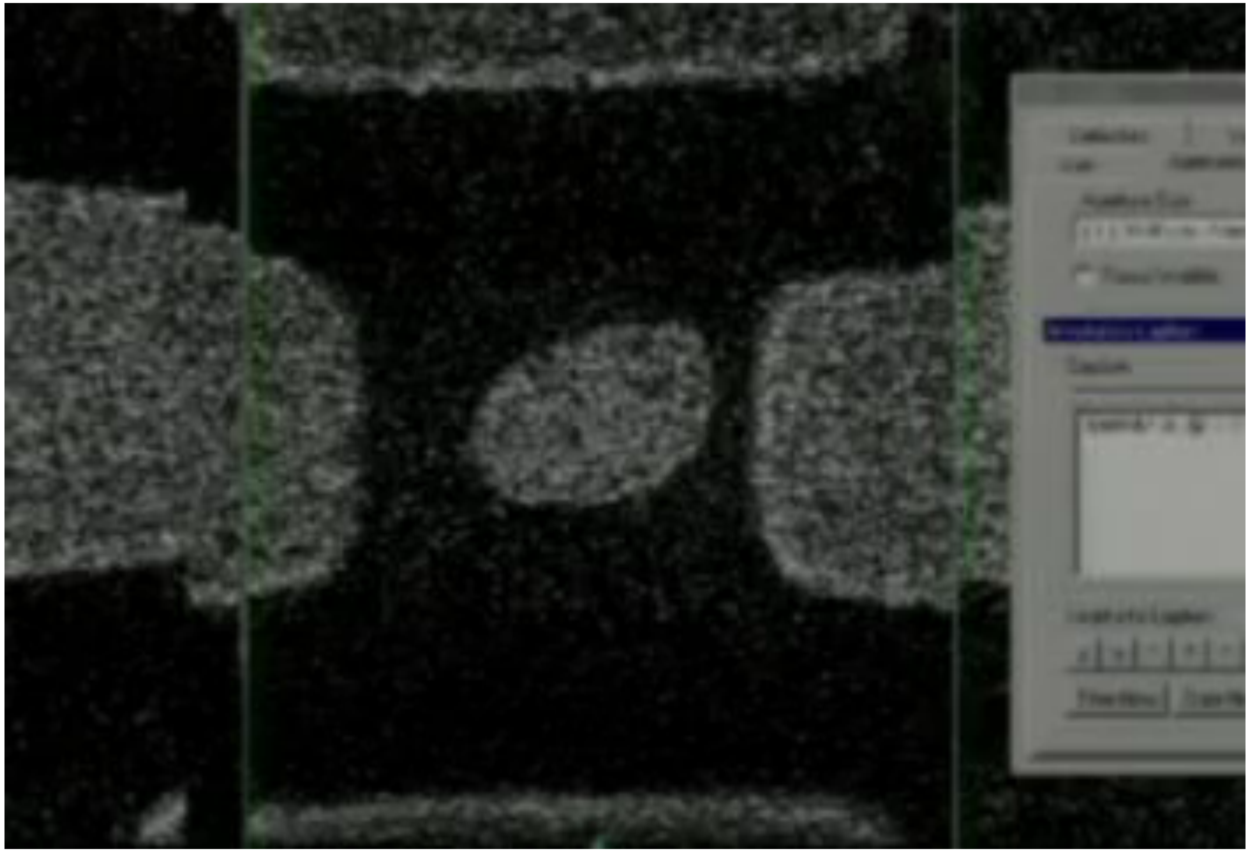

Nanomotor

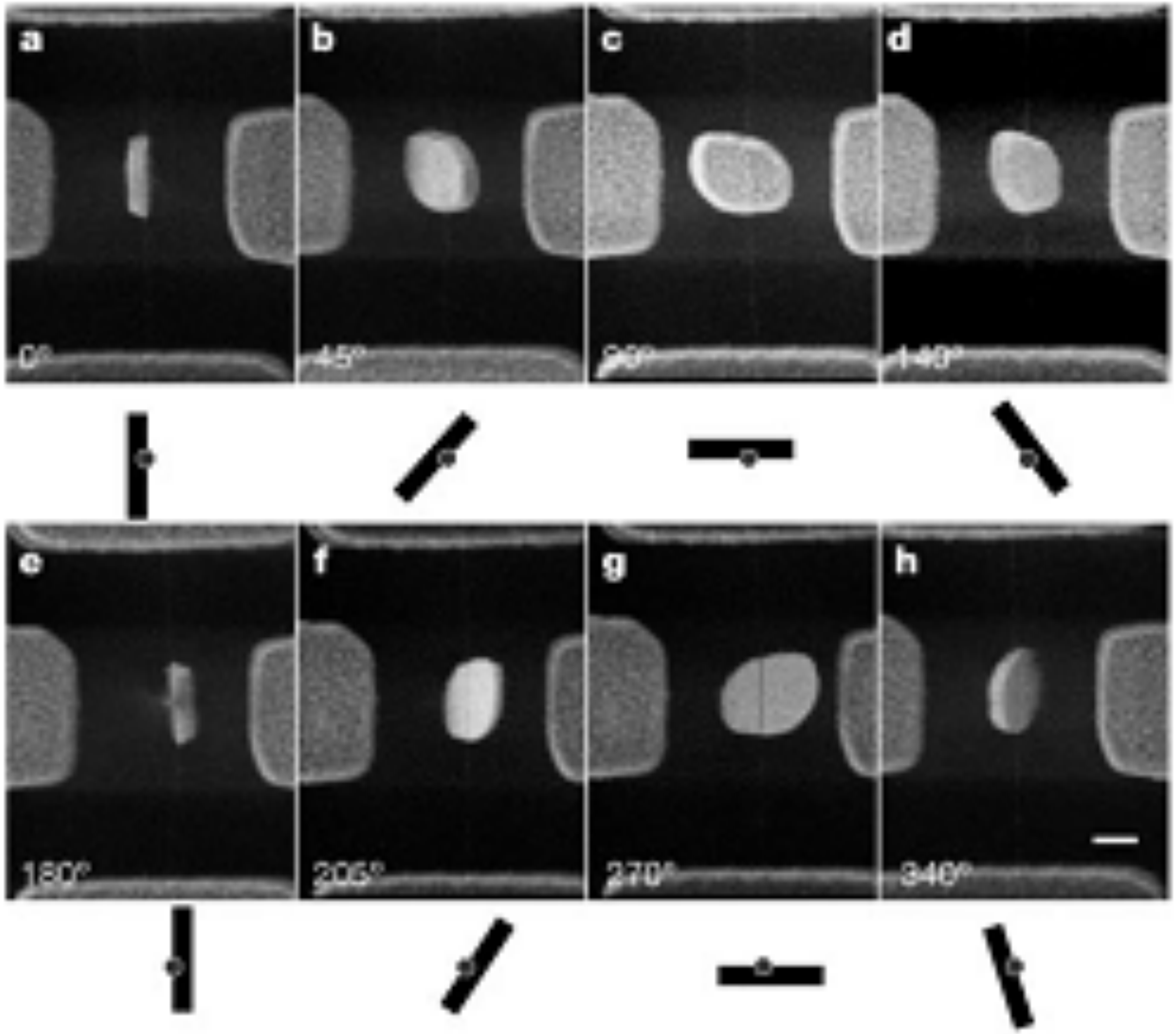

Application of gate voltage leads to rotation of the paddle
Friction and wear beween walls of the nanotube are negligble

Surface-tension driven motor

Current through Nanotube
leads to Atom motion

Growth of smaller sphere

Contact leads to fast
Mass exchange

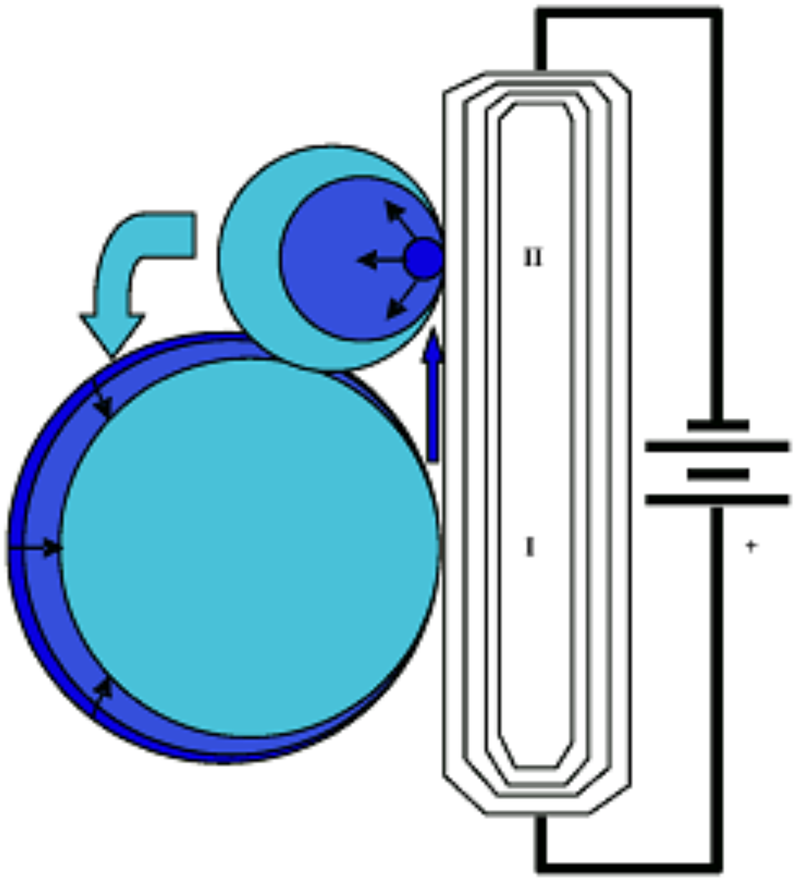

B.C. Regan, S. Aloni, K. Jensen and A. Zettl, Appl. Phys. Lett. 86, 123119 (2005)

Surface tension driven motor

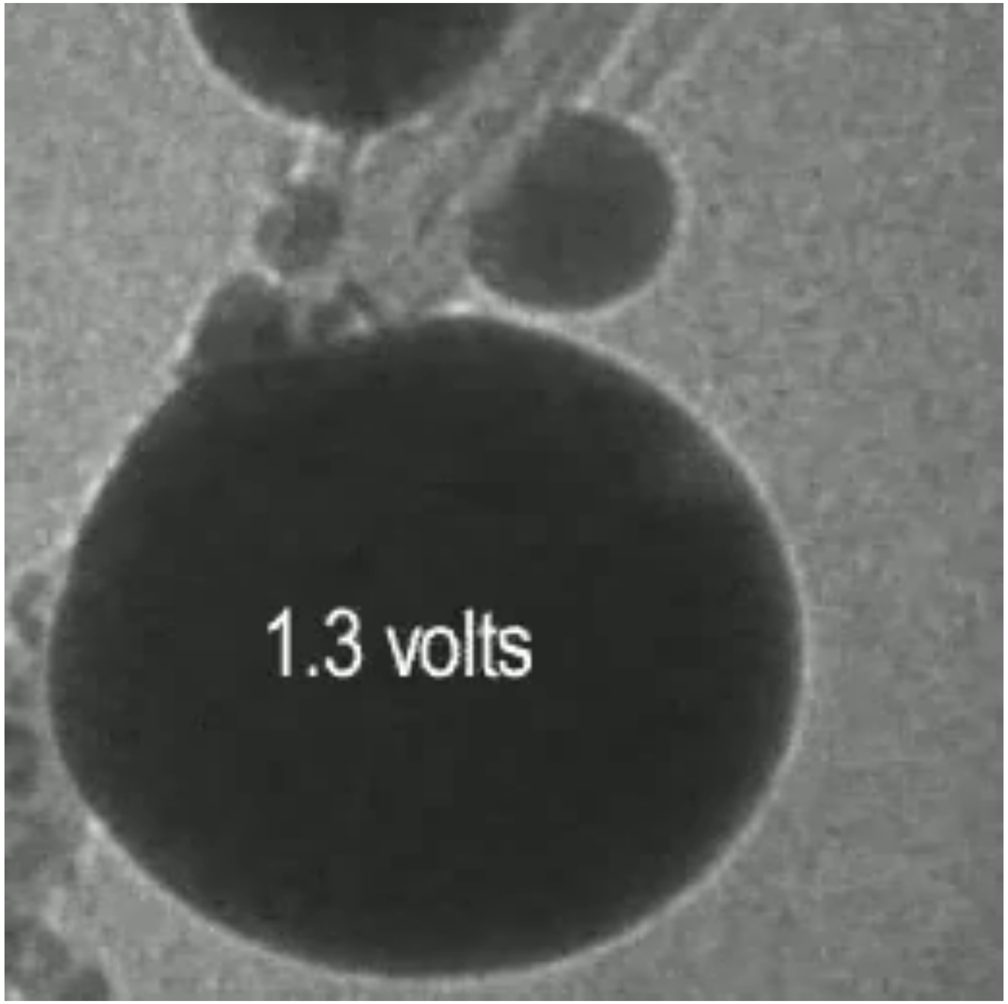

B.C. Regan, S. Aloni, K. Jensen and A. Zettl, Appl. Phys. Lett. 86, 123119 (2005)

Surface-tension driven motor

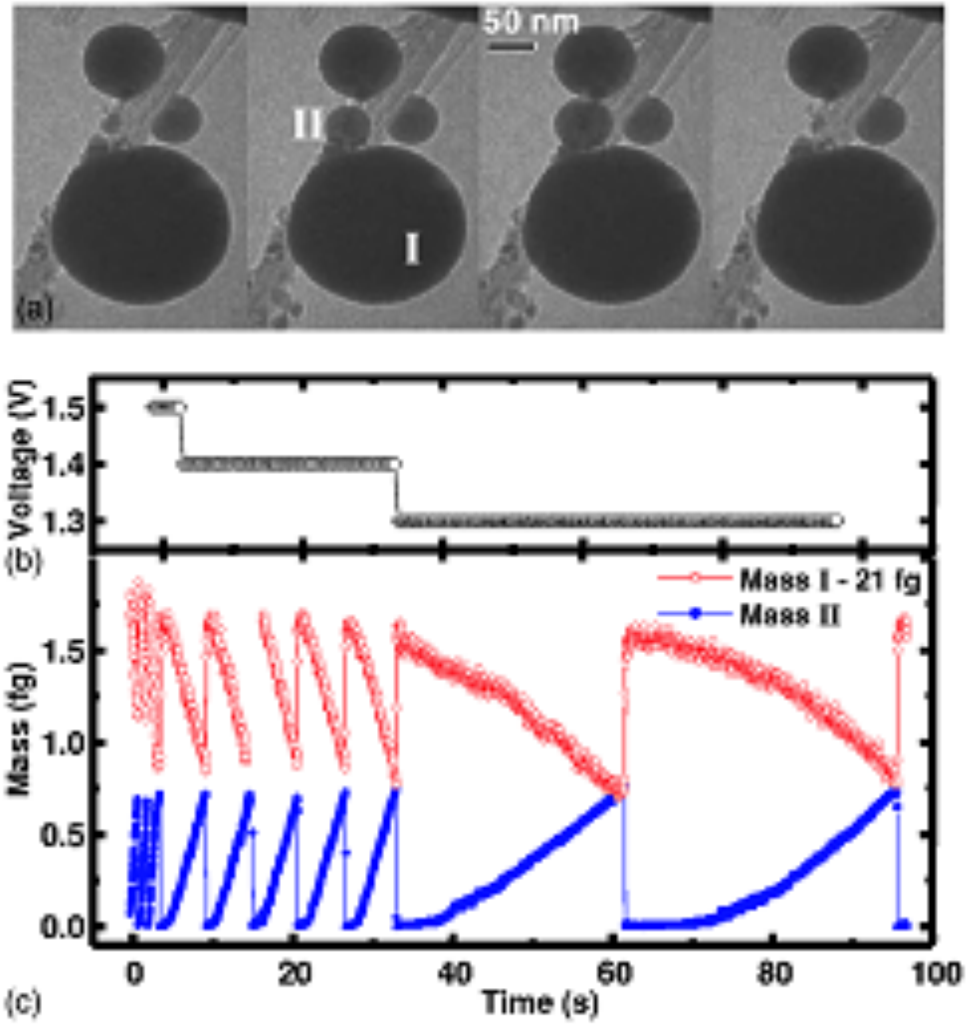

Frequency depends on applied voltage (current through tube)

Surface tension driven devices

B.C. Regan, S. Aloni, K. Jensen and A. Zettl, Appl. Phys. Lett. 86, 123119 (2005)

Nanodroplets and Superhydrophobicity

How do nanodroplets behave, compared to macroscopic droplets?
What is the influence of roughness on contact angles?

Young's Equation

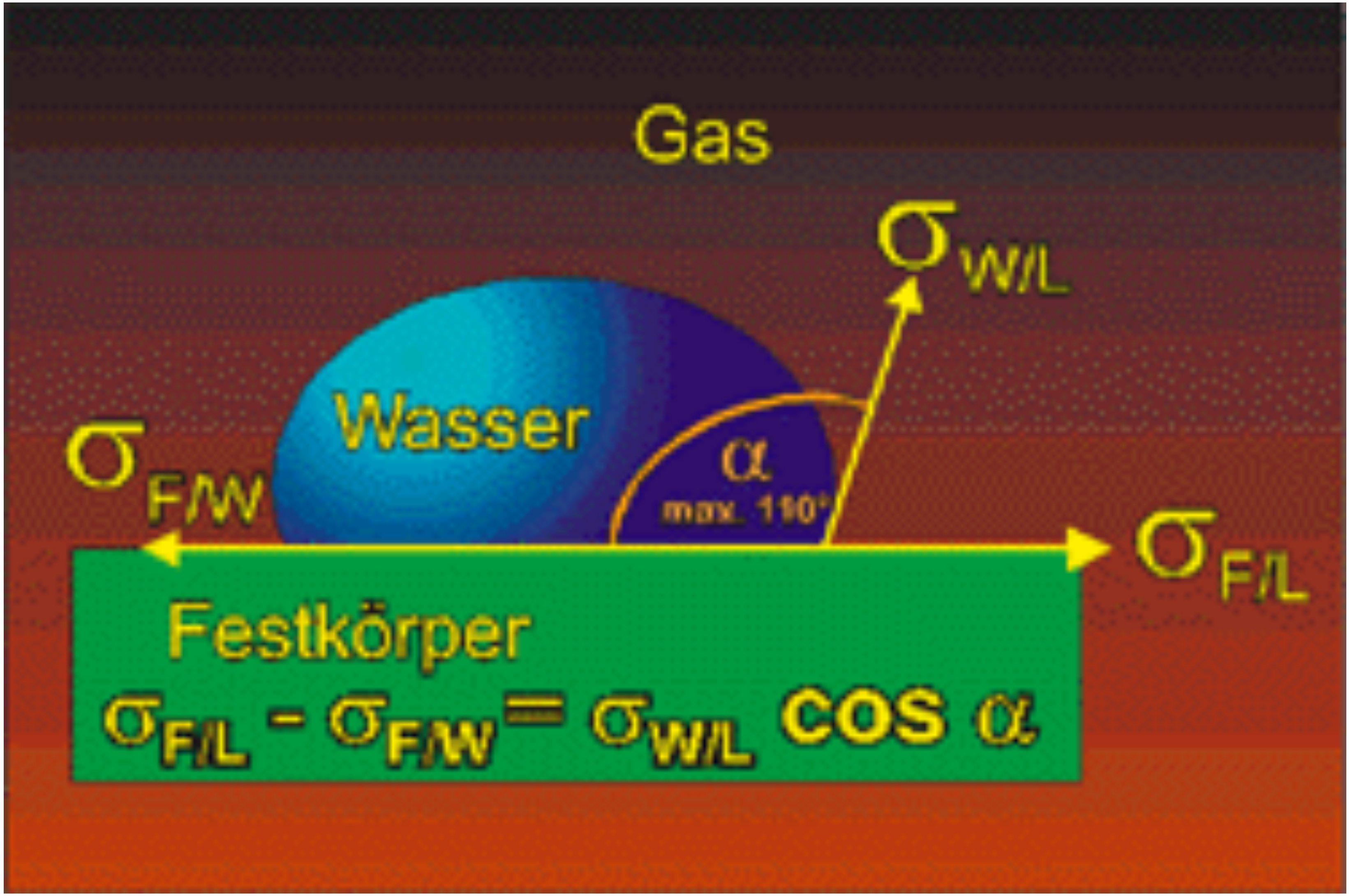

Lotus-Effect

Lotus-Effect

Lotus Flower

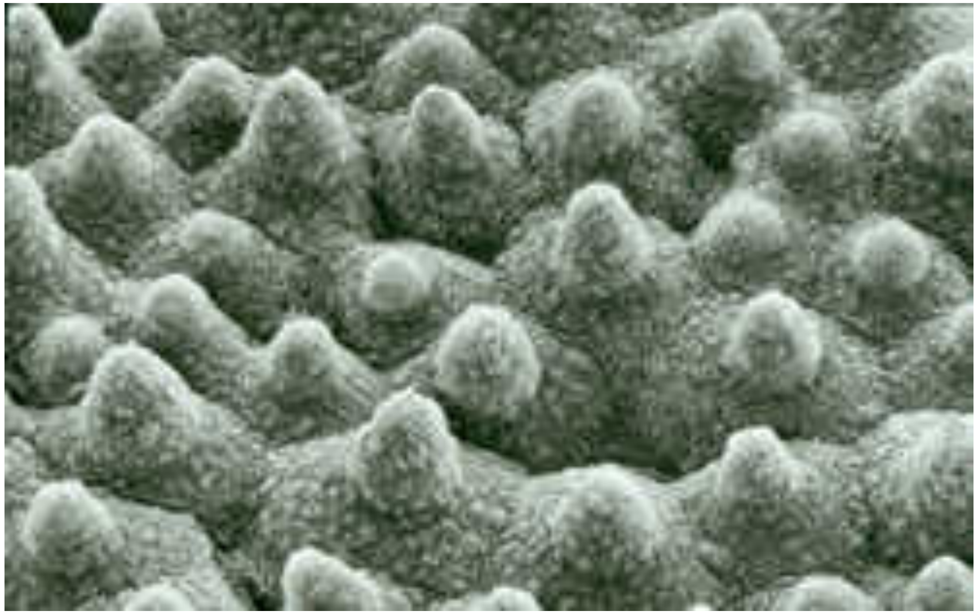

Surface of the Lotus Flower

Lotus-Effekt

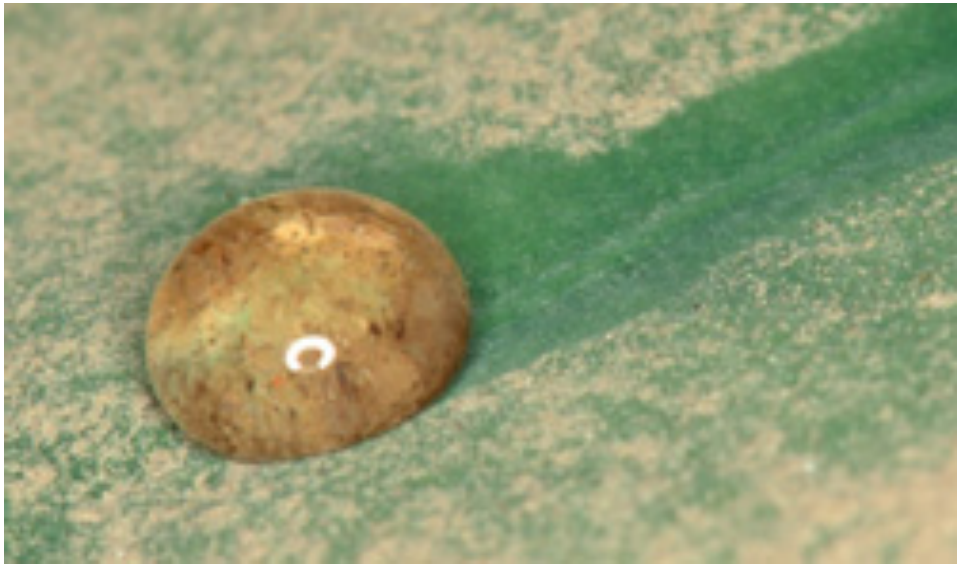

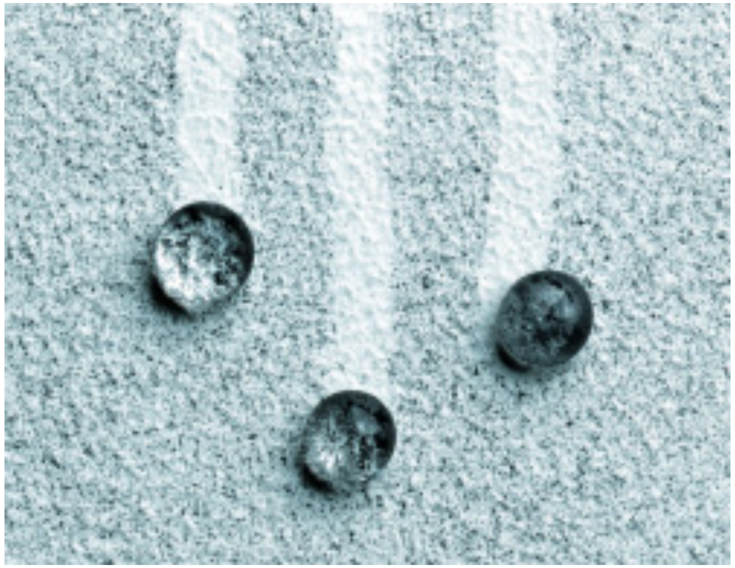

Dust particles are swept away

Self-cleaning paint

Superhydrophobicity

$$\gamma_{SL} + \gamma_{lv} \cos\Theta = \gamma_{sv}$$

Youngs Equation

$\Theta = 0^{\circ}$ $\Rightarrow$ hydrophilic

$\Theta > 90^{\circ}$ $\Rightarrow$ hydrophobic

$\Theta > 150^{\circ}$ $\Rightarrow$ superhydrophobic

Experimental evidence:
Rougness increases contact angles from 100-120 º
to 150-175 º !

Wenzel vs. Cassie Model

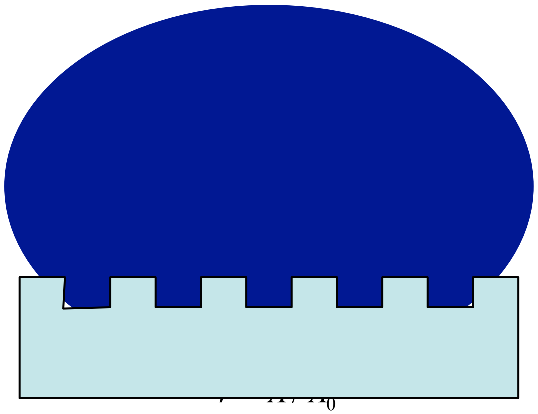

Wenzel

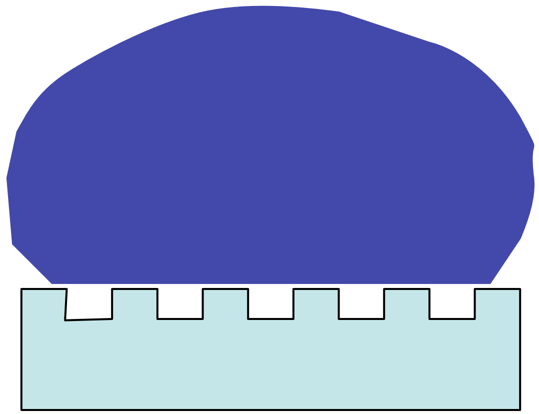

Cassie

$$\cos\Theta_0 = r\cos\Theta$$

$$r = A / A_0$$

$$\cos\Theta_0 = -1 + \Phi(1 + \cos\Theta)$$

$$A = \Phi A_0$$

A.B.D. Cassie and S. Baxter, Trans. Faraday. Soc. 40, 546 (44)

Cassie-Modell

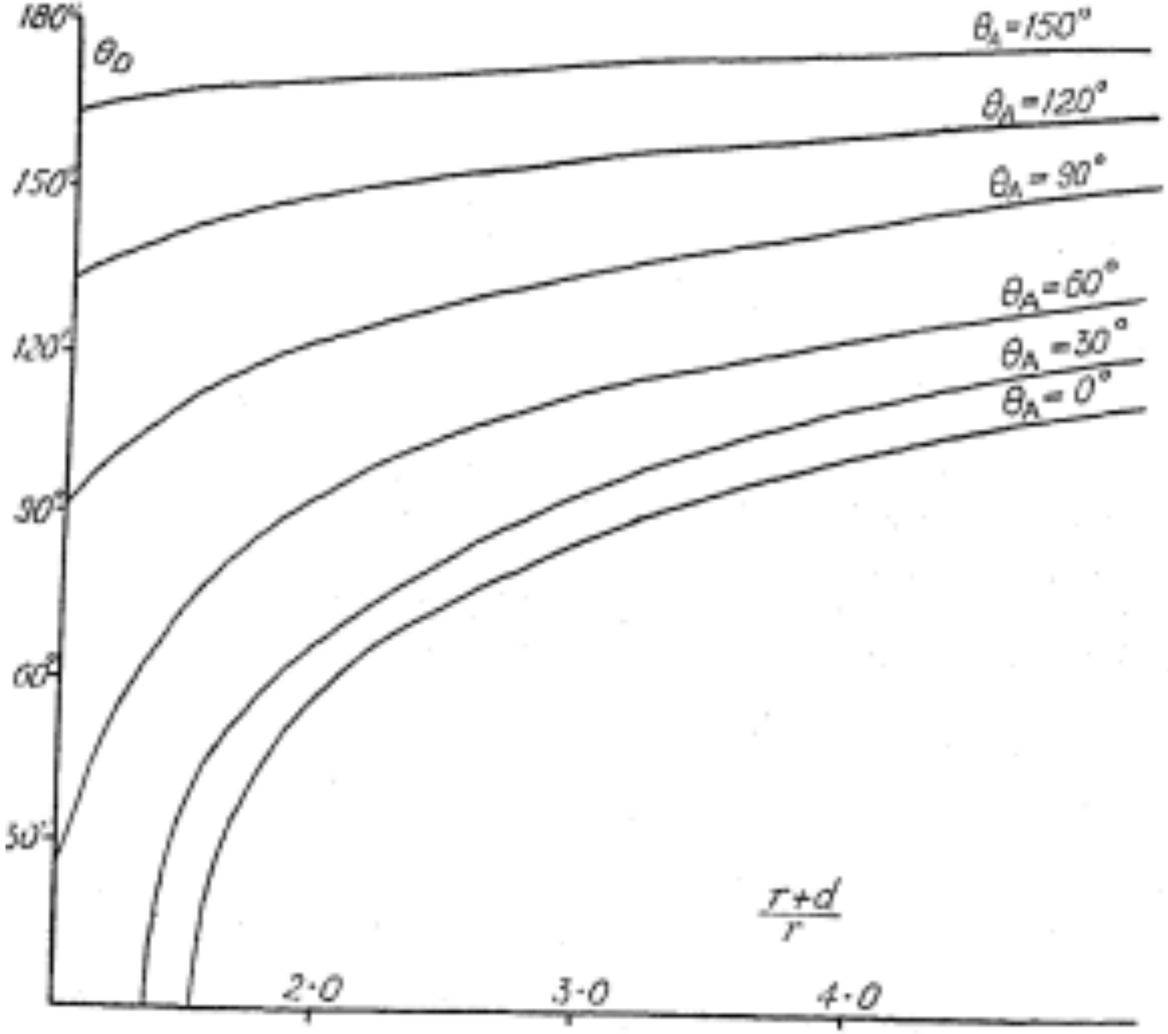

FIG. 3.—Apparent advancing contact angle.

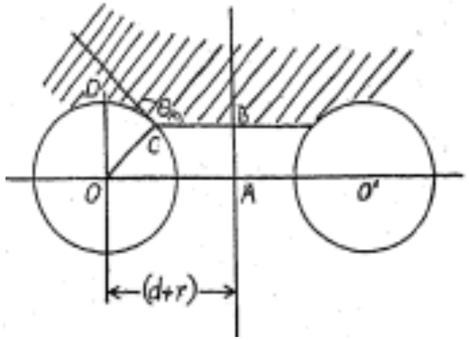

Fibers with radius r

A.B.D. Cassie and S. Baxter, Trans. Faraday. Soc. 40, 546 (44)

Nanodroplets: Wetting and Roughness

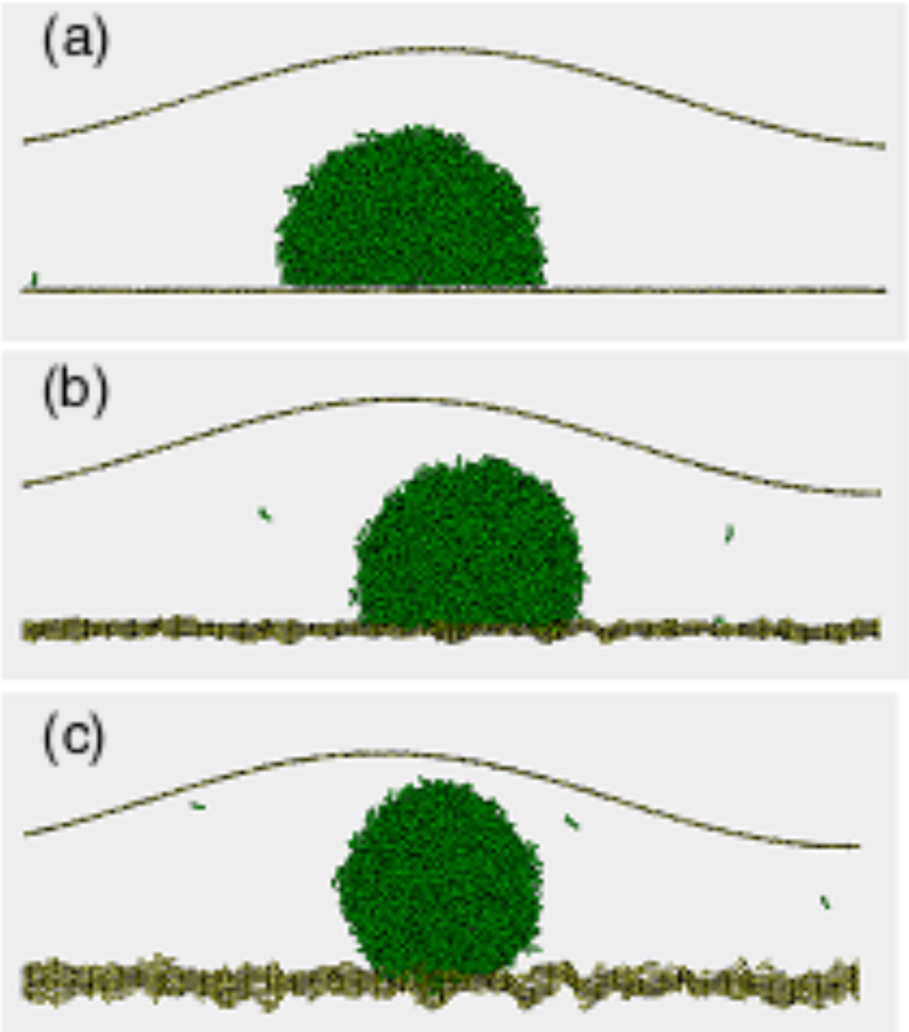

MD-Simulations of Octane nanodroplet on a flat surface (a) and rough surface rms= 2:3 A and rms=4:8 A

C. Yang et al., Phys. Rev. Lett. 97, 116103 (2006)

Comparison of MD-simulations with models

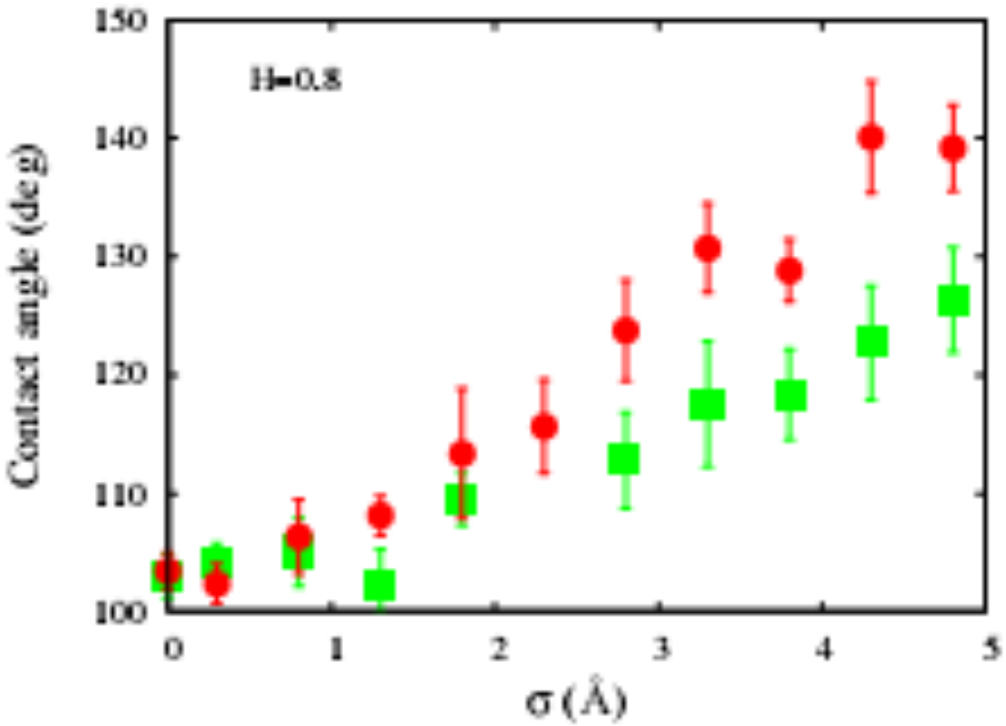

MD-Simulations

Cassie-model

Contact angle increases with rms-roughness but not with fractal dimension
⇒ Agreement with Cassie-model

Advancing and Receding contact angle are equal after 1ns

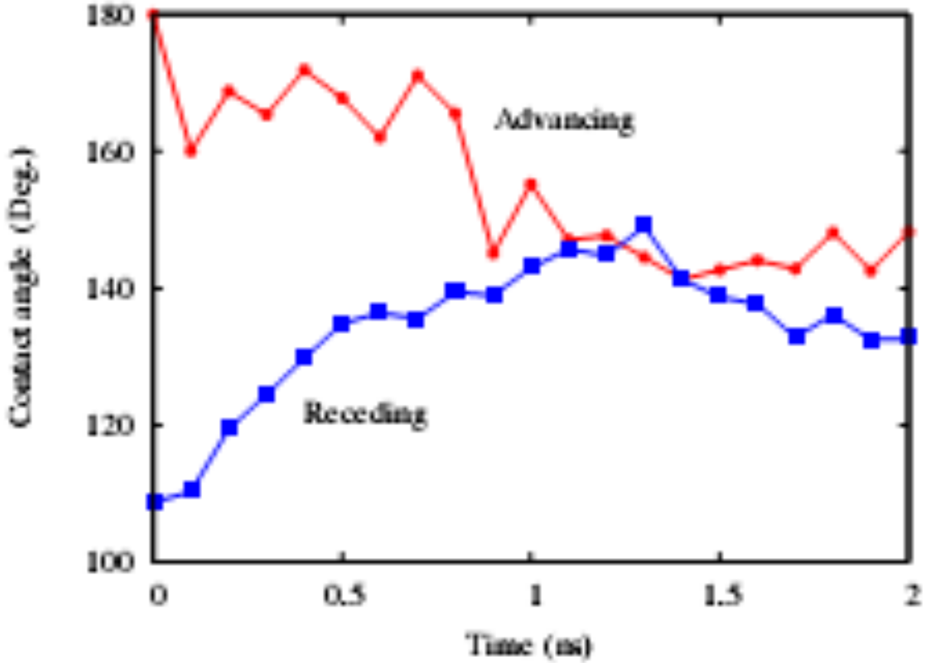

Thermal activation between Wenzel-state and Cassie-state is
Possible for nanodroplet; not for macroscopic droplet! Hysteresis

Transition between Cassie-state and Wenzel-state

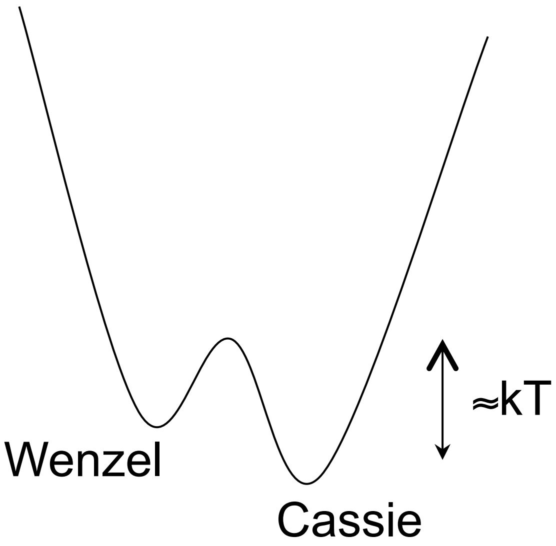

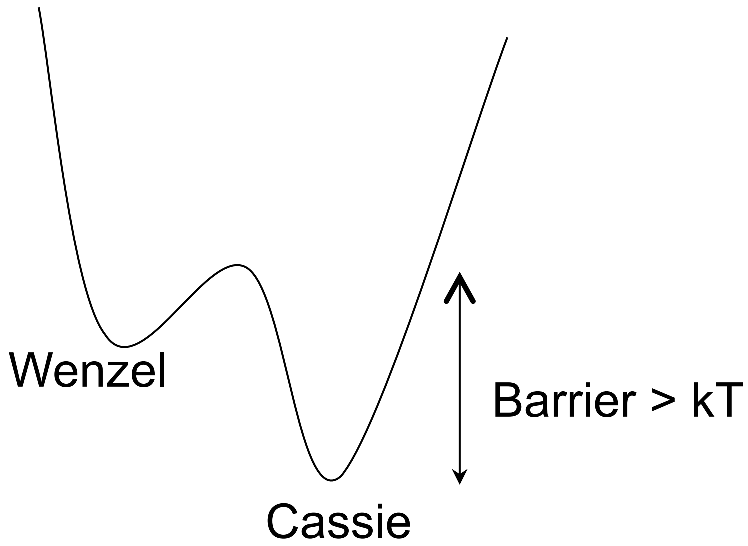

Nanodroplet
⇒Transition by thermal activation
⇒No hysteresis

Macrosopic droplet
⇒If droplet is pushed into Wenzel it is an irreversible transition
⇒hysteresis

Nanotech Business Suit

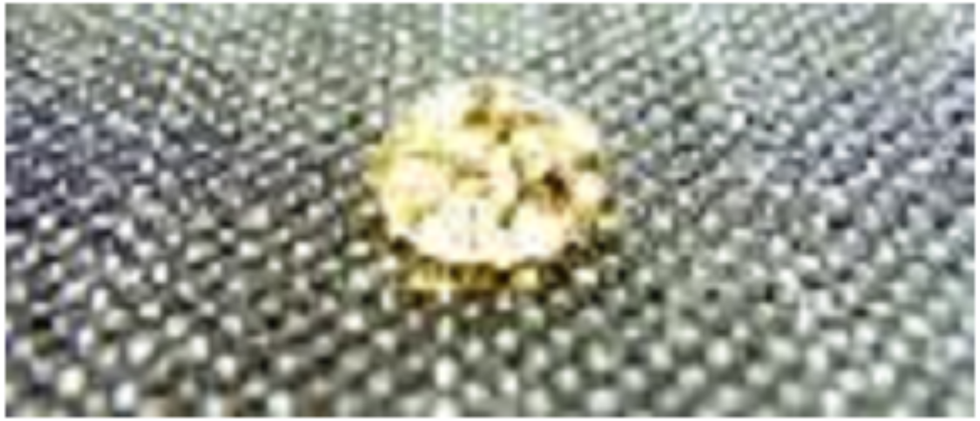

Using ultra-fine processing technologies, Miyuki Keori Co. has developed a business suit that repels water and even oil and stays comfortable. The suit is difficult to stain with wine or olive oil. The maker processed the suit by spraying extremely small chemical particles on its surface, each as small as 30 nanometers.

Dynamic force detection

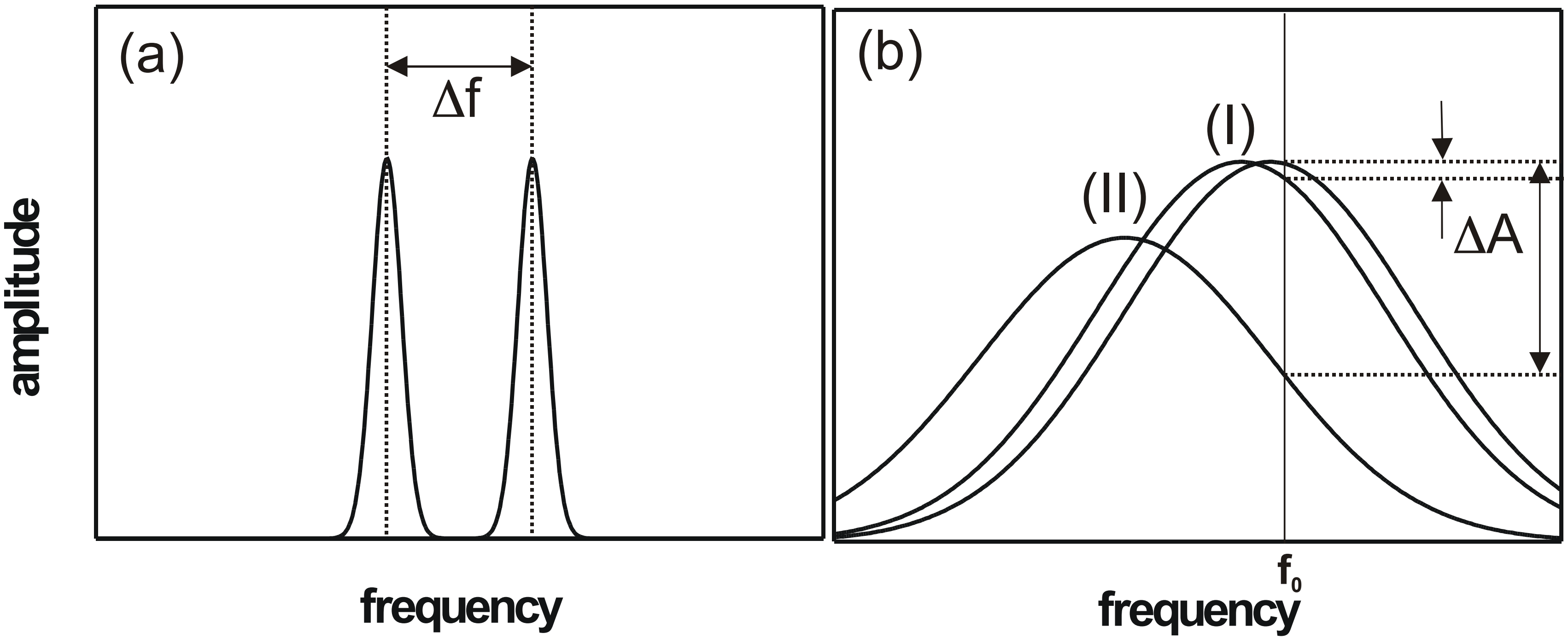

Cantilever is excited to oscillate, frequency shift and amplitude are measured for force detection

(a) high Q-factor (vacuum)

sharp resonance, detection of frequency shift: non-contact mode, Dynamic Force Microscopy

(b) low Q-factor (air, liquid)

fast amplitude response, detection of amplitude: intermittent contact or tapping mode

R. Garcia, R. Perez, *Surf. Sci. Rep.* **47**, 197 (2002)

How to measure small forces?

$$F_{\min} = \sqrt{\frac{2k_B T \Gamma \Delta\omega}{\pi}}$$

$$\Gamma = \frac{k}{\omega_0 Q}$$

$Q=10^6$
$\omega_0=10^4$Hz
k=1mN/m
T=4K
$\Delta\omega$=1Hz
$\Rightarrow F_{min} \approx 10^{-18}$N=1aN

k_B: Boltzmann constant
T: Temperature
B: Bandwidth
k: spring constant
Q: Q-factor
ω_0: Resonance frequency
Γ: Damping coefficient

High Q
Low temperature
Low spring constant k

Advantages of Dynamic Force Microscopy

- Avoid jump into contact
    - Spring constants k > 10 N/m
    - Rather large amplitudes $kA > F_{adh}$ (A=2-60nm)
- Reduced damage of the surface due to lateral forces
- Preparation of probing tips (similar to STM)
- Atomic resolution in non-contact modes
- Differentiation of force contributions
- High force sensitivity:

$$F_{\min} = \sqrt{\frac{4kk_BTB}{Q\omega_0}} \approx 10^{-15}\,\frac{\mathrm{N}}{\sqrt{\mathrm{Hz}}}$$

Setup for tapping mode

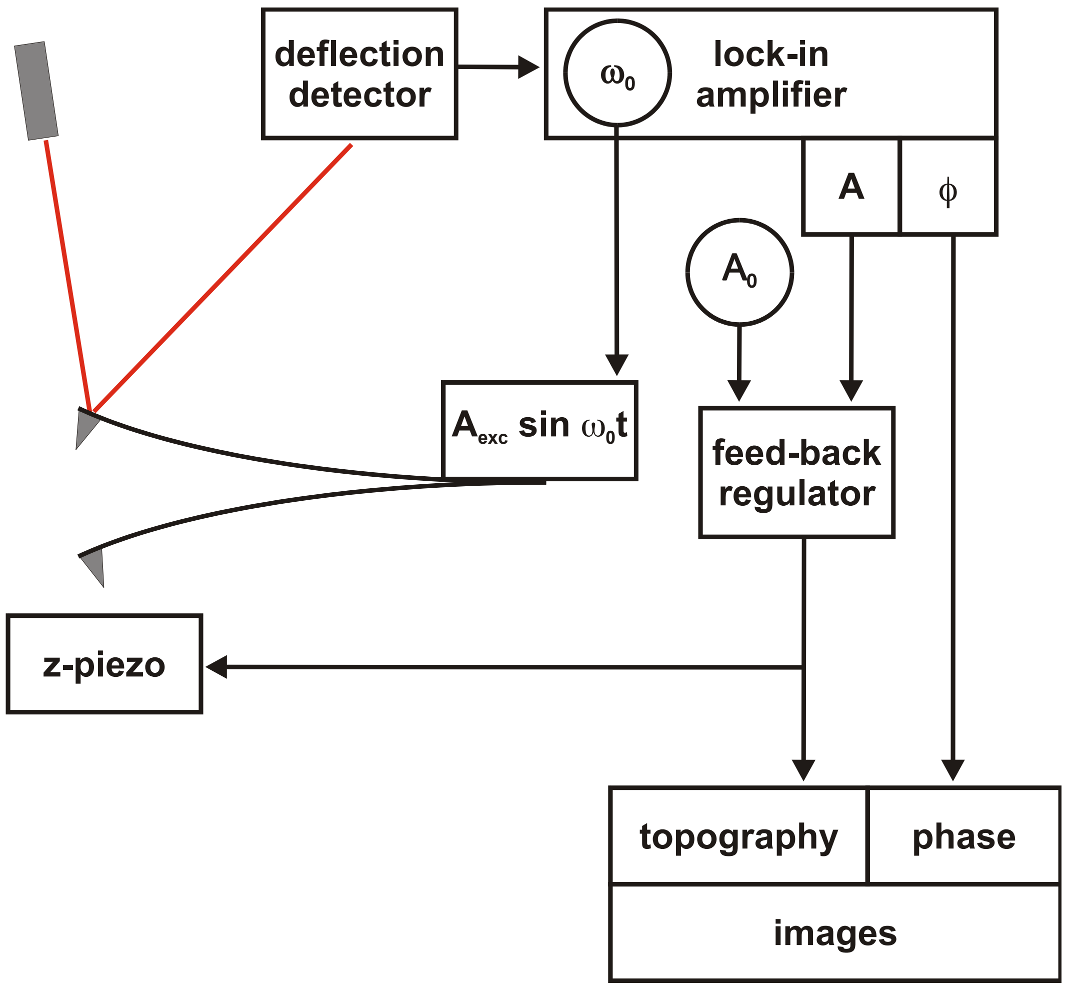

Setup for Dynamic Force Microscope

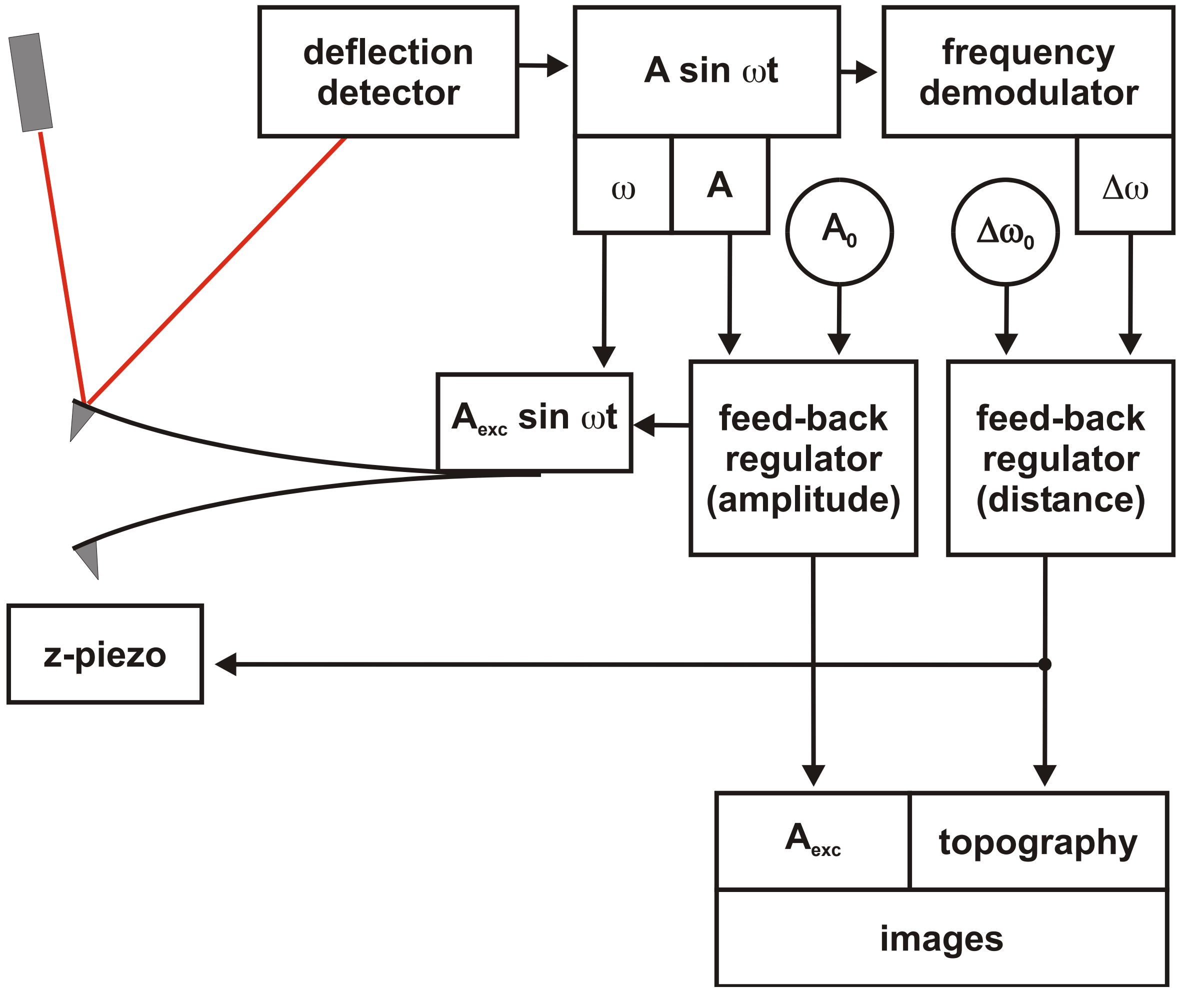

How to measure forces in dynamic force microscopy

For **small amplitudes** A, compared to the interaction length,

The frequency shift Δf is related to **force gradients** $k_{ts}=dF_{ts}/dz$

$$\Delta f(z_c) = \frac{f_0}{2k} k_{ts}(z_c)$$

The tip-sample force can be determined by integration

Forces in nc-AFM

Frequency modulation: $f_0 = \frac{1}{2\pi}\sqrt{\frac{k}{m^*}}$ $\Delta f = -\frac{f_0}{2k}\frac{\partial F_{tot}}{\partial z}$

$\Rightarrow$ measured topography = surface of constant $\frac{\partial F}{\partial z}$

$$F_{tot} = F_{chem} + F_{mag} + F_{el} + F_{vdW}$$

bonding between tip and sample atoms (only for d < 5 Å)

only for magnetically sensitive tips

$$F_{el} = -\frac{1}{2}\frac{\partial C}{\partial z}V^2$$

$$F_{vdW} = -\frac{HR}{6d^2}$$

Dynamic Mode, non-contact

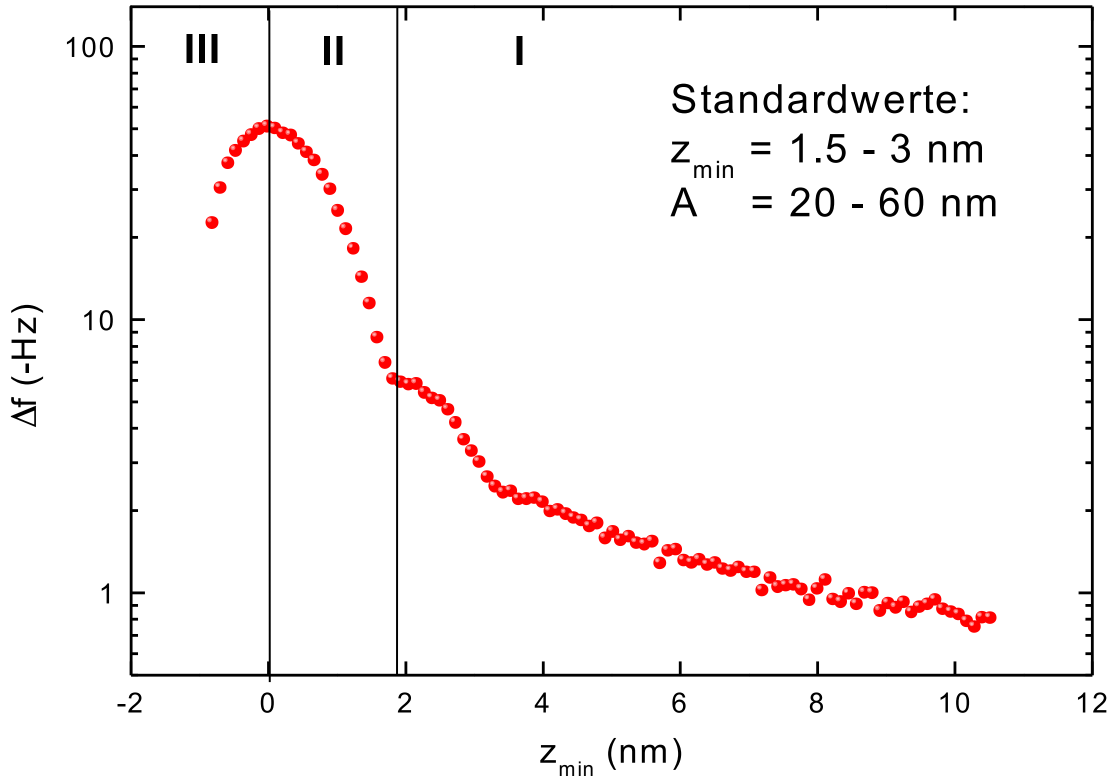

region I:
attractive forces
non-contact mode

region II:
attractive forces
atomic resolution

region III:
repulsive forces
tapping mode

Perturbation approach for the large amplitude case

The motion of the tip can approximately be described as a harmonic oscillator, where internal damping is compensated by the driving force:

$$m\ddot{z} = -kz + F_{tip-sample}$$

For large amplitudes, the motion is nearly harmonic and the frequency shift is given by :

$$\frac{\Delta f}{f} kA = \frac{1}{\pi} \int_0^{\frac{2\pi}{\omega}} \sin \omega t \; F_{tip-sample}\left(z(t)\right) dt$$

The force law can be reconstructed from the Δf(z)-curve.

Non-contact AFM on Si(111)7x7

(Constant frequency mode)

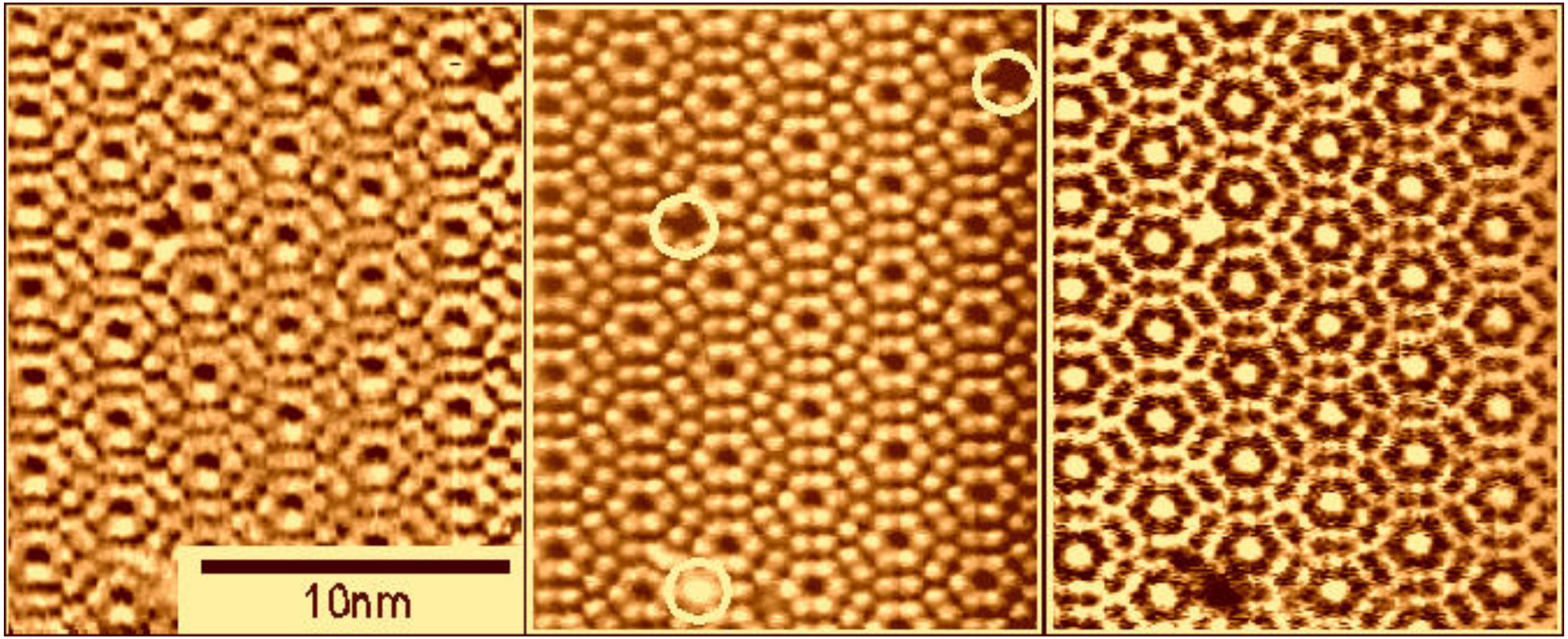

Topography	Tunneling Current	Damping
Δf=const. $\Delta z \approx 1$Å	$\overline{\Delta I_t} \approx$ 20pA	A_{exc}

f_0=156710Hz k=27N/m Q=16500 A=16.9nm Δf = -122Hz ($\Delta f/f$)kA = -0.35nN

R. Lüthi et al. *Surf. Rev. Lett.* 4, 1025 (1997)

Simulation of oscillating tip

$\alpha = 6.6°$

A = 16nm

f = 0.1 Hz

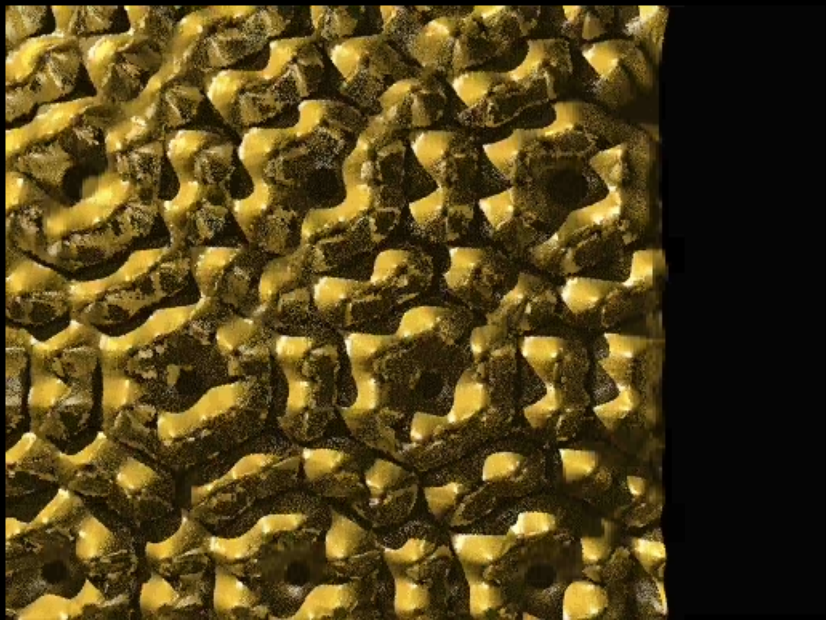

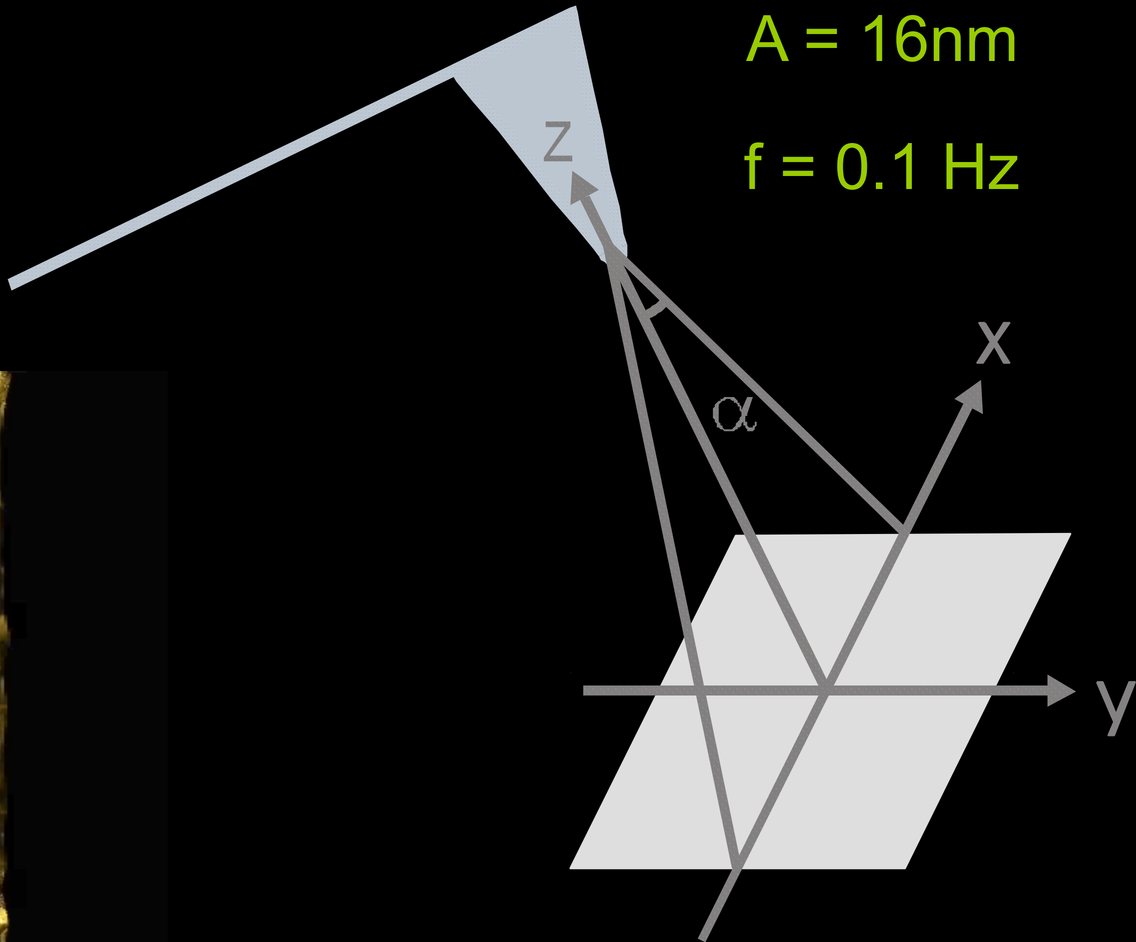

Short range interaction

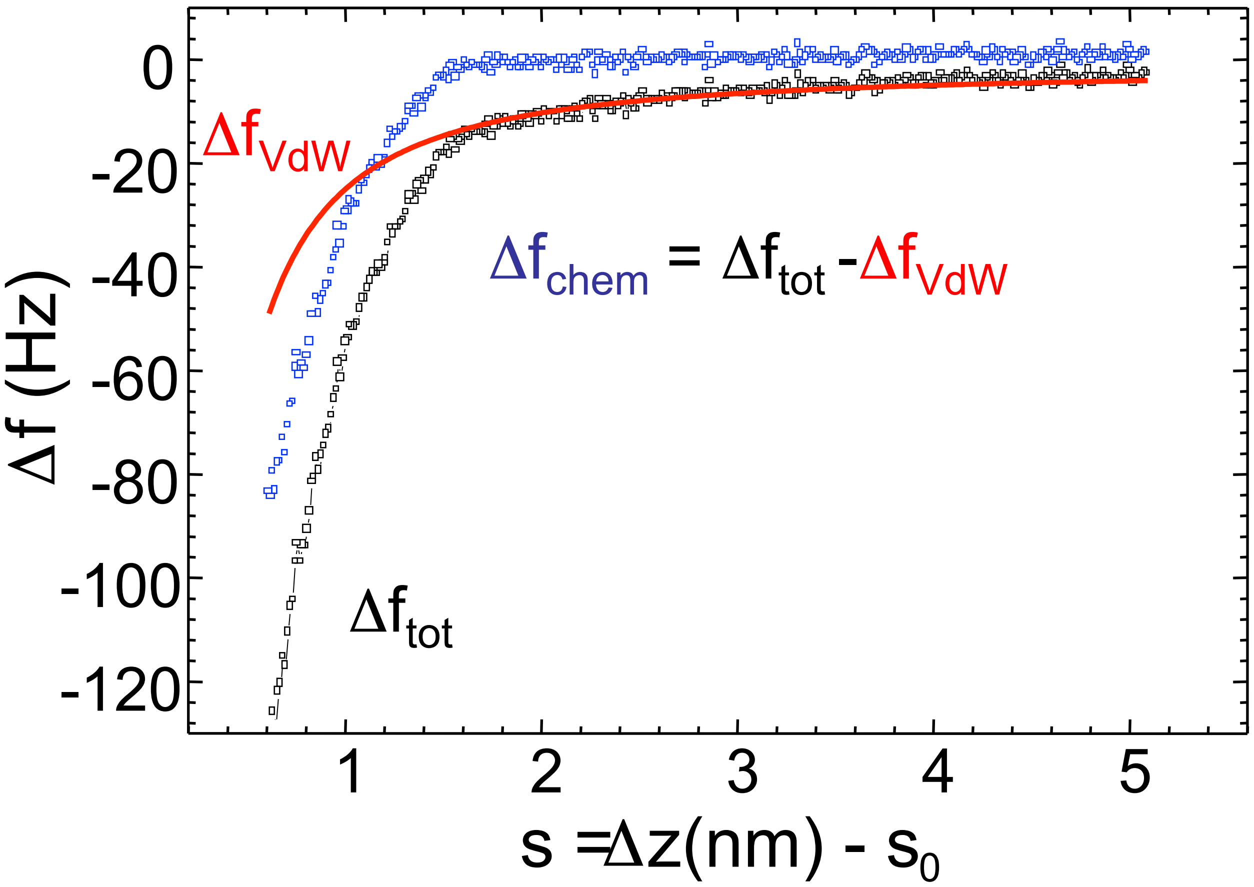

$$\Delta f_{chem} = \frac{f_0}{kA}\frac{U_0}{\sqrt{2\pi A\lambda}}e^{-\Delta z/\lambda}$$

λ = 0.35 nm

U_0 = -4.7 eV

s_0 = 0.45 nm

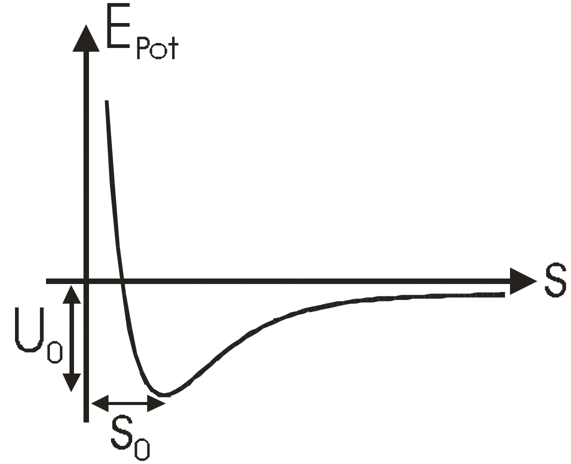

Carbon nanotubes as probing tips for nc-AFM

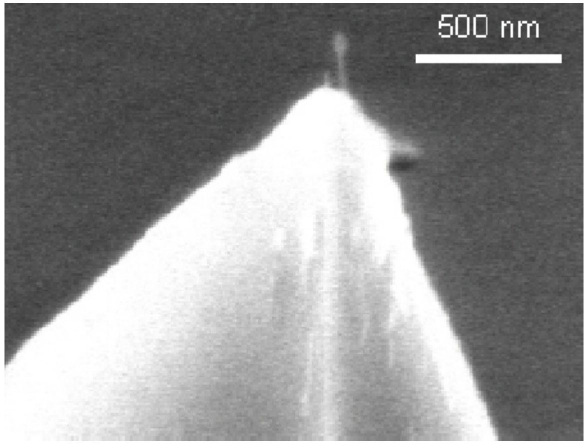

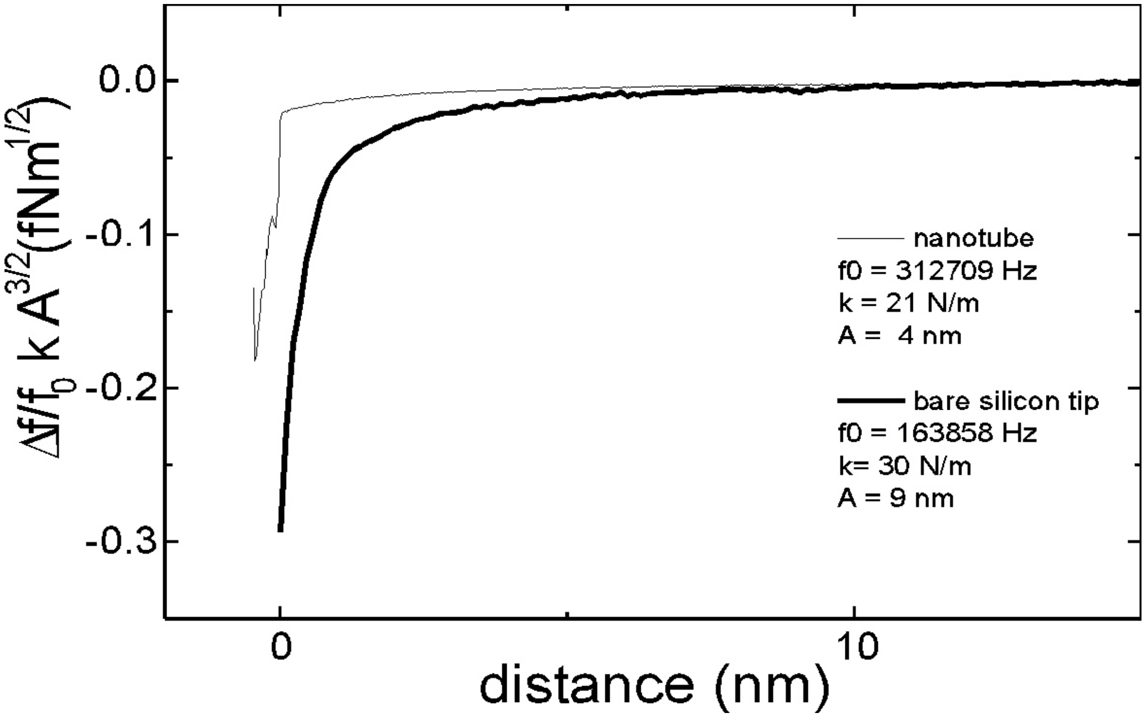

⇒ Long-range forces are reduced

True atomic resolution on NaCl(001)

(Insulator surface with point defects)

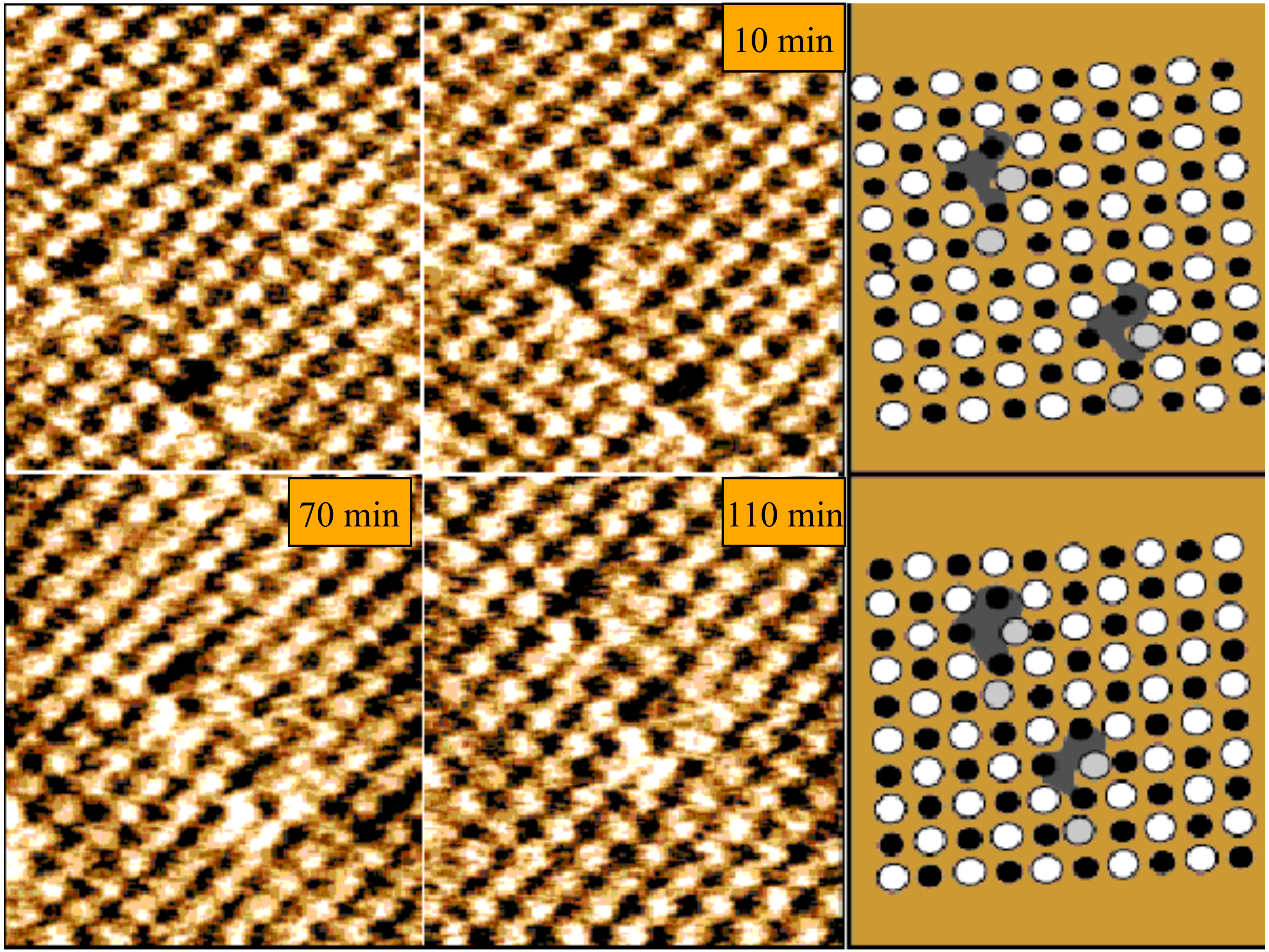

M. Bammerlin et al., *Probe Microscopy* **1**, 3 (1997)

True-atomic resolution at step edges of NaCl(001)-thin films on Cu(111)

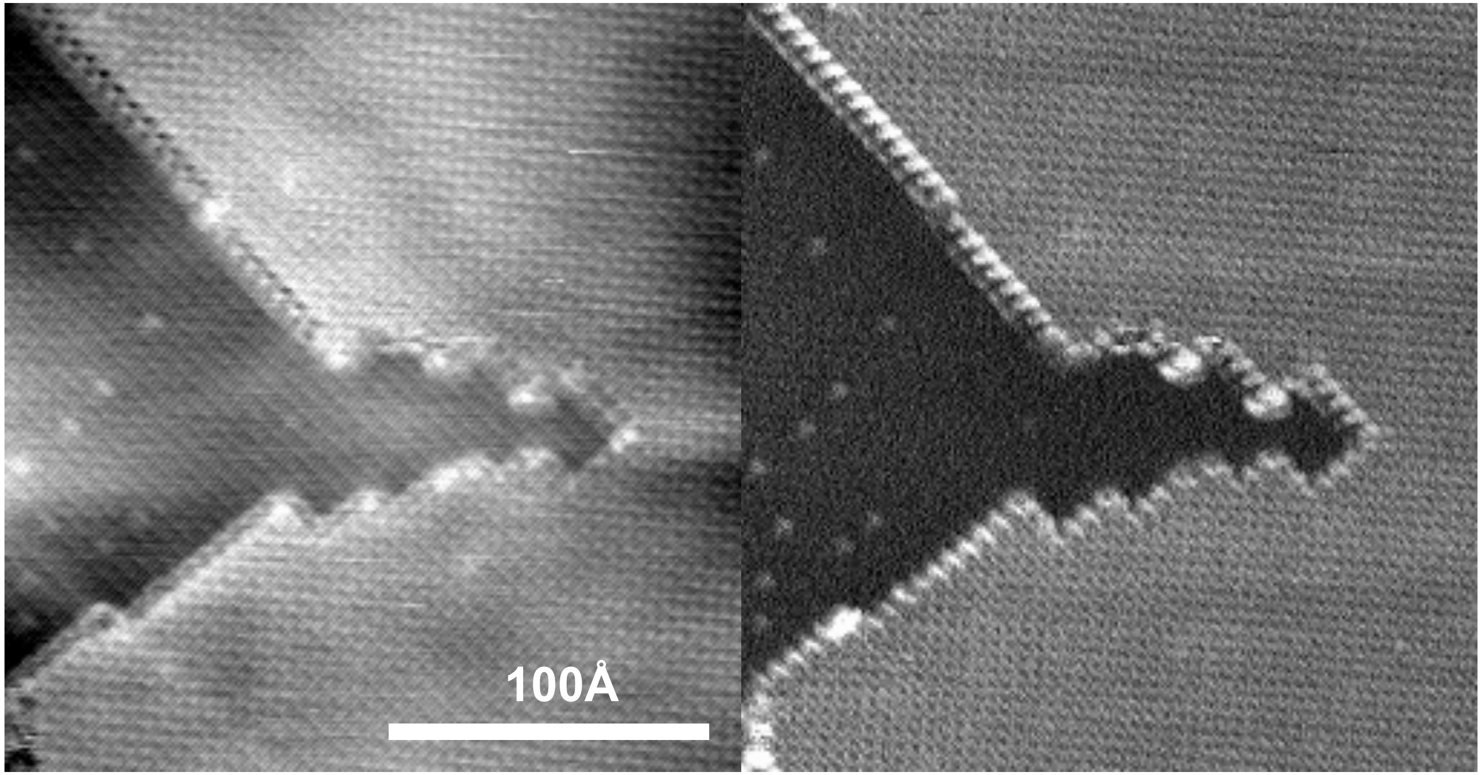

Topography　　　　Excitation Amplitude (A_{exc})

k=26N/m f_0=158.3kHz   A=0.7nm   Δf= -185Hz   (Δf/f)kA = -0.02nN

⇒ Step atoms and kink sites give different contrast

Theory of nc-AFM on Ionic Surfaces

$\gamma \approx 35°$
R ≈ 10nm

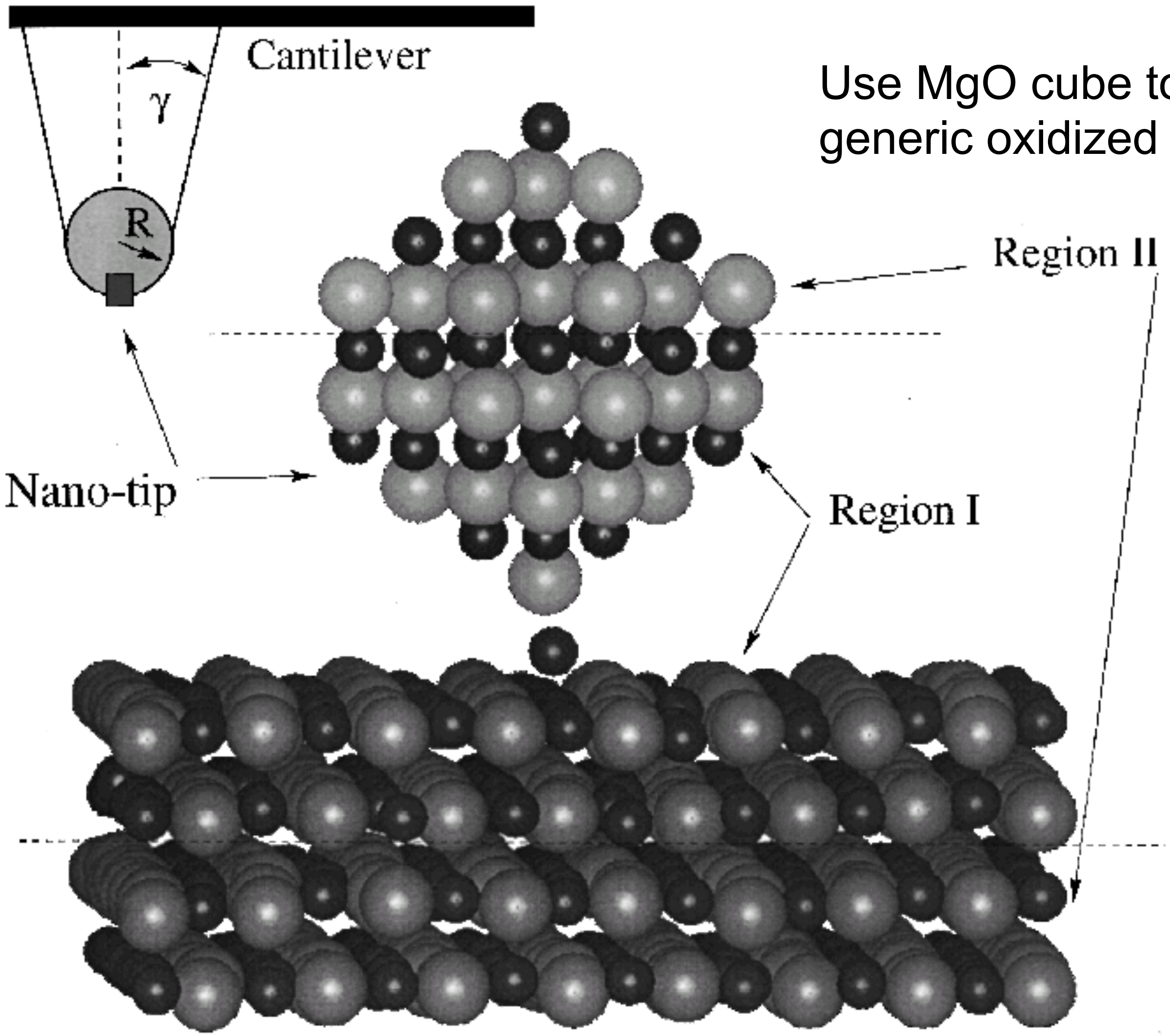

Use MgO cube to represent generic oxidized nano-tip

R. Bennewitz et al., Phys. Rev. B 62 (2000) 2074

Molecular nanowires on KBr

Topography Damping

100 nm

24 nm

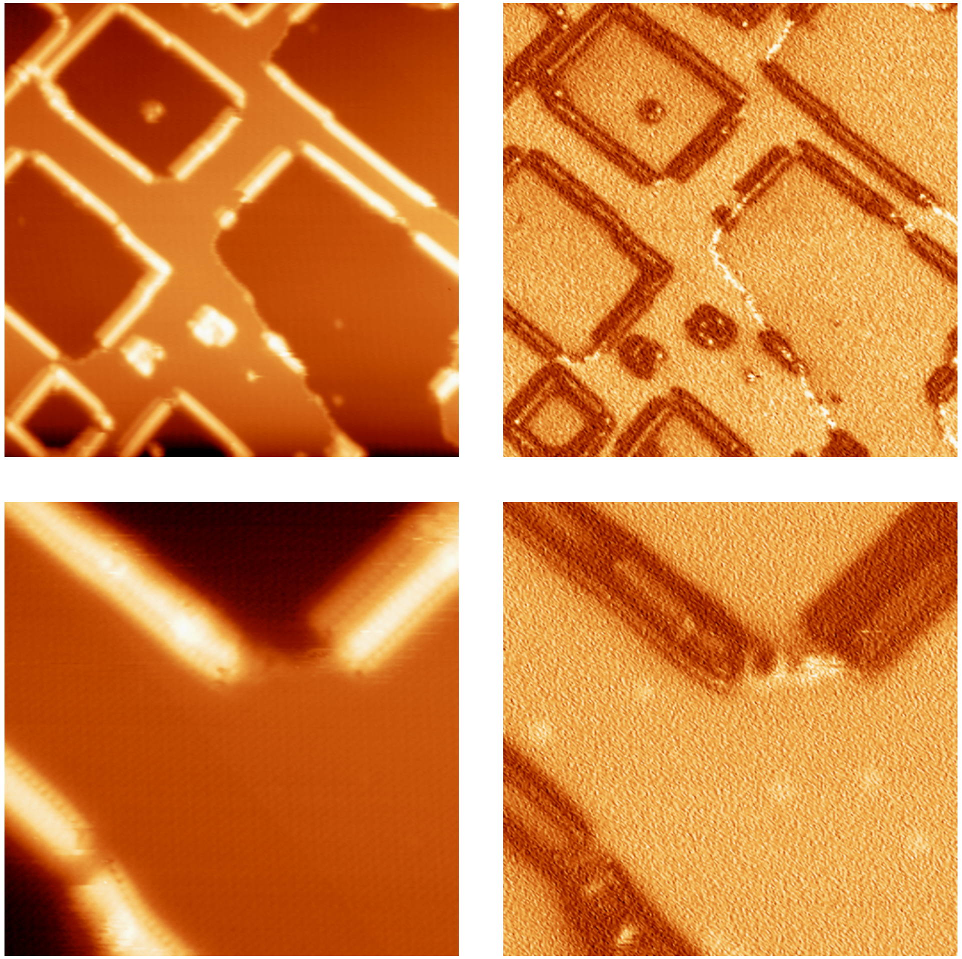

- “Asymmetric” porphyrins on KBr with pits
- Straight edges are decorated
- Image height approx 1nm, Single molecules ?

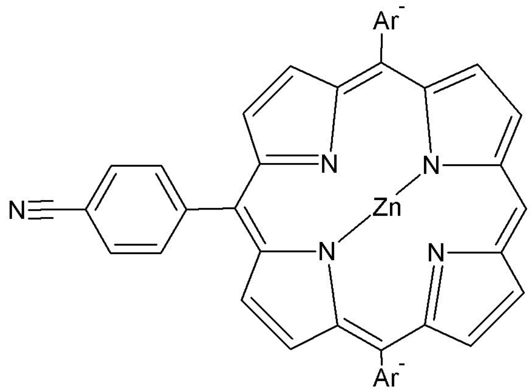

Nano-Switzerland

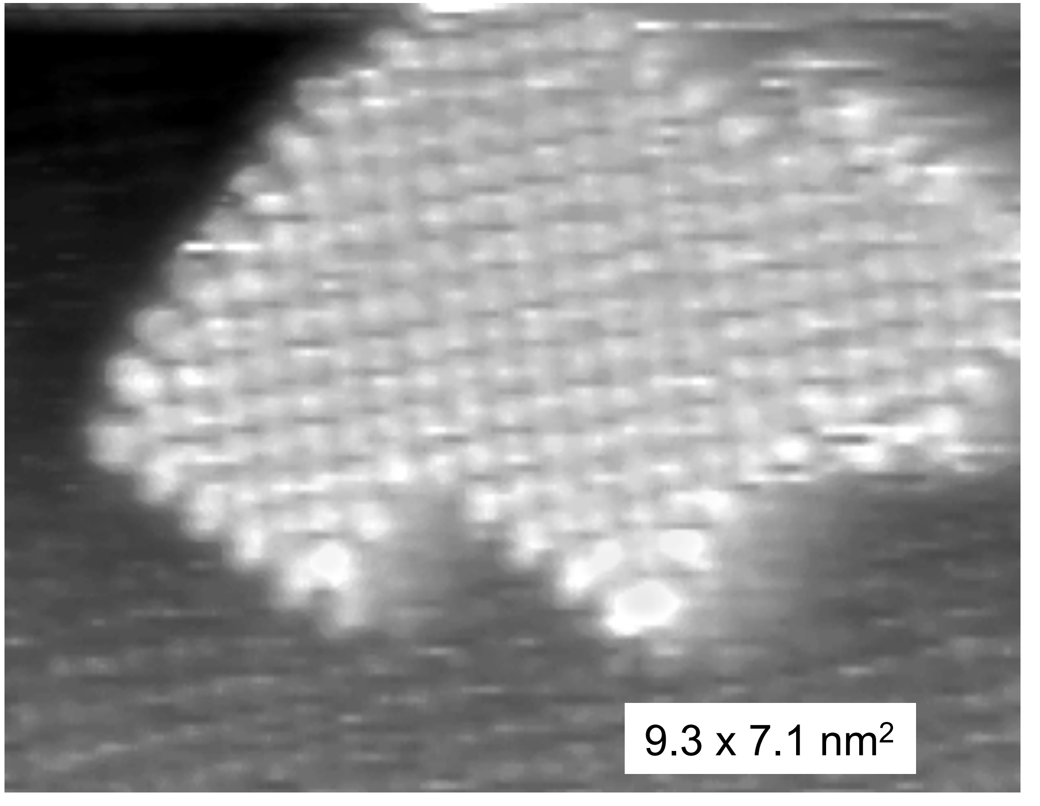

NaCl-Islands consisting of 120 atoms

Pendulum geometry

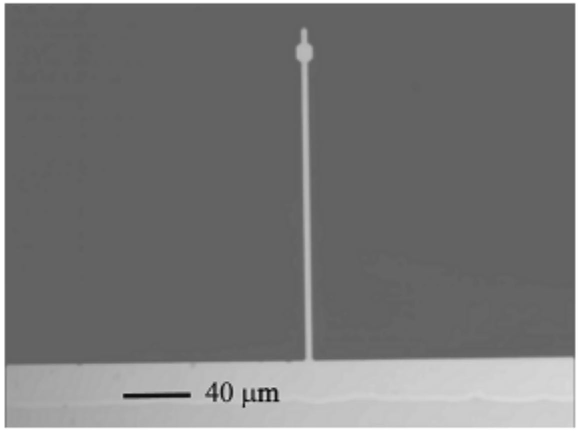

k≈mN/m
No snap in to contact!

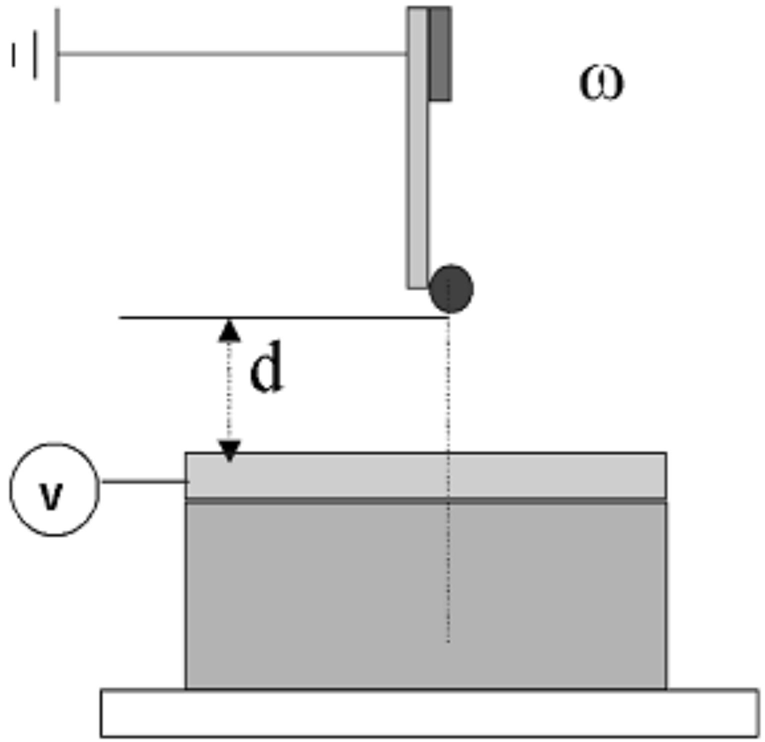

Magnetic Resonance Force Microscopy: Detection of single electron spins vertically mounted cantilevers (pendulum)

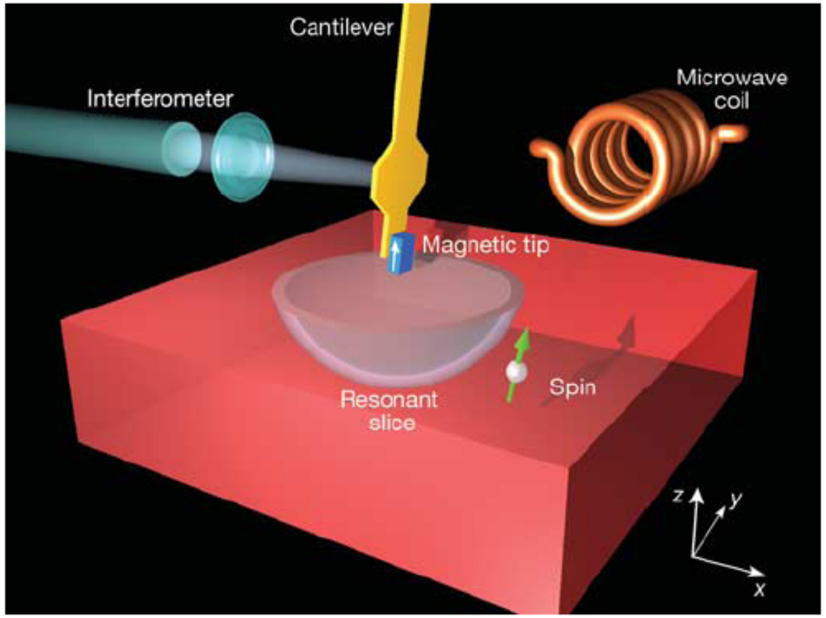

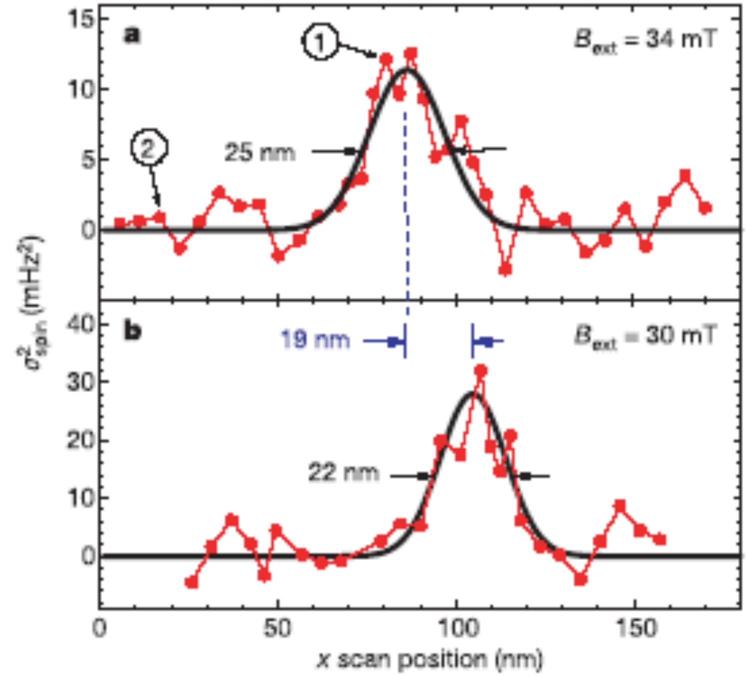

D. Rugar et al., Nature 430, 329 (2004)

Atomare Reibung
und Kontrolle von Reibung

How to understand atomic friction?
Can we avoid atomic friction?
Can we control friction?

Friction on the Nanometer-scale: Atomic-Stick Slip

Atomic stick-slip

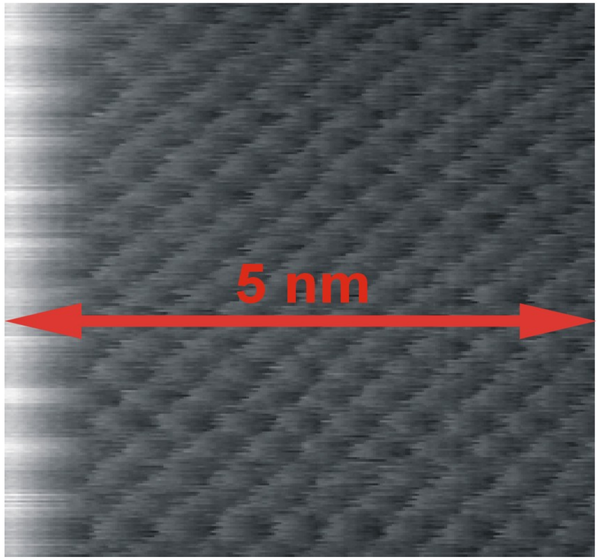

KBr(001)-crystal

Friction loop

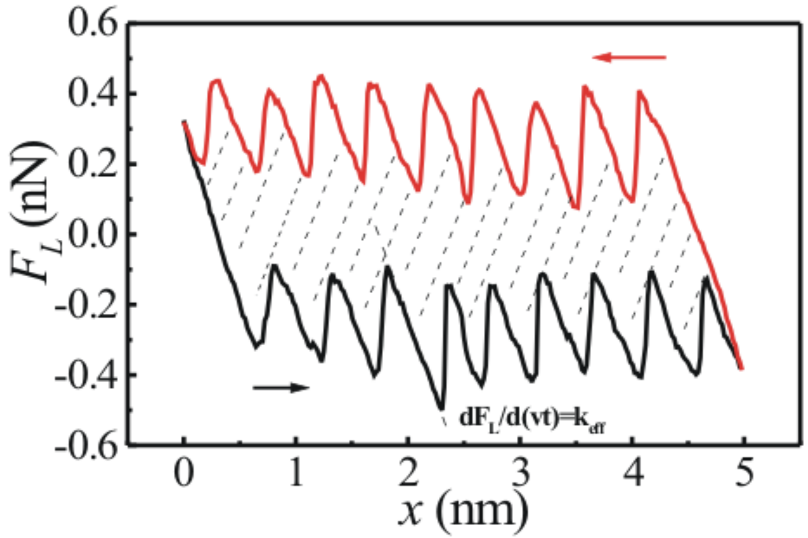

F_N = 0.44 nN

E_{diss} = 1.4 eV (per slip)

Velocity dependence of atomic friction

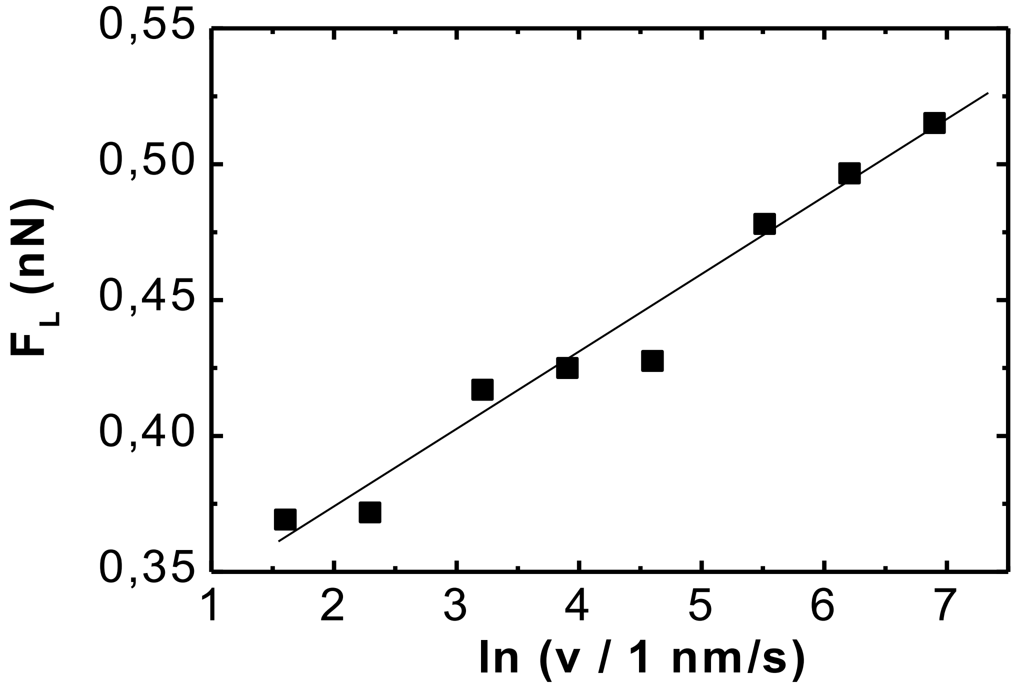

- Friction increases with the logarithm of velocity
- The slope of the curve increases with the applied load

E. Gnecco et al., *Phys. Rev. Lett.*, **84**, 1172 (2000)

Interpretation of velocity dependence

Tomlinson model:

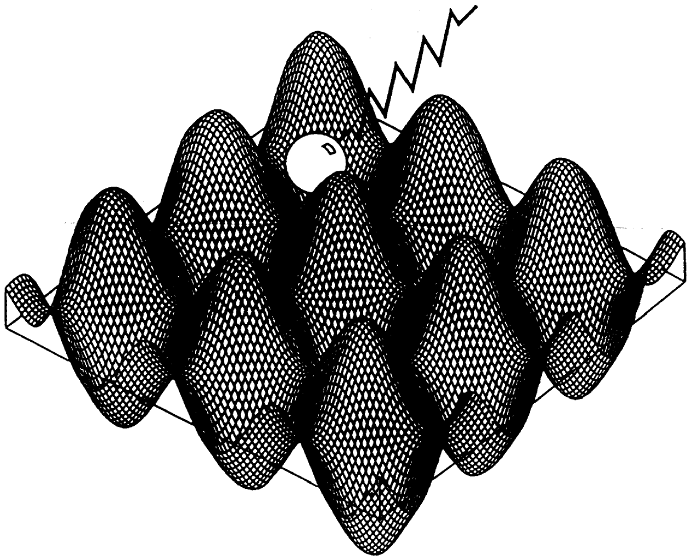

thermal activation:

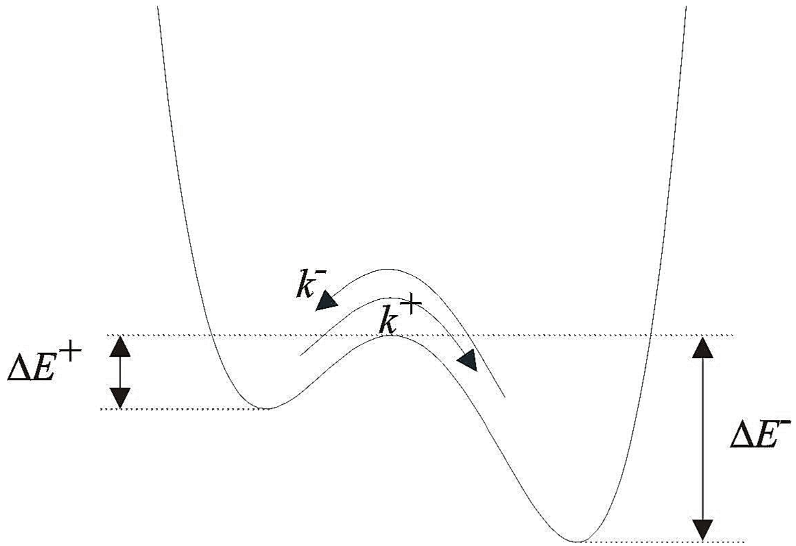

$$\rightarrow \quad F_L(v) = F_L + \frac{k_B T}{\lambda} \ln \frac{v}{v_1}$$

Transition to Ultralow Friction on NaCl(001)
UHV FFM with sharp tip vs. Prandtl-Tomlinson model

k_x = 29 N/m, k_z = 0.05 N/m, v_x = 3 nm/s, const. z
Scans along [100] showing maximum variation

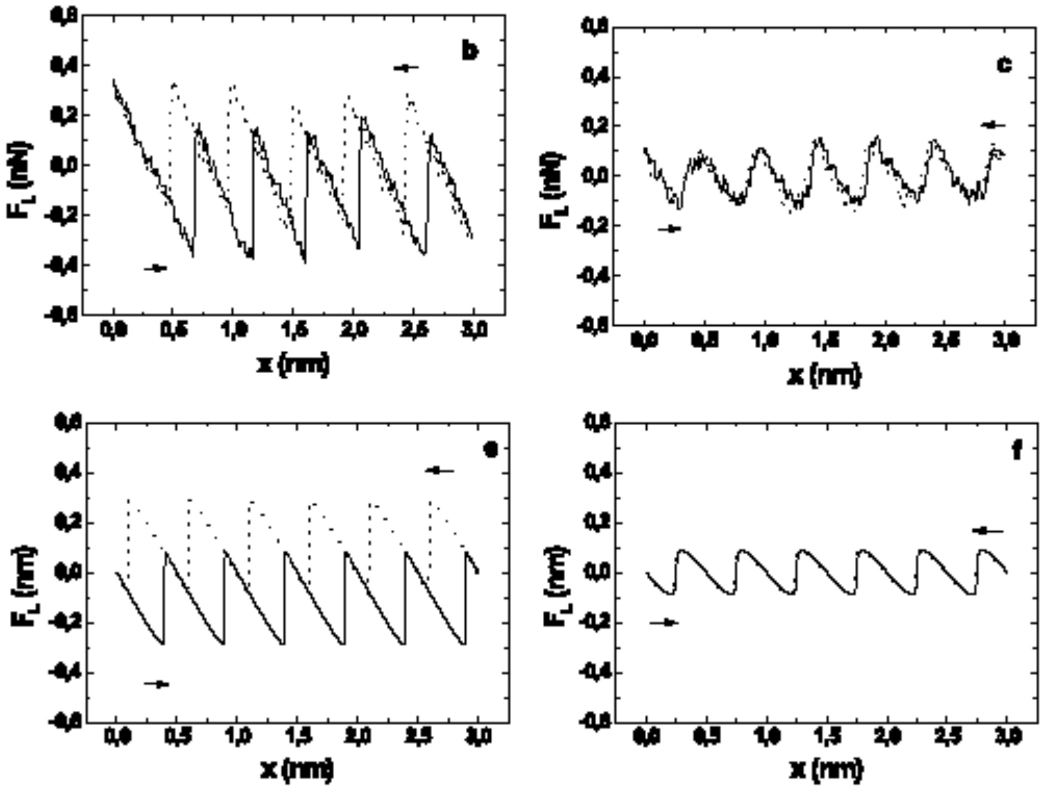

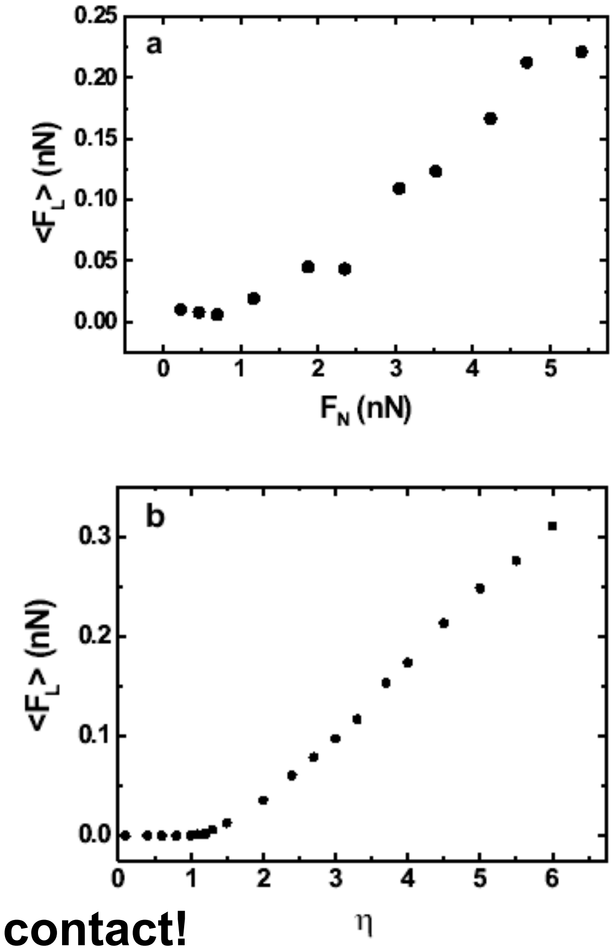

Stick-slip **Continuous sliding in contact!**

$\eta > 1$ **$\eta < 1$** **mean load $F_N = F_z + 0.7$ nN**

A. Socoliuc et al., *Phys. Rev. Lett.* **92**, 134301 (2004)

1d-Prandtl-Tomlinson-Model

Potential energy:

$$U = -\frac{E_0}{2}\cos\left(2\pi\frac{x_t}{a}\right) + \frac{1}{2}k(x_t - x_s)^2$$

Stability criterion:

$$\frac{\partial U^2}{\partial x_t{}^2} = \frac{2\pi^2}{a^2}E_0\cos\left(2\pi\frac{x_t}{a}\right) + k > 0$$

$$\eta = \frac{2\pi^2 E_0}{ka^2} = \pi^2\frac{E_0}{ka^2/2}$$

η < 1: unique sliding solution
η > 1: instabilities

η > 1

η = 3

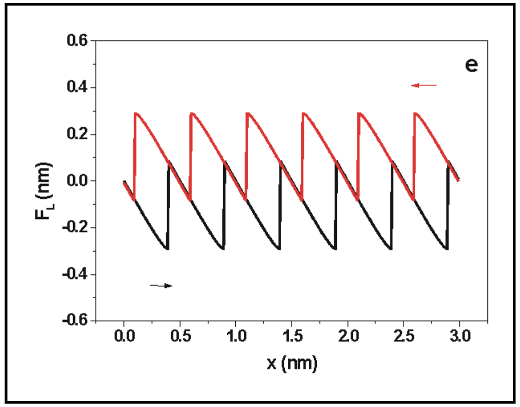

η < 1

η = 1

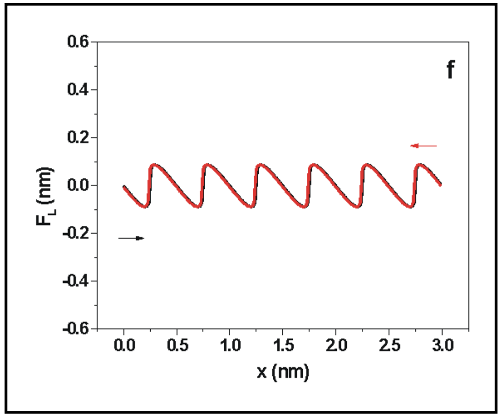

Instability Criterium

1d: Effective spring constant equals 2nd derivative of adiabatic potential between tip and sample

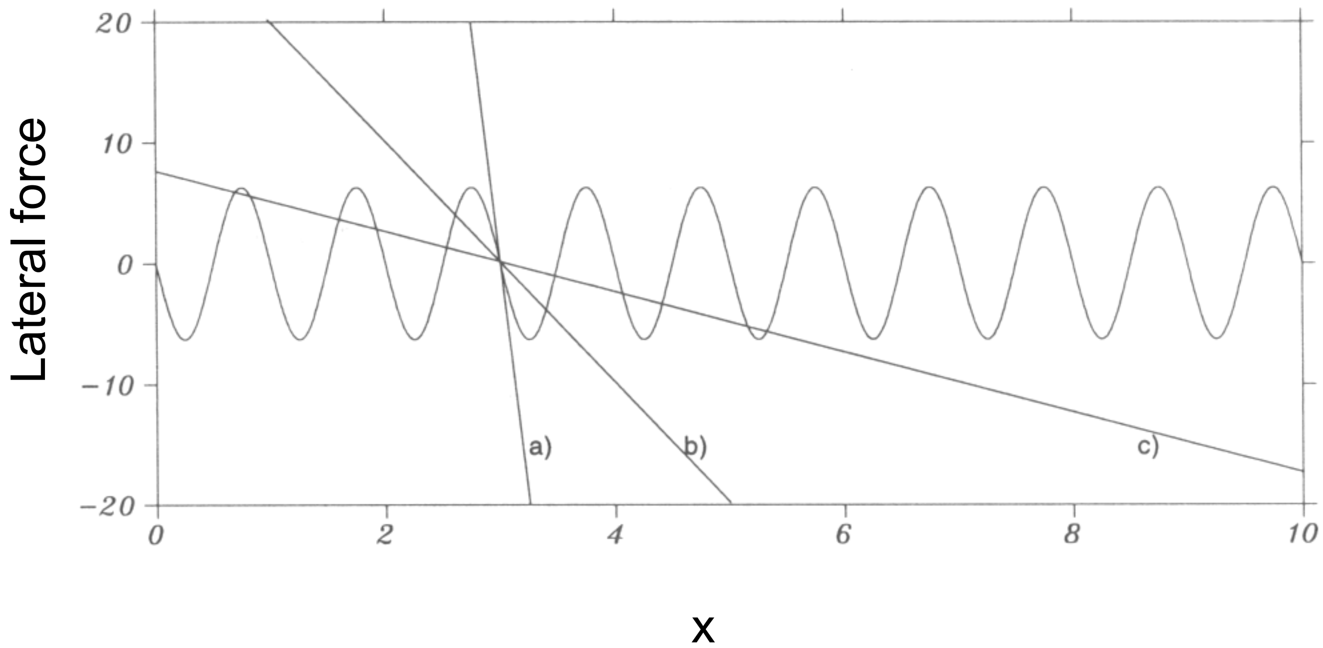

Dependence of Tomlinson Parameters

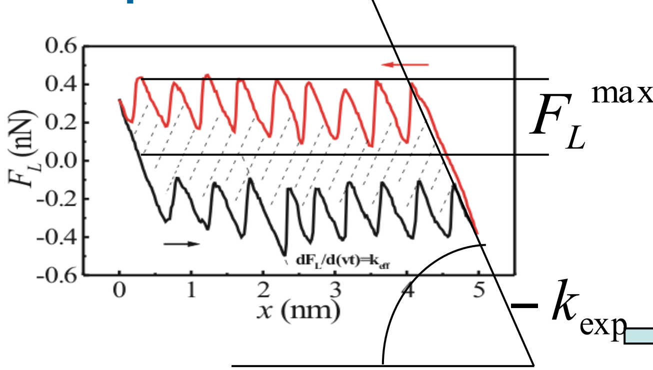

$$E_0 = \frac{aF_L^{max}}{\pi}$$

$$\eta = \frac{2\pi F_L^{max}}{k_{exp}a} - 1$$

$$k = \frac{\eta + 1}{\eta} k_{exp}$$

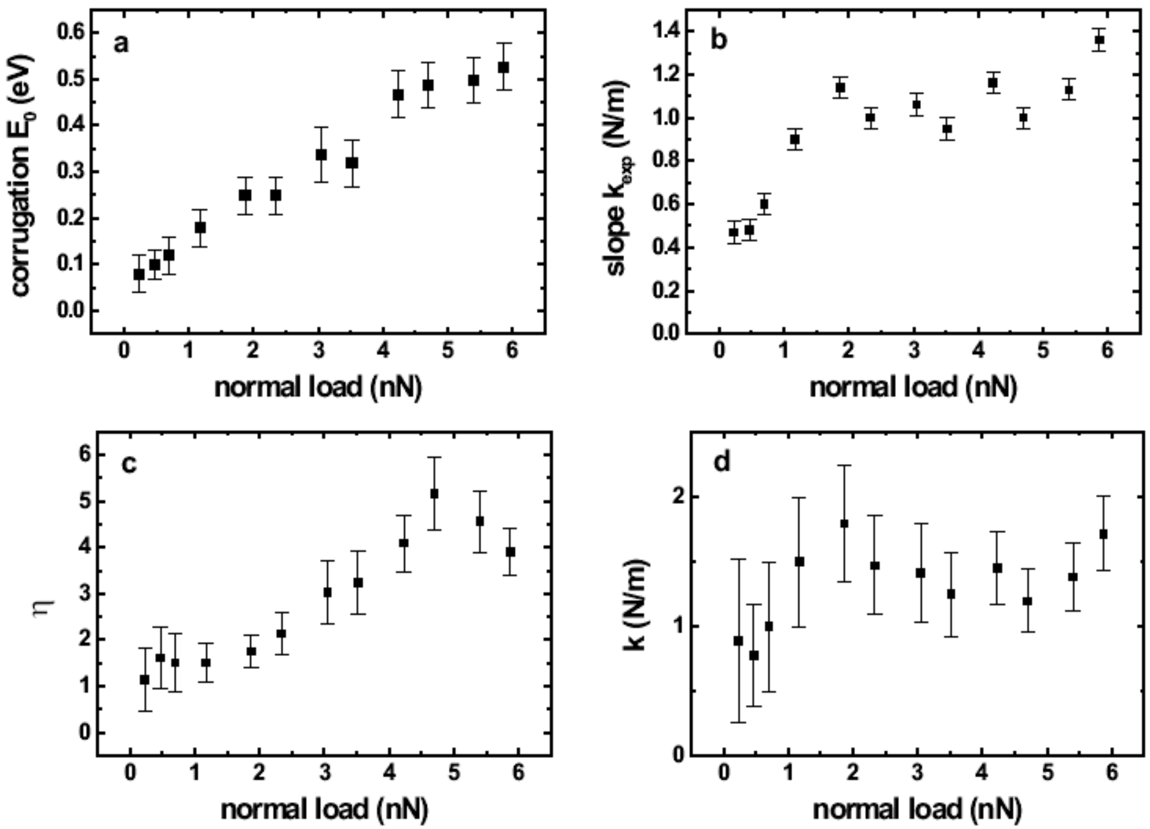

E_0: linear increase with normal forces

k: rather independent (contact area const.?)

Lateral contact stiffness

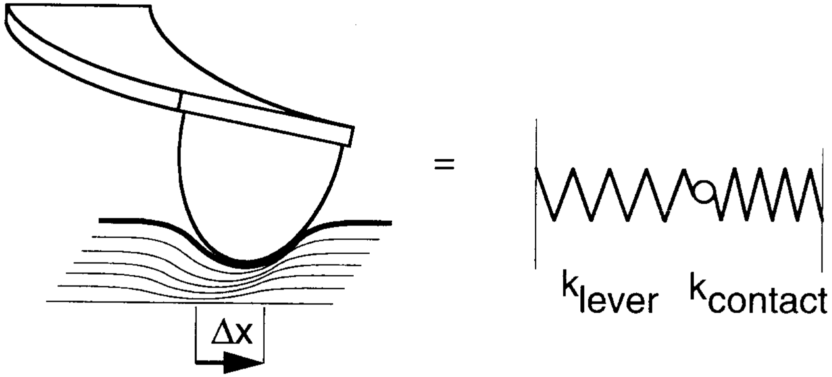

$$\frac{1}{k} = \frac{1}{k_{lever}} + \frac{1}{k_{tip}} + \frac{1}{k_{contact}}$$

R. Carpick et al, Appl. Phys. Lett. 70, 1548-1550 (1997)

Here: k_{lever}=29N/m » k $\Rightarrow$ $k_{contact} \approx$ 1-2N/m

Continuum model :

$k_{contact}$= 8 a G $\Rightarrow$ a < 1Å ?

$\Rightarrow$ Atomistic model needed

Simulations: KBr cluster tips against KBr(001)
10x10x6 slab (fixed boundaries), SciFi code (L.N. Kantorovich et al.)
Buckhingham short-range + shell model Coulomb pair potentials

U. Wyder, A. Baratoff, E. Gnecco, T. Trevethan and L. N. Kantorovich

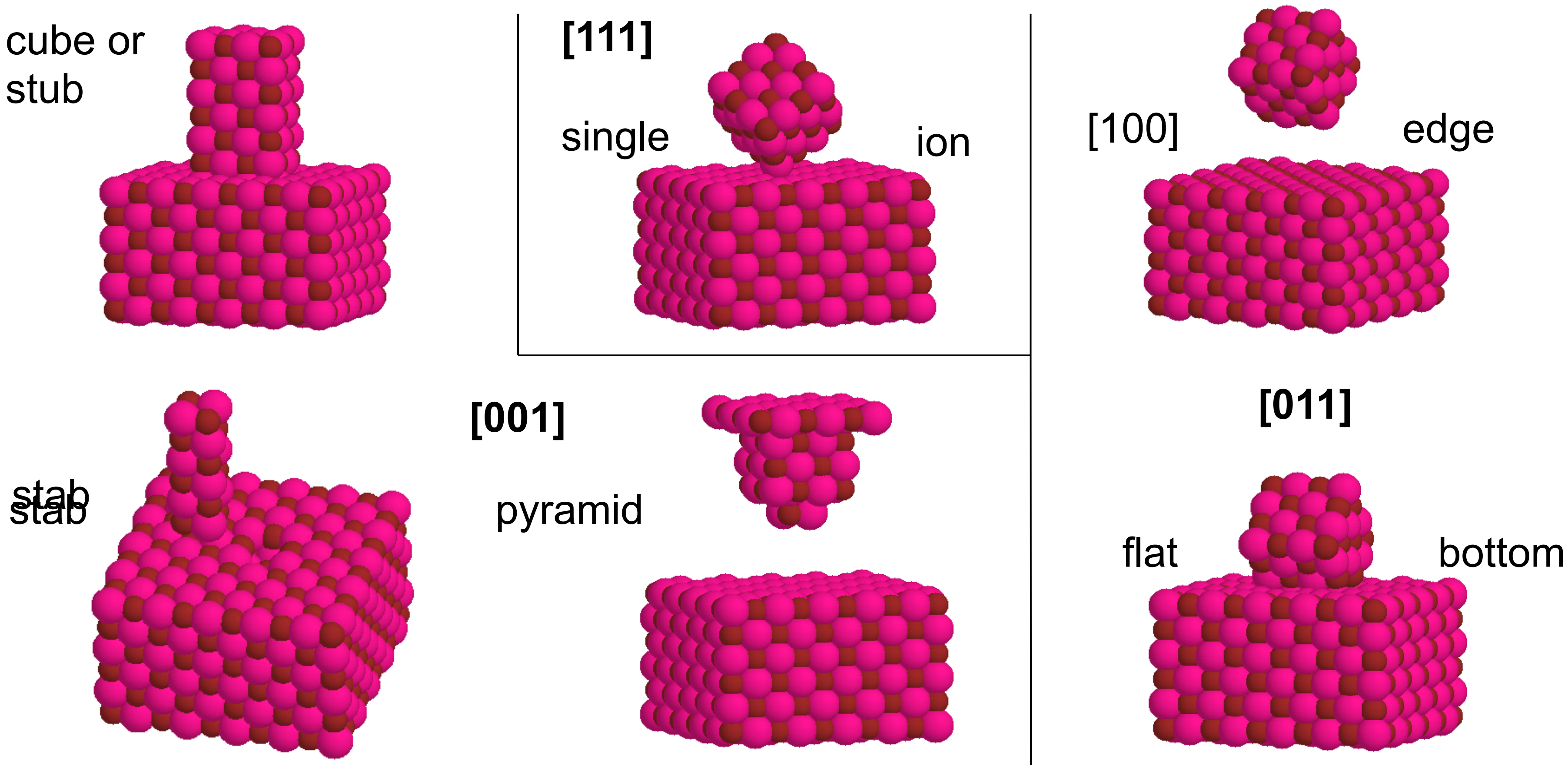

Tip top layer(s) frozen; **<100> scans at constant z (corrugation unaffected** by **van der Waals attraction** which, together with **soft cantilever k_z** causes **jump to/from contact in experiment**

Atomistic Simulation of the Tip-Sample Interaction

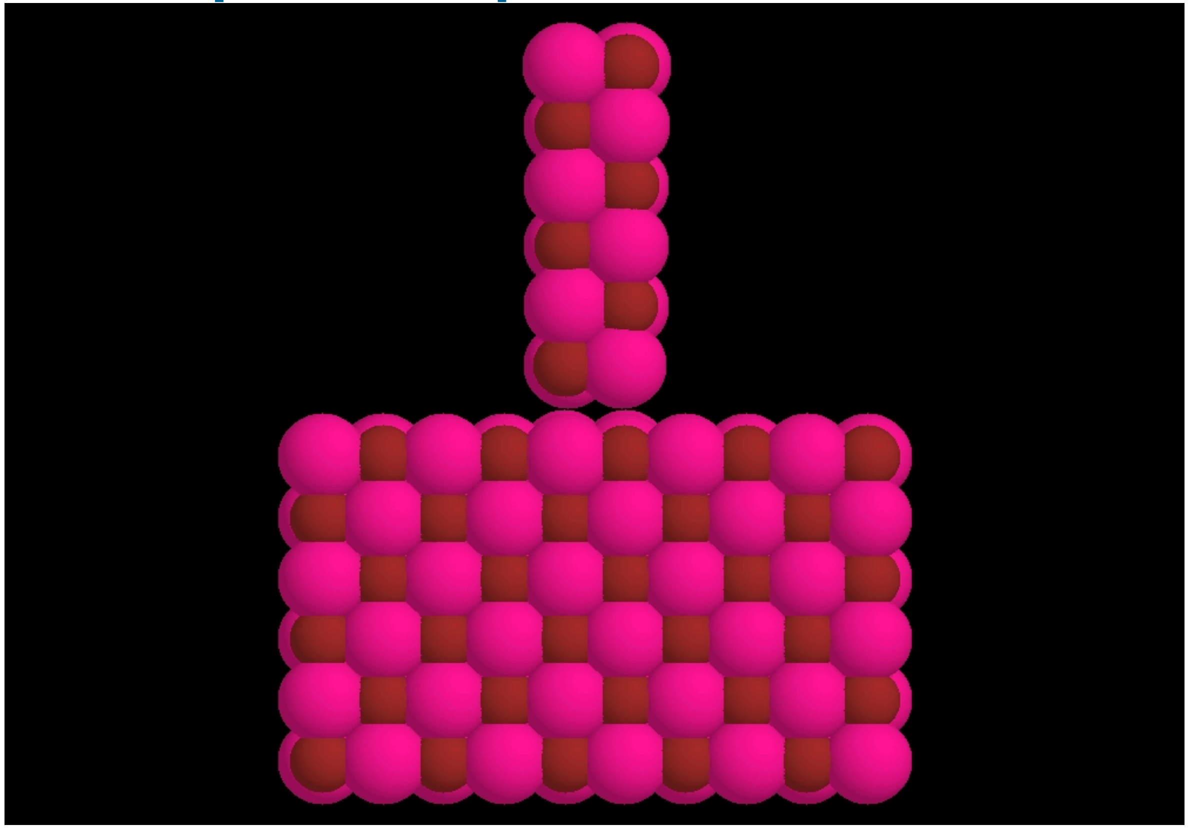

Quasi-static atomistic simulation using pair potentials

L. Kantorovich, T. Trevethan, King's College London

U. Wyder, A. Baratoff, University Basel

[111] K-terminated Tip

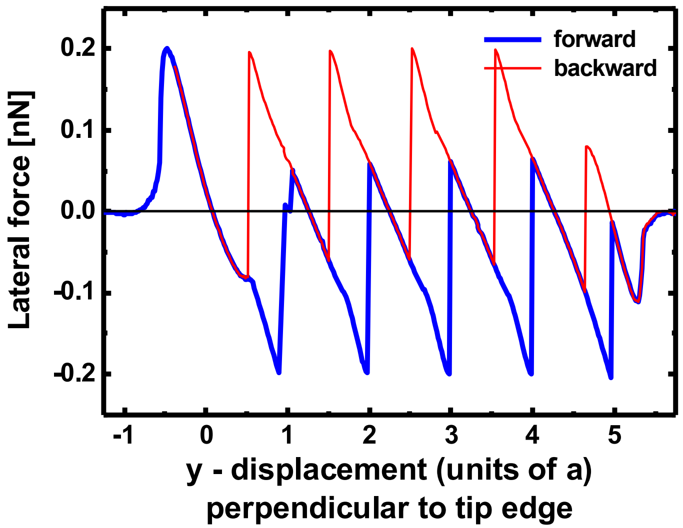

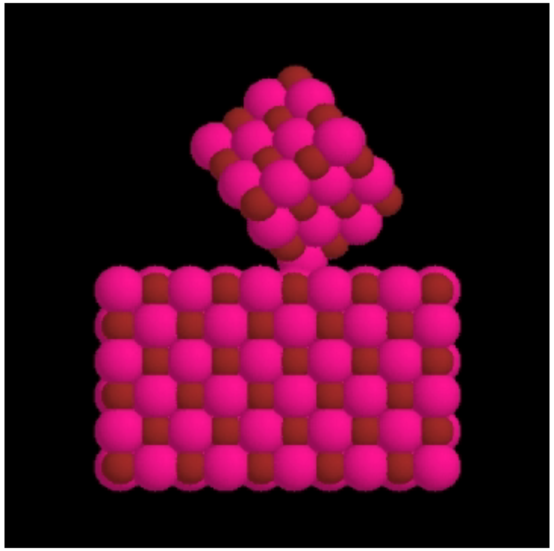

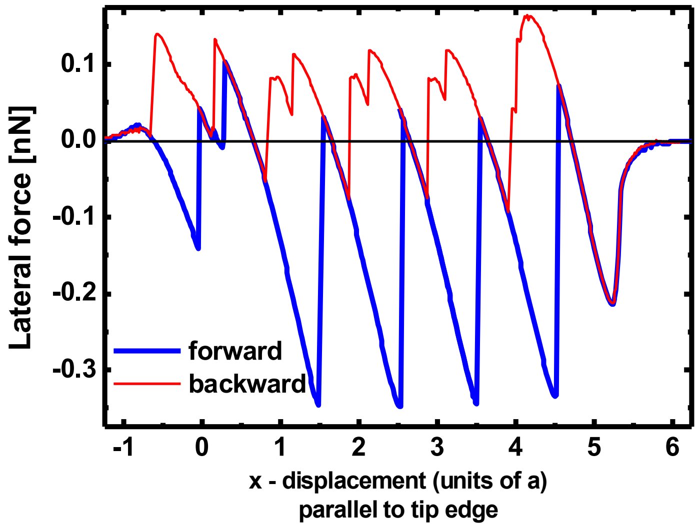

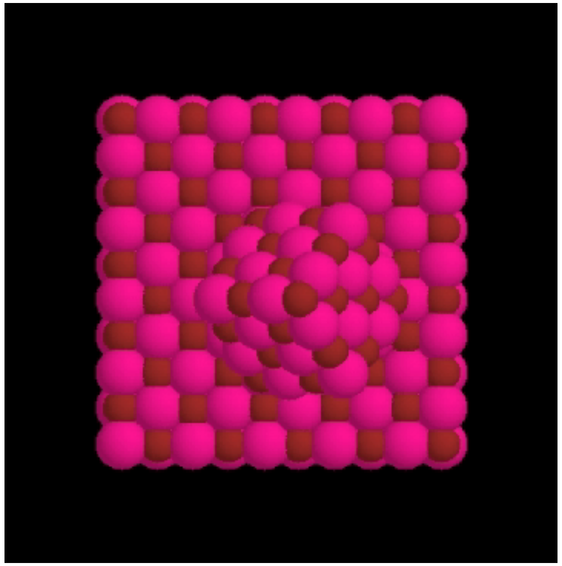

Can we switch friction on and off?

AC voltages were applied across thin KBr and NaCl crystals:

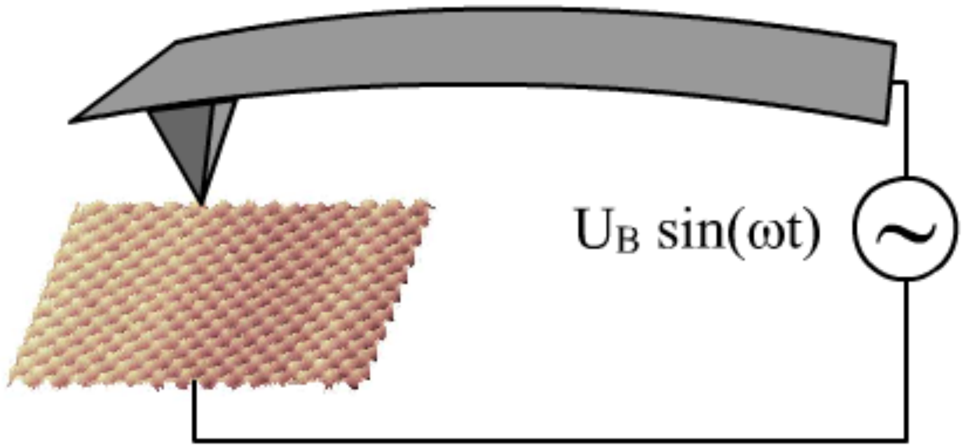

- Capacitive interaction between lever and sample holder $\propto U_B^2$
- Coulomb interaction $\propto U_B$

Controlling Friction: Actuation of Nanometer-Sized Contacts

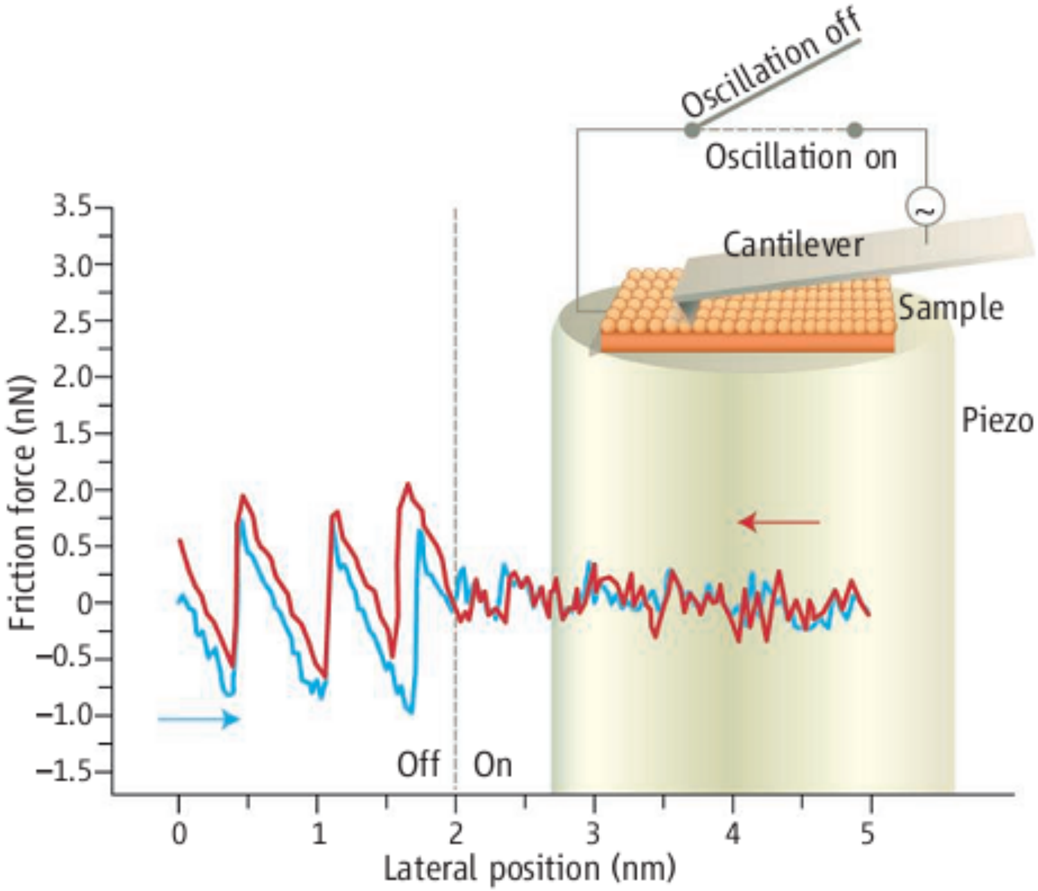

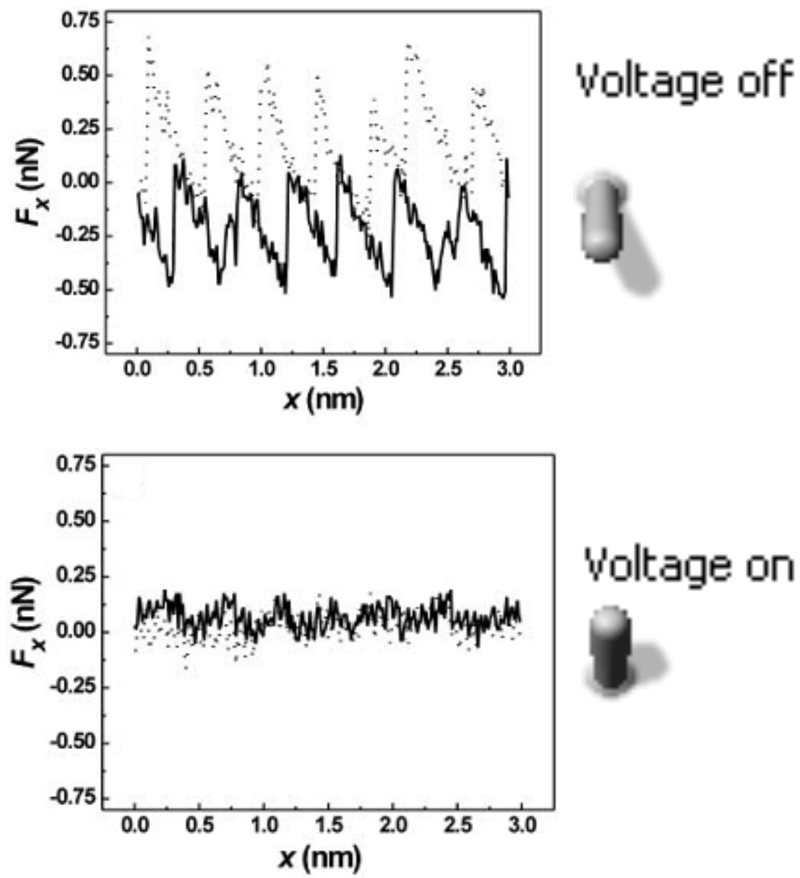

A. Socoliuc, E. Gnecco, S. Maier, O. Pfeiffer, A. Baratoff, R. Bennewitz, E. Meyer, *Science* **313**, 207 (2006)

Frequency dependence of friction

Friction:

Thermal noise:

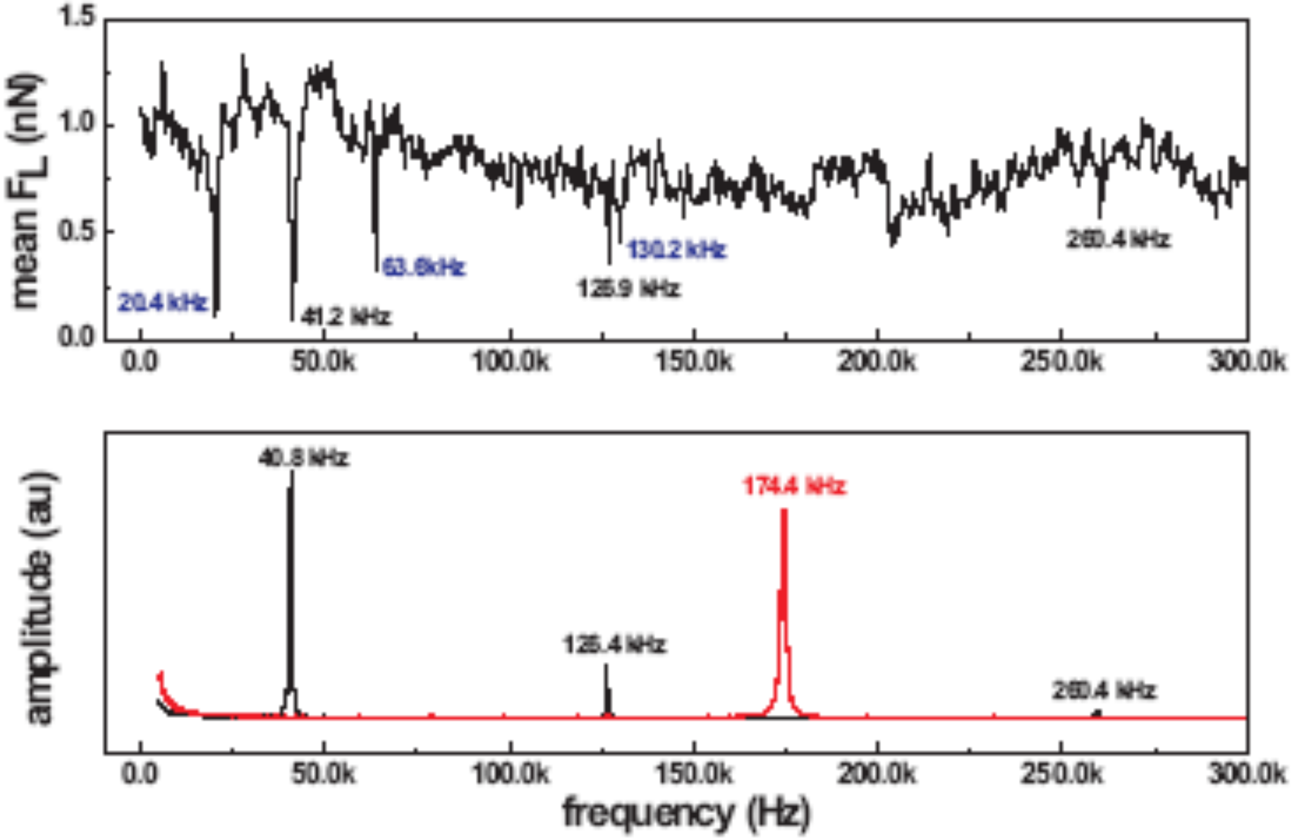

- Friction is “switched off” only if $f_{exc} = f_{norm}$ or (1/2) f_{norm}
- No effect when $f_{exc} = f_{tors}$!

Frequency dependence of friction

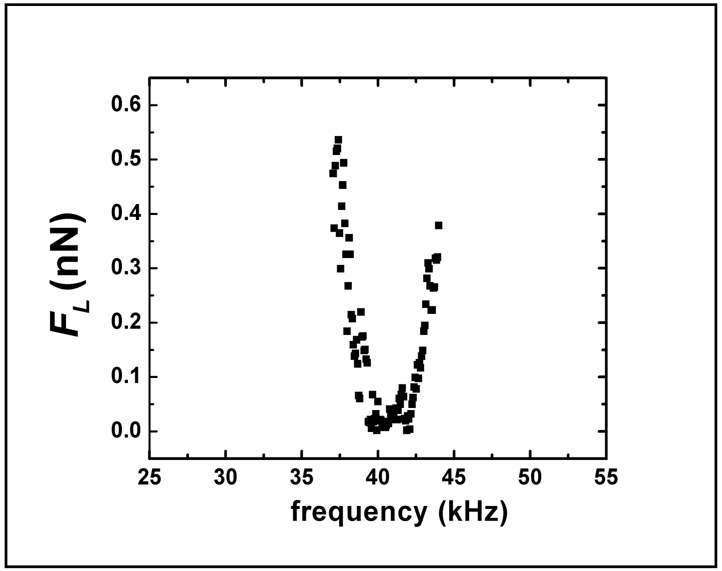

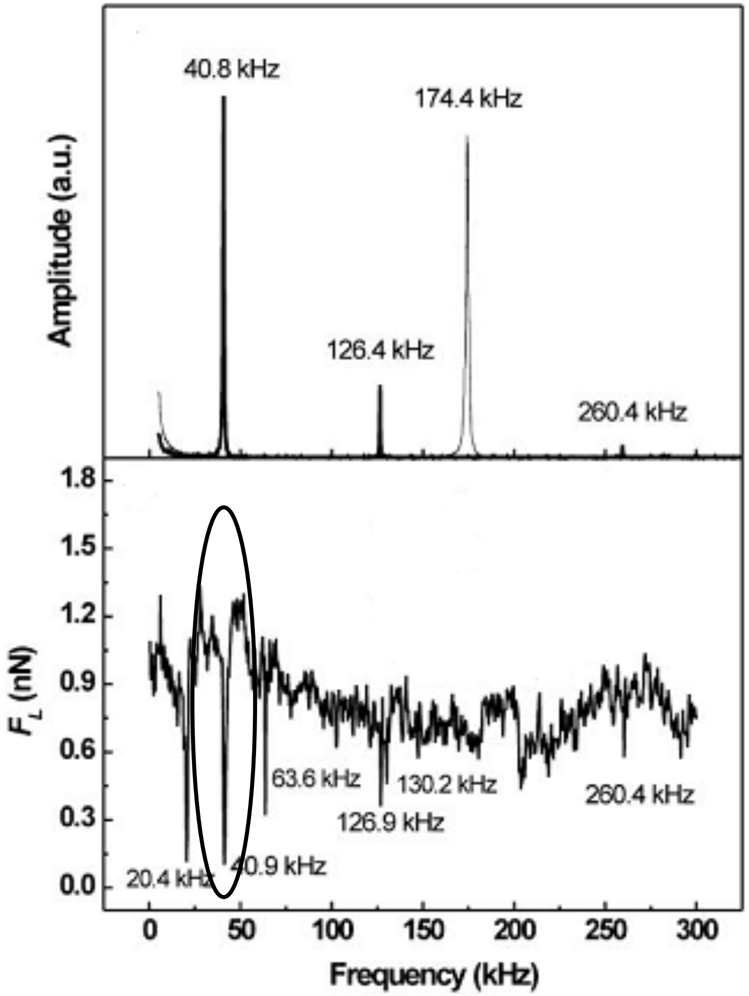

Reduction of friction at and resonance
Frequencies of the the bending modes f and f/2

Voltage dependence of friction

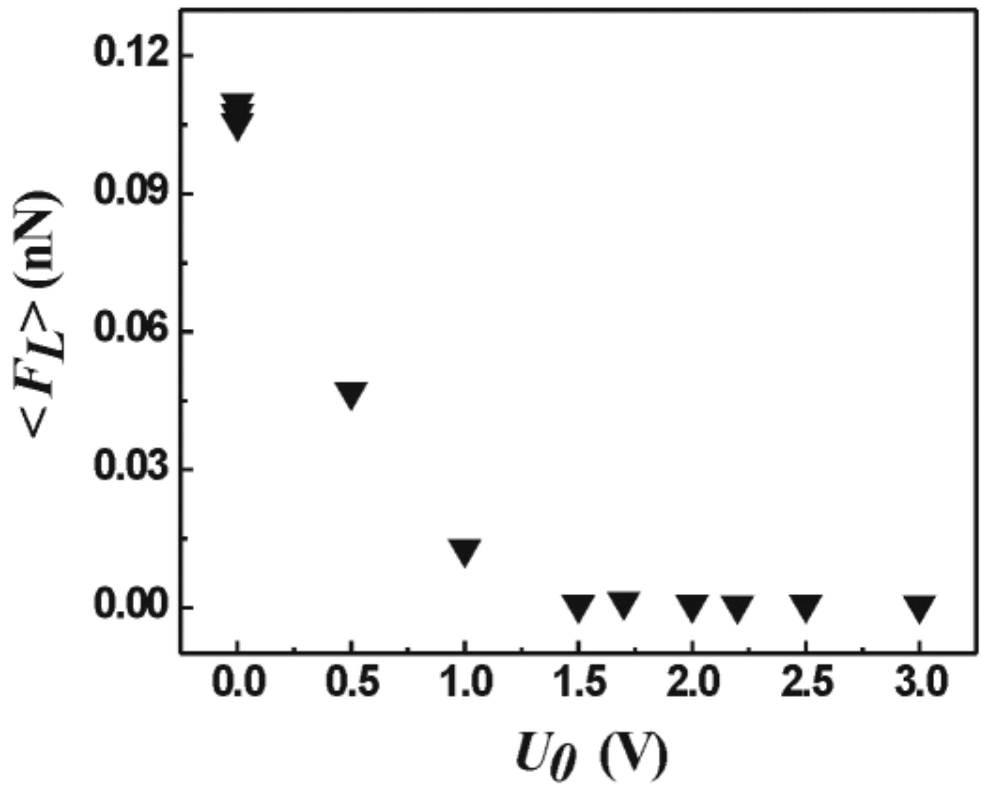

- Friction goes down to zero increasing the excitation amplitude !

Interpretation of Dynamic Superlubricity

- In the Tomlinson model: We replace E_0 with $\boxed{E_0\,(1+\alpha \cos \omega t)}$
- The parameter α increases with the applied voltage

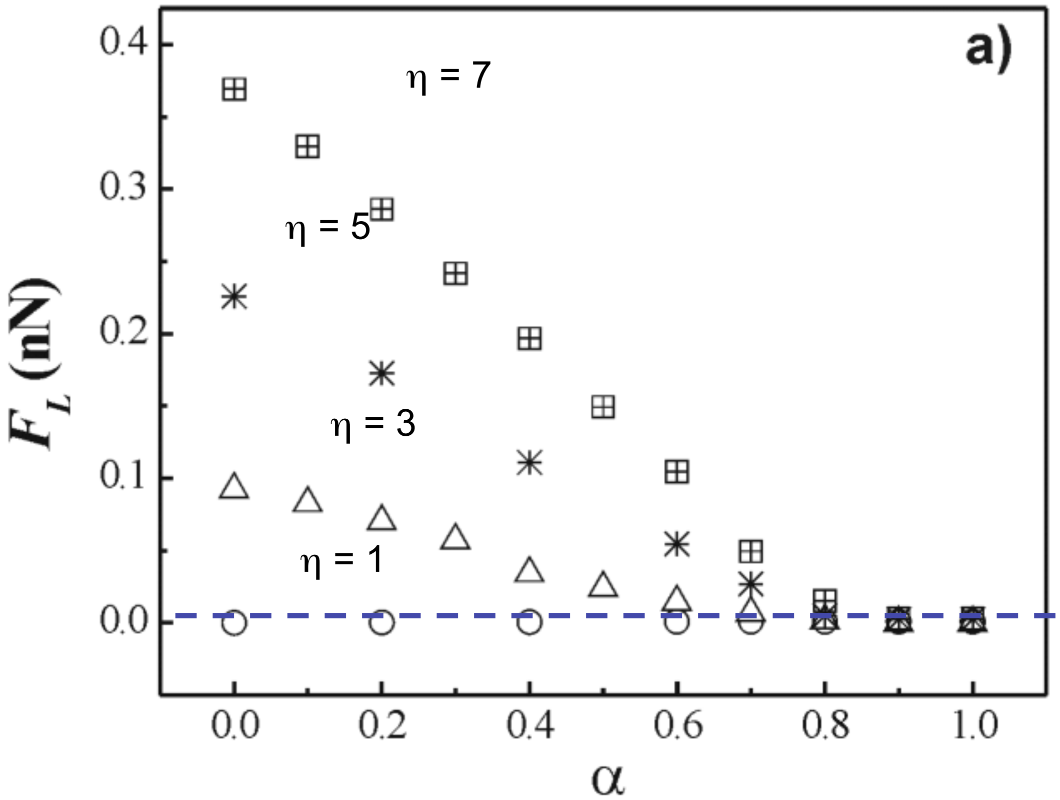

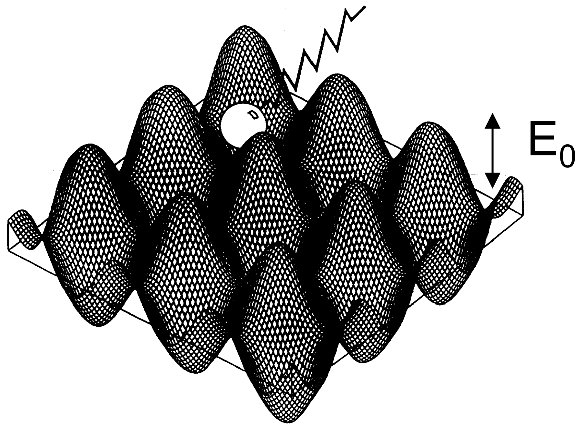

Friction decreases when $\alpha \to 1$

New parameter η_{min}

- The parameter $\boxed{\eta_{min} = \eta\,(1-\alpha)}$ determines superlubricity

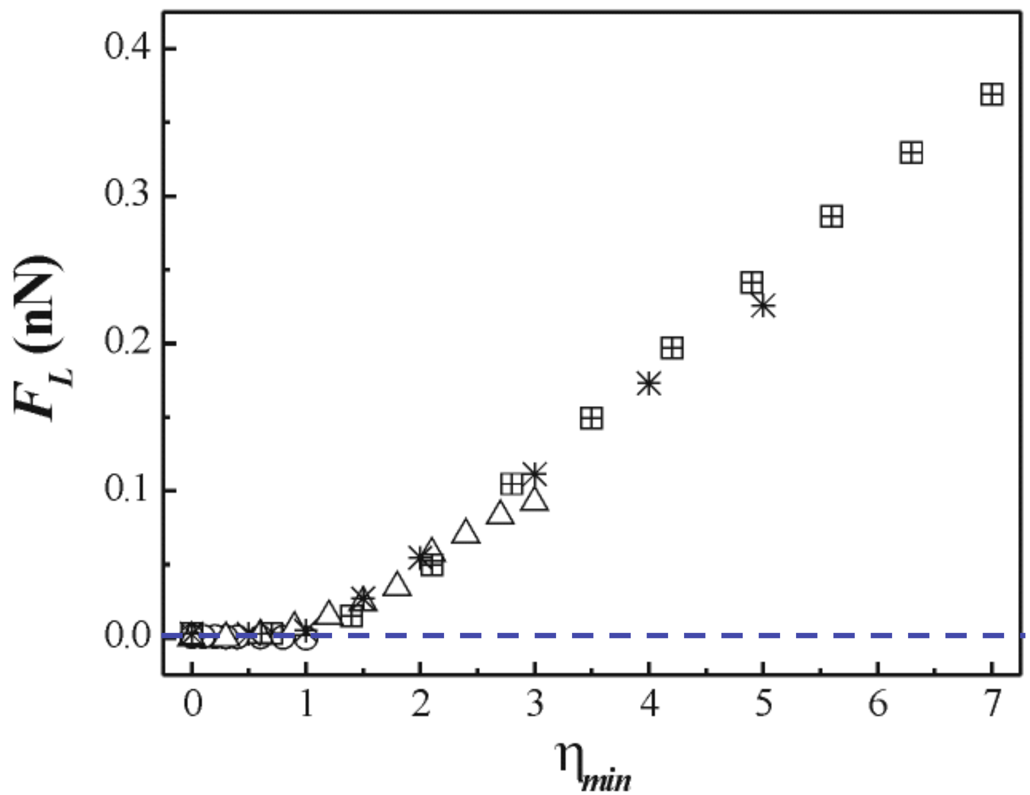

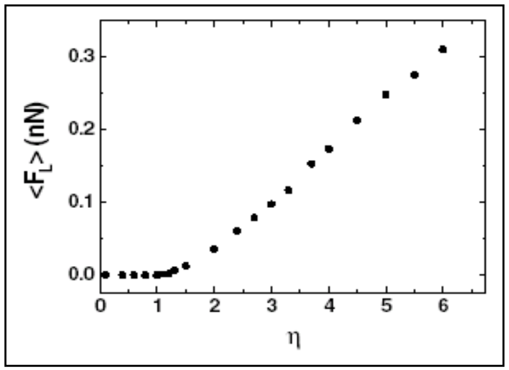

“Static” case

„Phase“ diagram of friction

• A "**phase diagram**" in the η-α plane can be drawn:

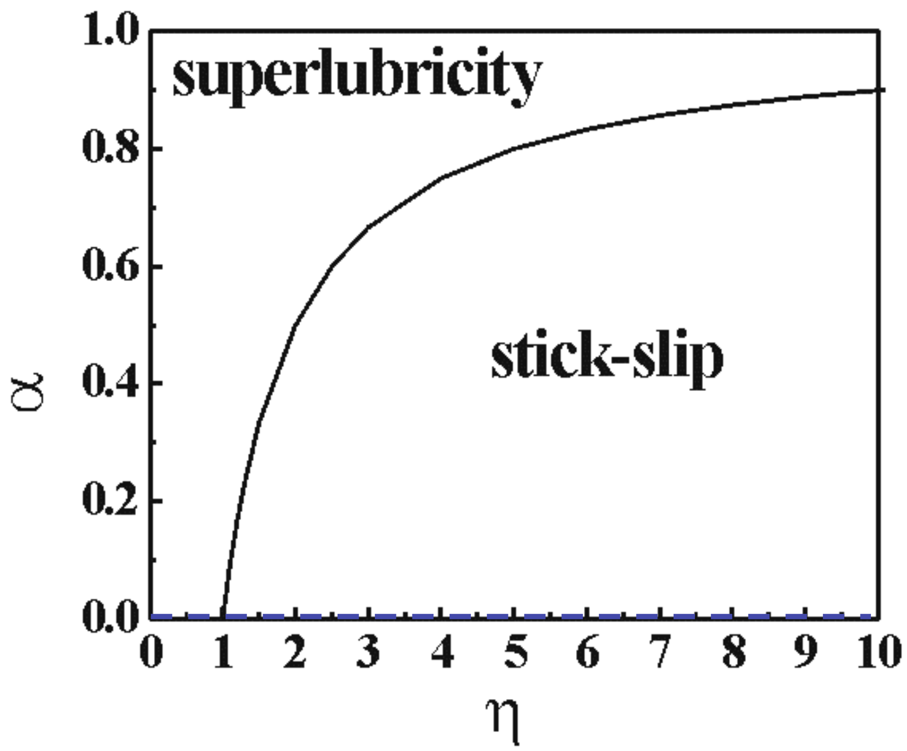

$$\boxed{\alpha_{cr} = 1 - \frac{1}{\eta}}$$

"Static" SL

A. Socoliuc et al., Science 2006

Modulation of the Energy barrier by actuation of the nano-contact

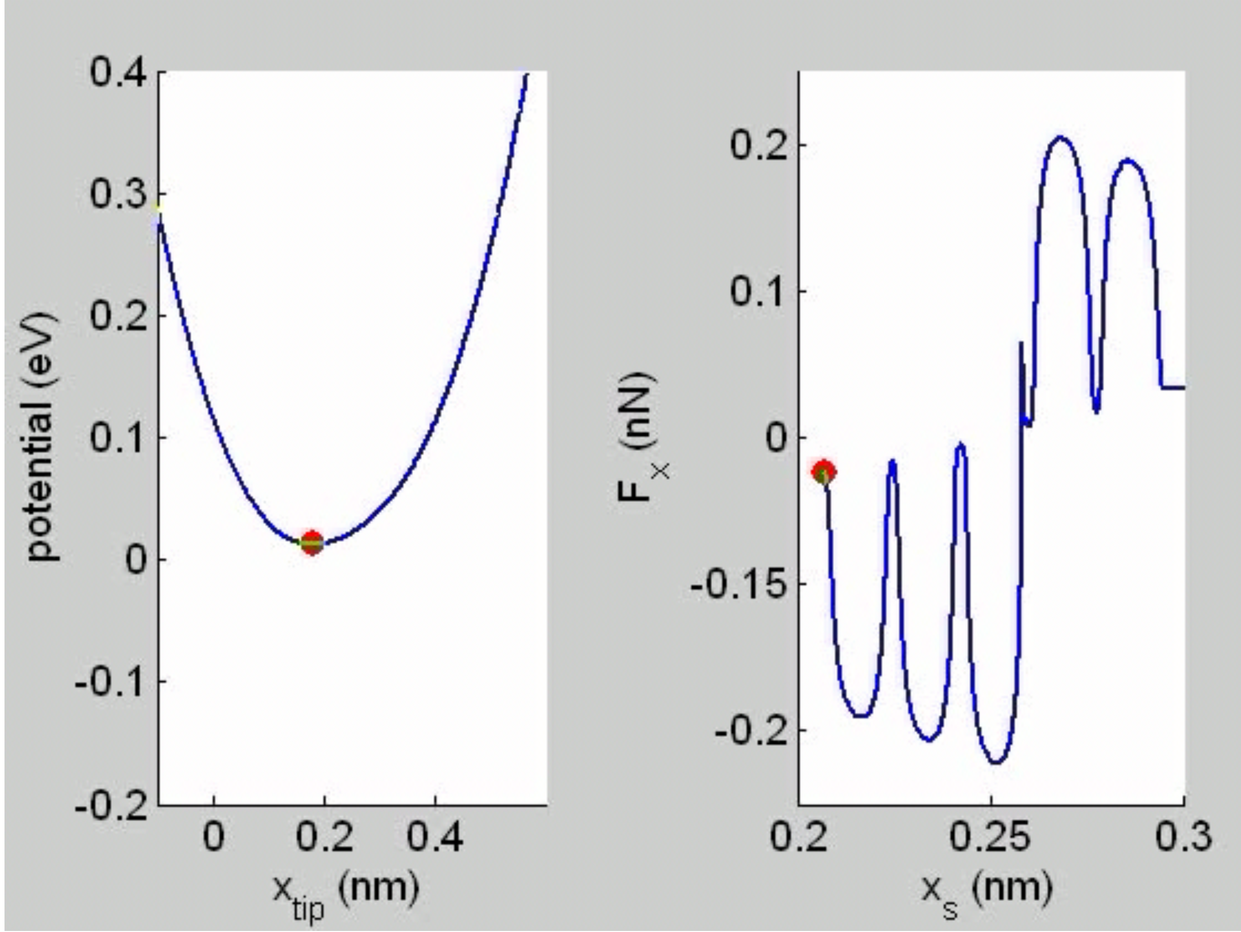

Standard parameters for the Tomlinson model with excitation:
0.5 times critical damped

Parameters: eta=4, alpha=0.9, f=567Hz, v=10e-9m/s, gamma=1e-6kg/s, m=8e-13kg, a=0.5e-9m, c=1N/m

Ultralow friction on the macroscopic scale?

- Normal force per asperity is limited to 1nN
- Macroscopic weight of 1g ≈ 10mN has to be distributed to 10^7 mini-tips (≈ array of 3'000 x 3'000 tips)

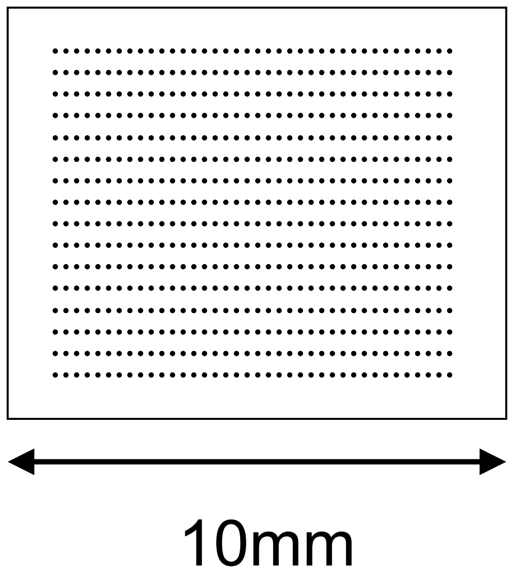

Tips with a spacing of 3μm

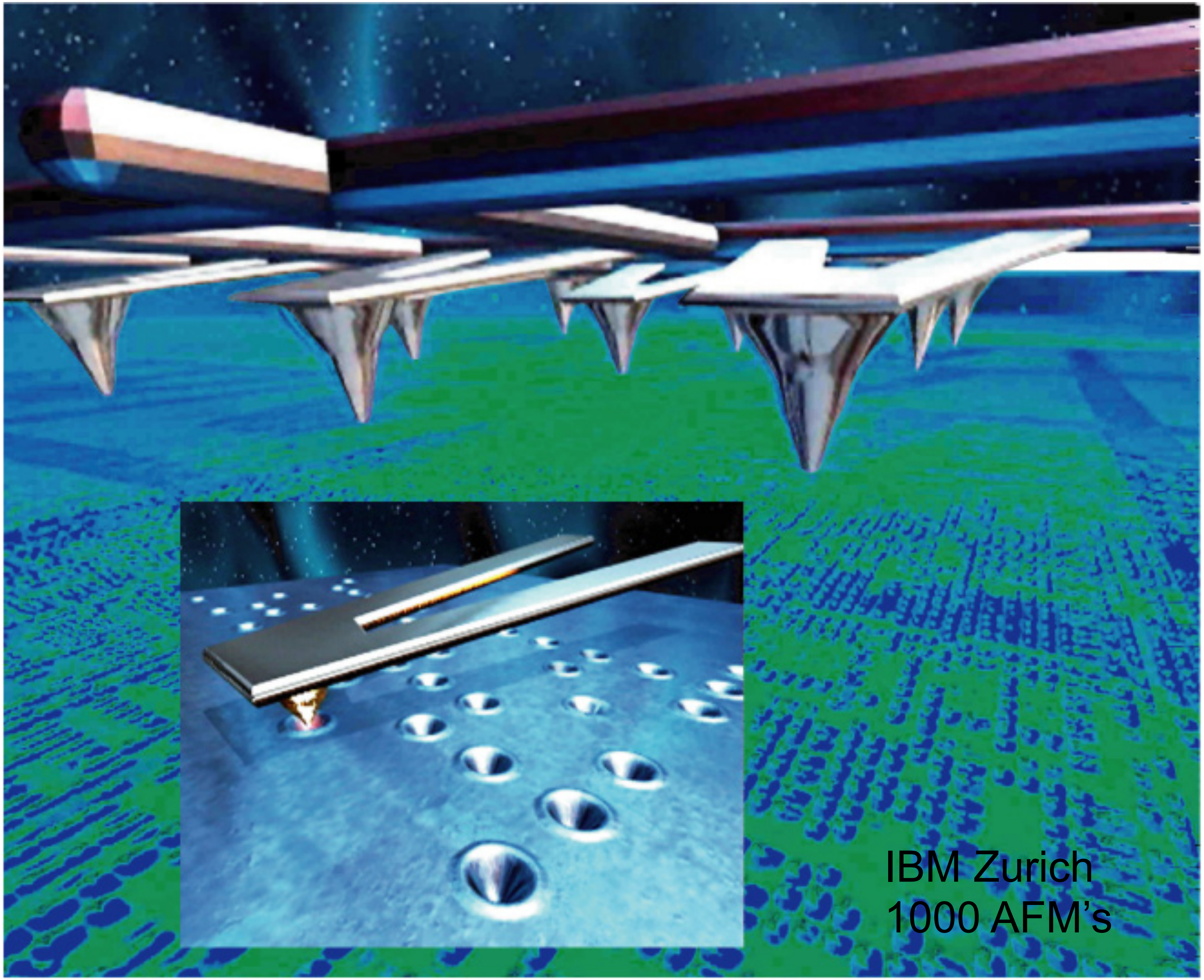
IBM Zurich
1000 AFM's

MEMS-Devices

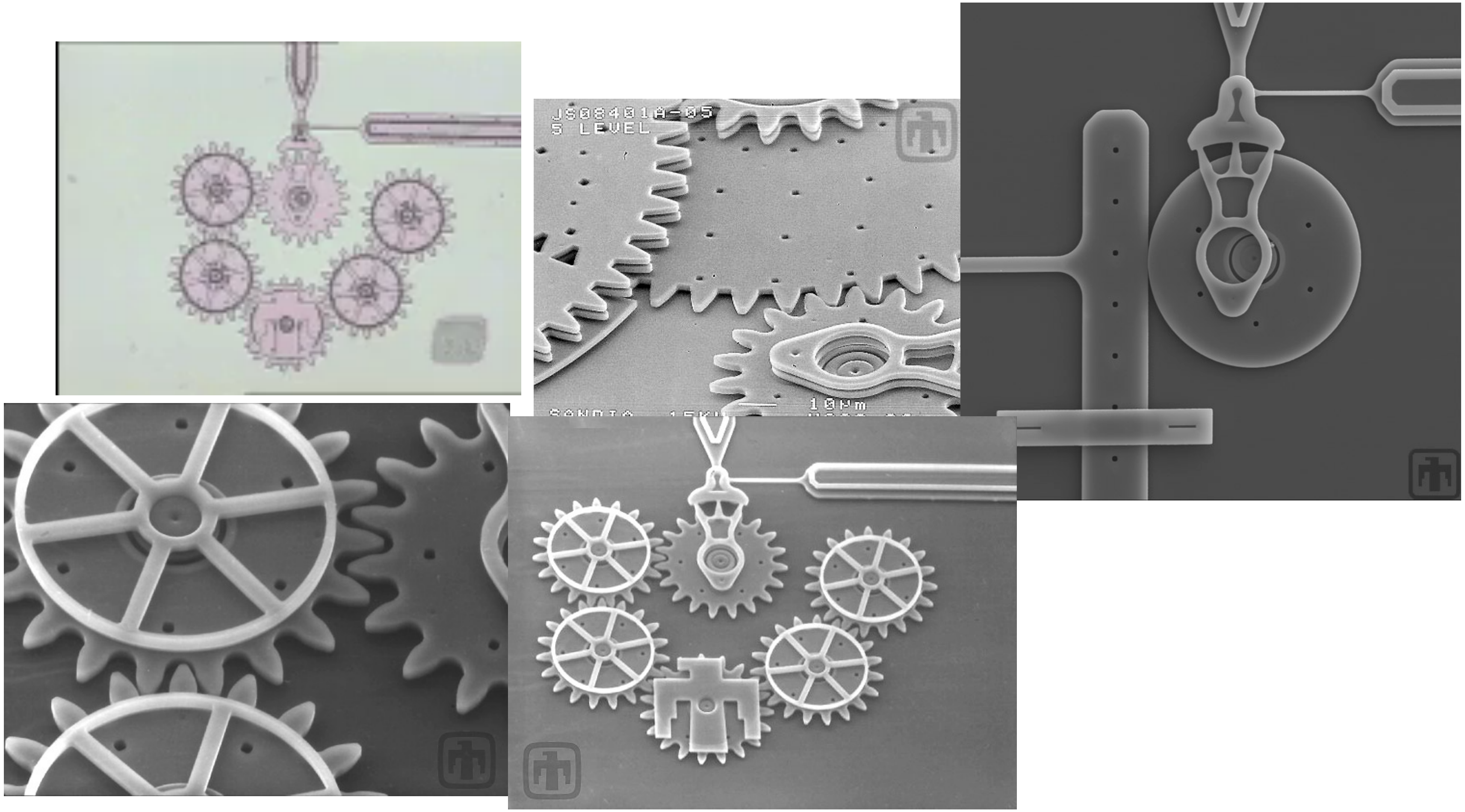

Courtesy of Sandia National Laboratories, SUMMiTTM Technologies, www.mems.sandia.gov"

Gecko uses nanometer-sized contacts to climb walls

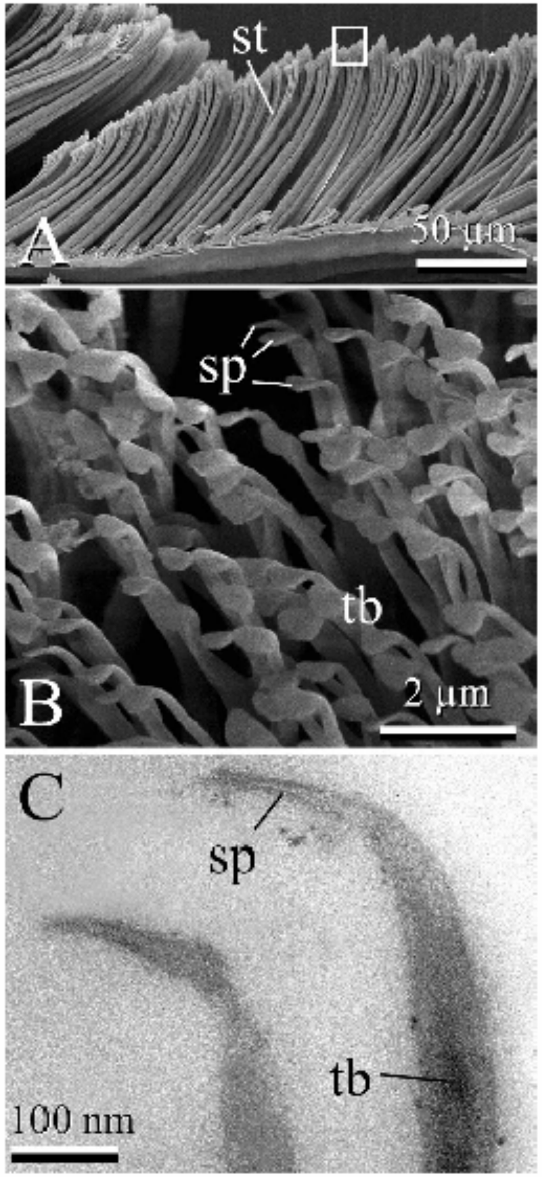

Gecko is able to control the contact area on all length scales

From B. Persson and S. Gorb JCP, 119, 11437 (2003)

Other forms of "superlubricity "

- **Thermolubricity** (Krylov et al., PRE 2005):

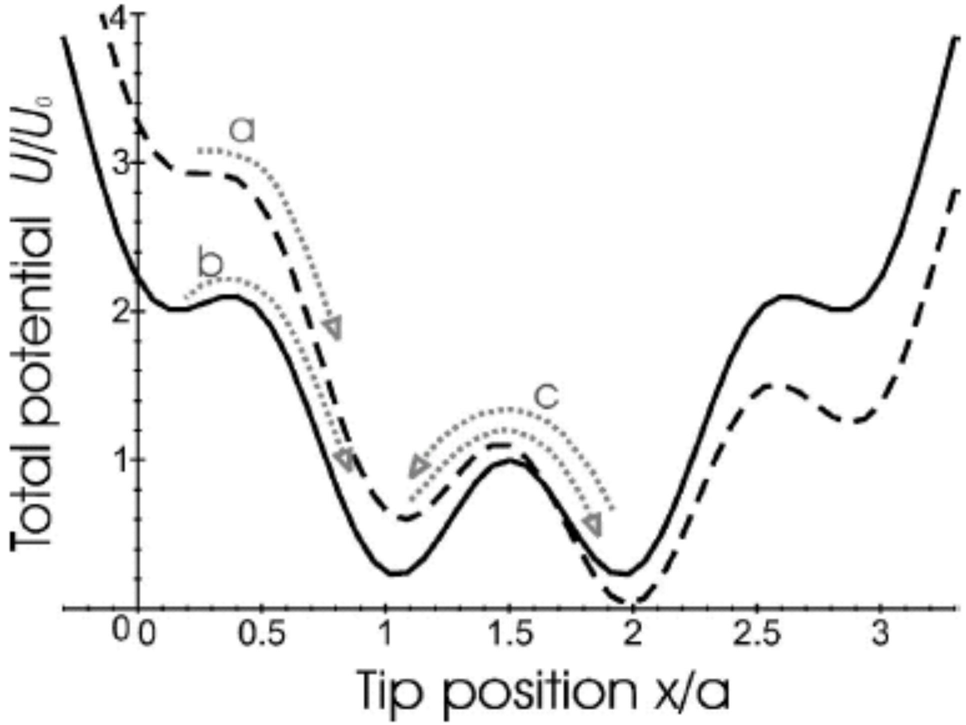

(taking "backjumps" into account → friction vanishes at low speed)

Other forms of "superlubricity"

• **Structural lubricity** (Dienwiebel et al., PRL 2004):

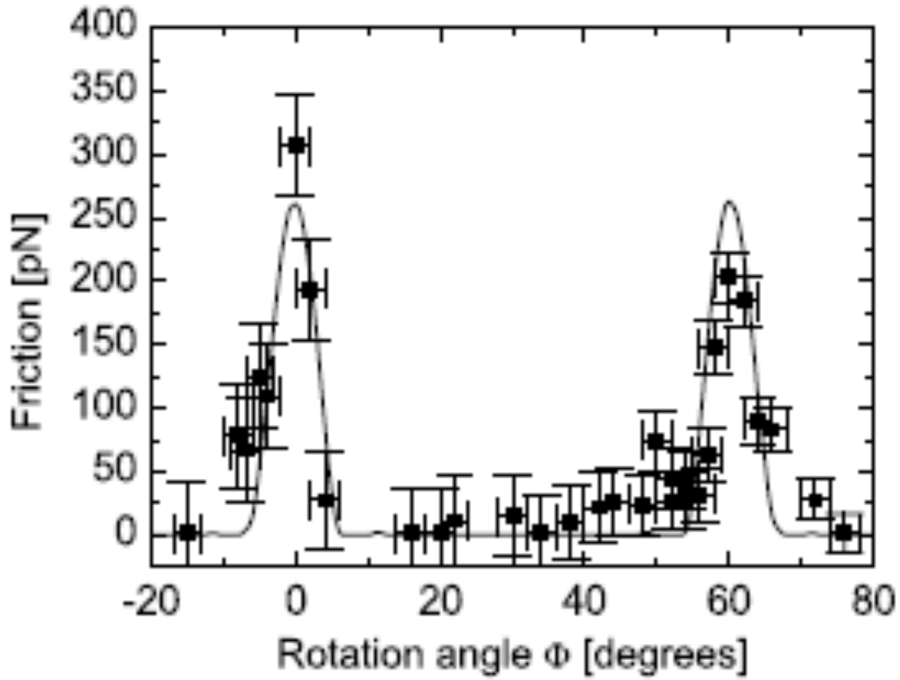

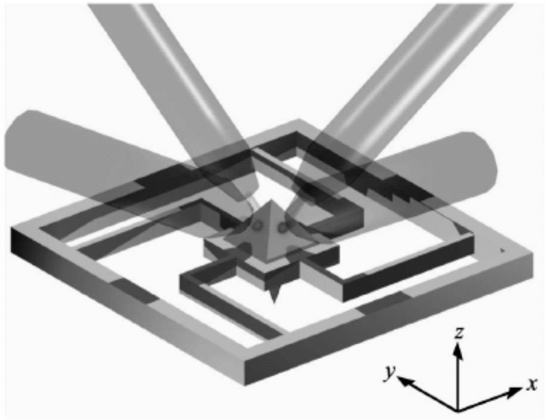

(two mismatched graphite flakes sliding past each other)

Transitions to negligible friction in different dry contacts

Graphite against rotated flake picked up by tip

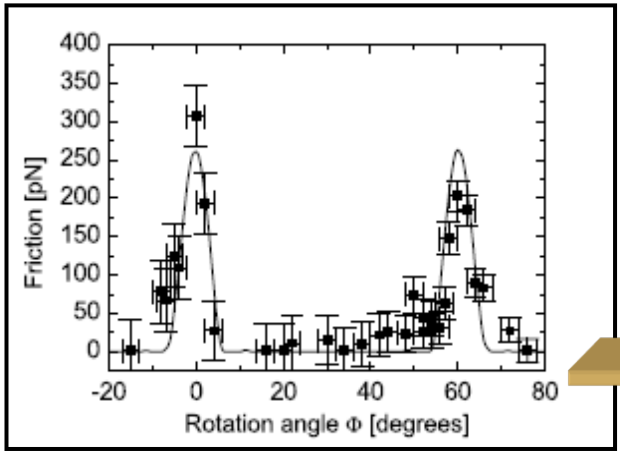

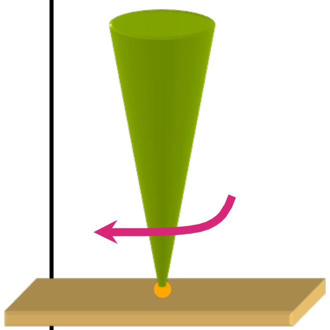

M. Dienwiebel et al. PRL 92, 126101 (2004)

NaCl(001) cleaved in UHV

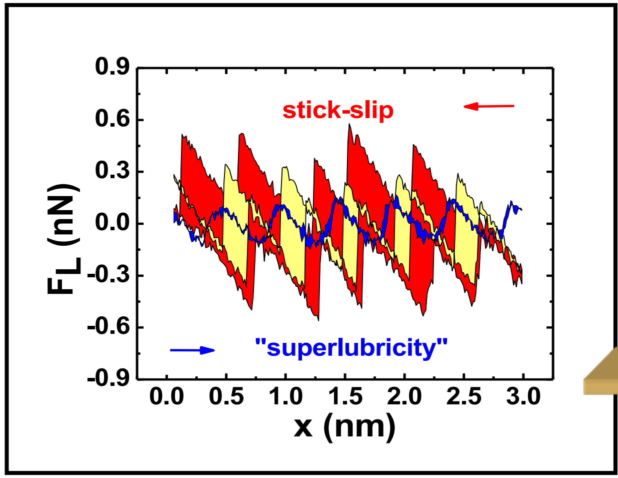

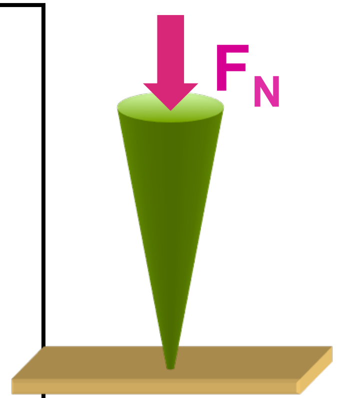

A. Socoliuc et al. PRL 92, 134301 (2004)

Effective corrugation on graphite reduced at low velocities at fixed room T

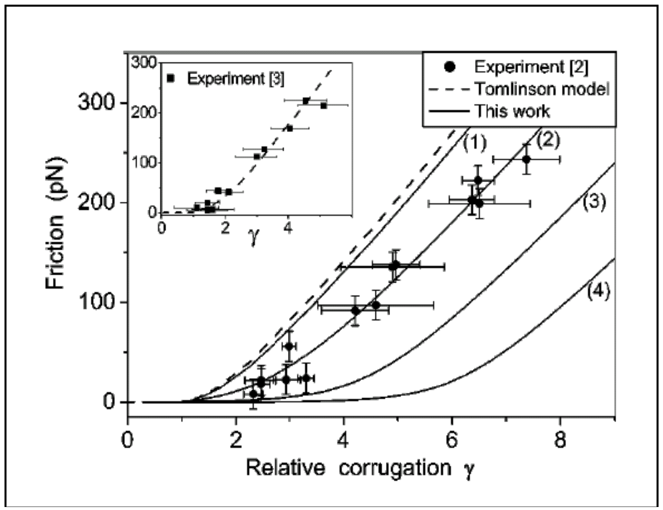

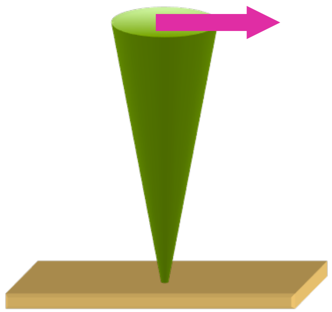

Thermal activation:
small velocity ~ high temperature

Like creep of dislocations
or vortices in type II superconductors

S.Yu Krylov et al. PRE 71, 065101(R) (2005)

Appendix: Calibration of lateral forces

Force calibration (2)

- Cantilever **thickness** also **from** the **resonance frequency**:

$$\boxed{t = \frac{2\sqrt{12}\pi}{1.875^2}\sqrt{\frac{\rho}{E}}f_0 l^2}$$

- ρ, E: density and Young modulus

(Nonnenmacher et al., JVSTB 1991)

- For pure silicon:

$$\rho = 2.33 \cdot 10^3 \text{ kg/m}^3$$

$$E = 1.69 \cdot 10^{11} \text{ N/m}^2$$

Force calibration (3)

- **Normal** and **lateral spring constants** of cantilever:

$$\boxed{c_N = \frac{Ewt^3}{4l^3}} \qquad \boxed{c_L = \frac{Gwt^3}{3h^2 l}}$$

- G: shear modulus
- For pure silicon:

$$\rho = 2.33 \cdot 10^3 \text{ kg/m}^3$$

$$E = 1.69 \cdot 10^{11} \text{ N/m}^2$$

$$G = 0.5 \cdot 10^{11} \text{ N/m}^2$$

Force calibration (4)

- Next step: **sensitivity of photodetector**
- Force-distance curves on hard surfaces (e.g. Al_2O_3):

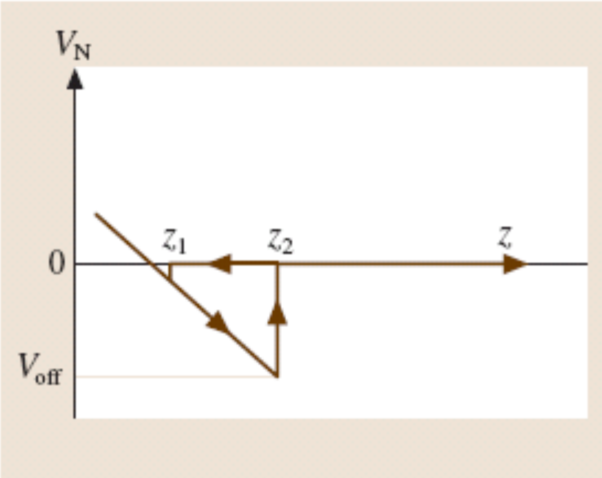

- Scanner movement = cantilever deflection
- Slope → sensitivity

Force calibration (5)

- **Normal** and **lateral forces**:

$$\boxed{F_N = c_N S_z V_N}$$

$$\boxed{F_L = \frac{3}{2} c_L \frac{h}{l} S_z V_L}$$

(if the light beam is above the probing tip!)

- V_N, V_L: normal and lateral signals

Force calibration (6)

• Alternative method #1: Tungsten **spheres attached to the tip** (Cleveland et al., RSI 1993)

• Frequency shift:

$$\boxed{f_0 = \frac{1}{2\pi}\sqrt{\frac{c_N}{M + m^*}}}$$

• M, m*: added mass and effective mass of the cantilever

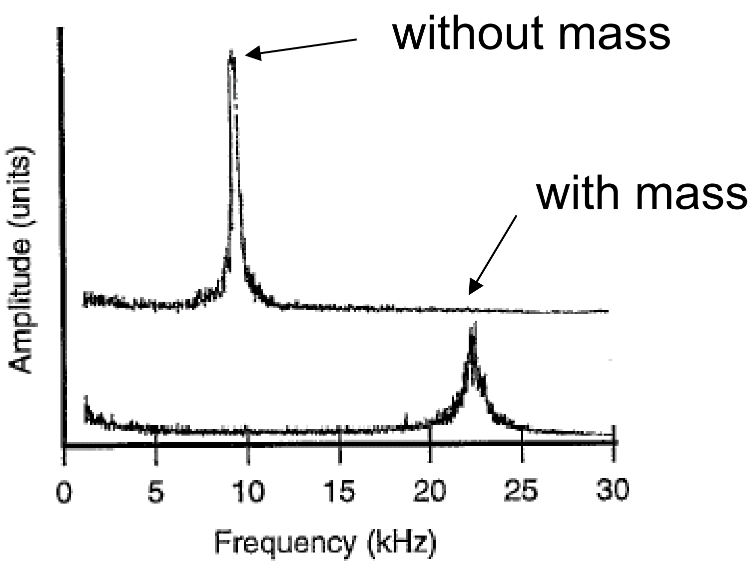

Force calibration (7)

• Alternative method #2: Spring constant **from thermal power spectrum** (Hutter et al., RSI 1993)

• Correct relation (Butt et al., Nanotech. 1995):

$$\boxed{c_N = \frac{4k_B T}{3P}}$$

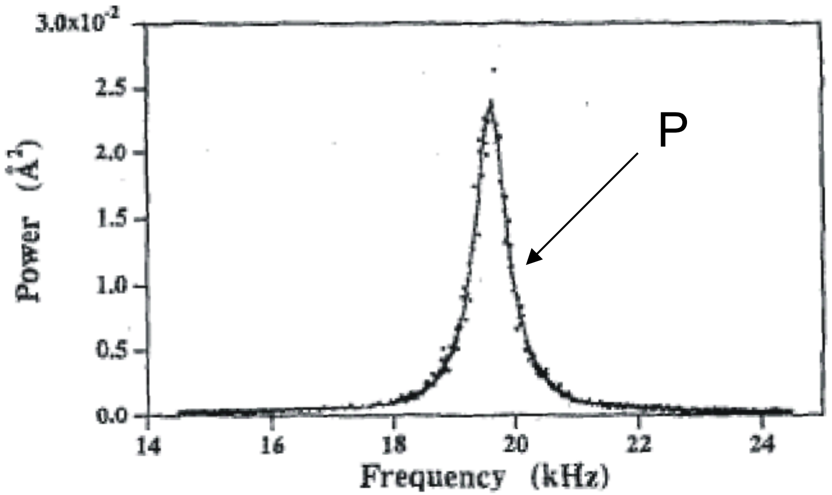

Force calibration (8)

• Different shapes → **Finite elements analysis** (alternative method #3)

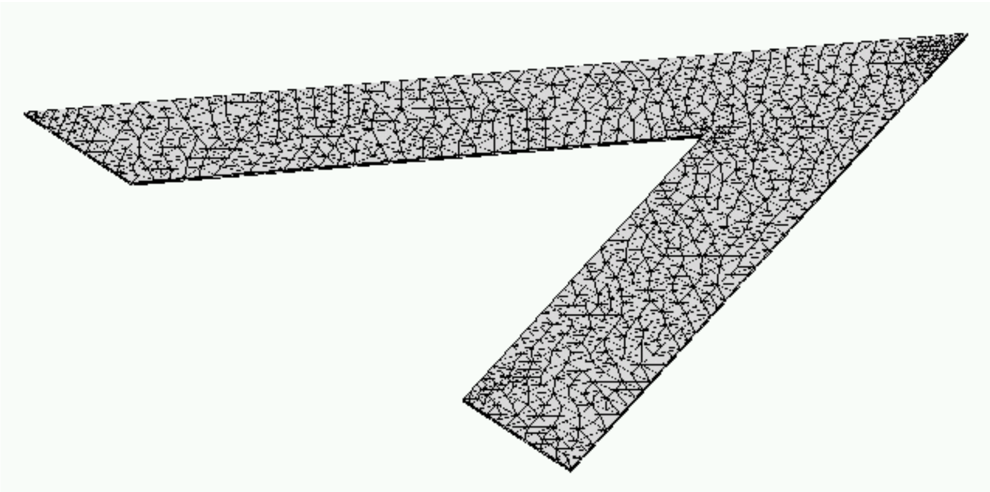

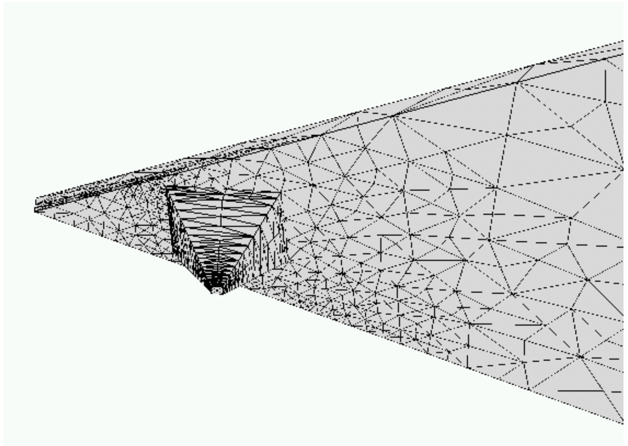

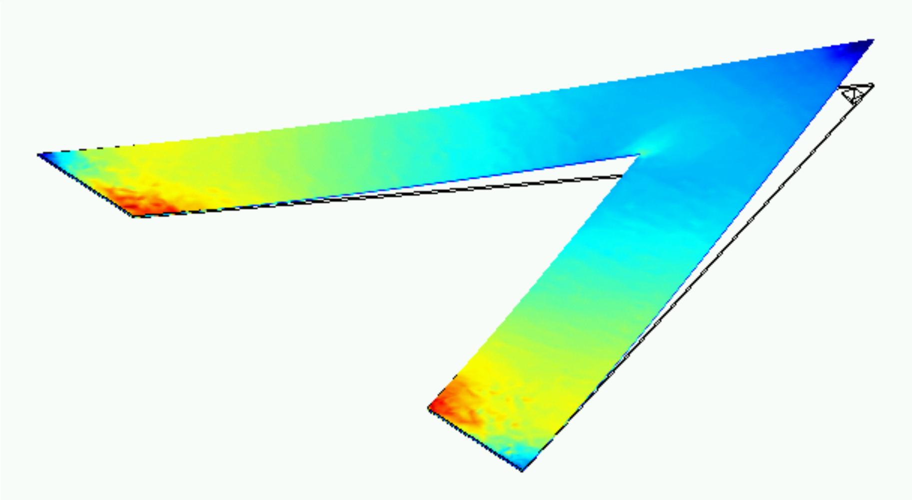

(Femlab™ 3.0)

Force calibration (9)

- Approximate relations hold for **V-shaped cantilevers** (Neumeister et al., RSI 1994):

$$c_L = \frac{Et^3}{3(1+\nu)h^2}\left(\frac{1}{\tan\alpha}\ln\frac{w}{d\sin\alpha} + \frac{L\cos\alpha}{w} - \frac{3\sin 2\alpha}{8}\right)^{-1}$$

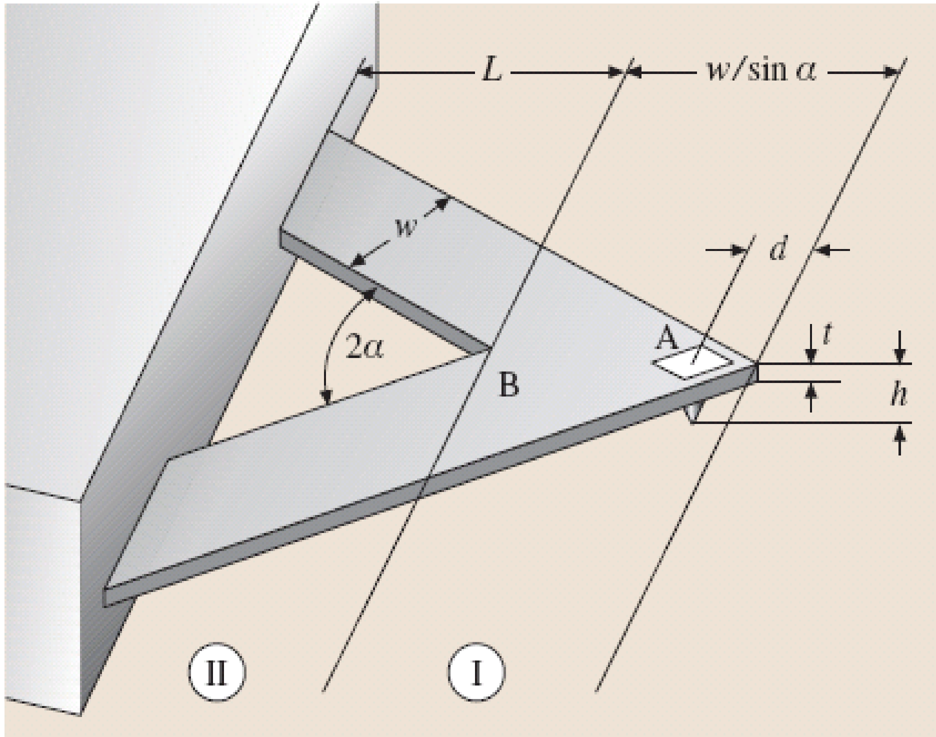

Force calibration (10)

• Alternative method #4: Scanning over profiles with **well-defined slope** (Ogletree et al., RSI 1996)

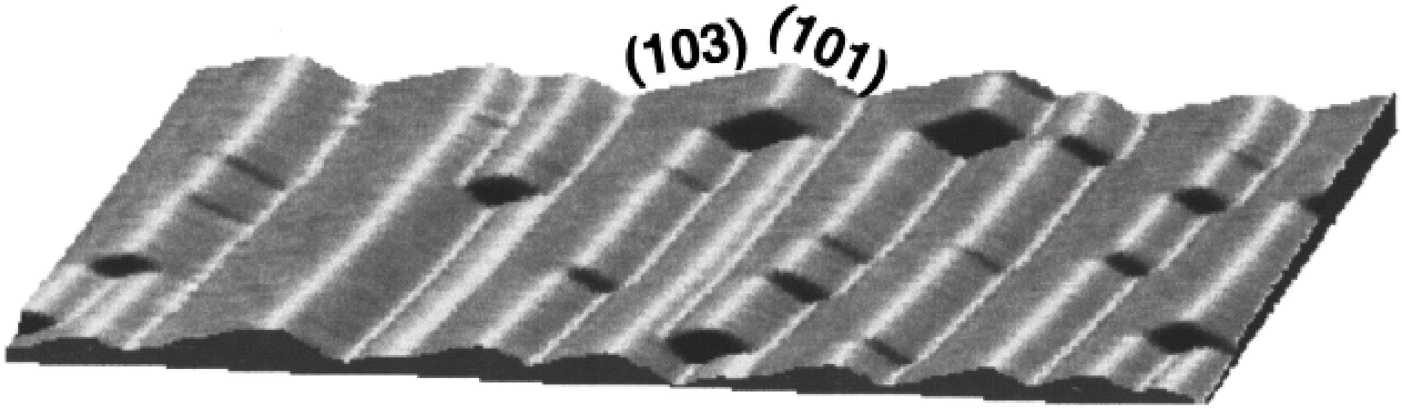

Commercially available grating:

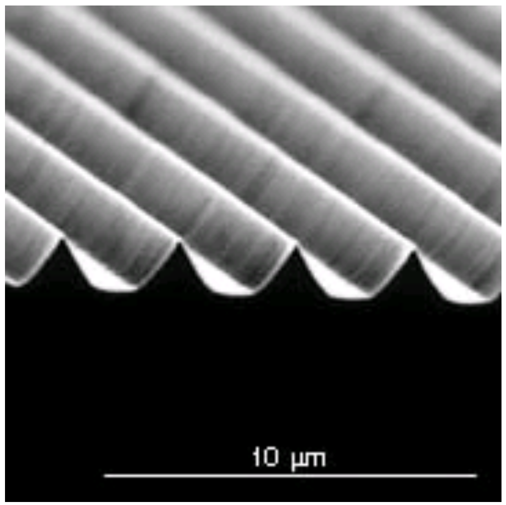

(TGG01, NT-MDT, Moscow)

Force calibration (11)

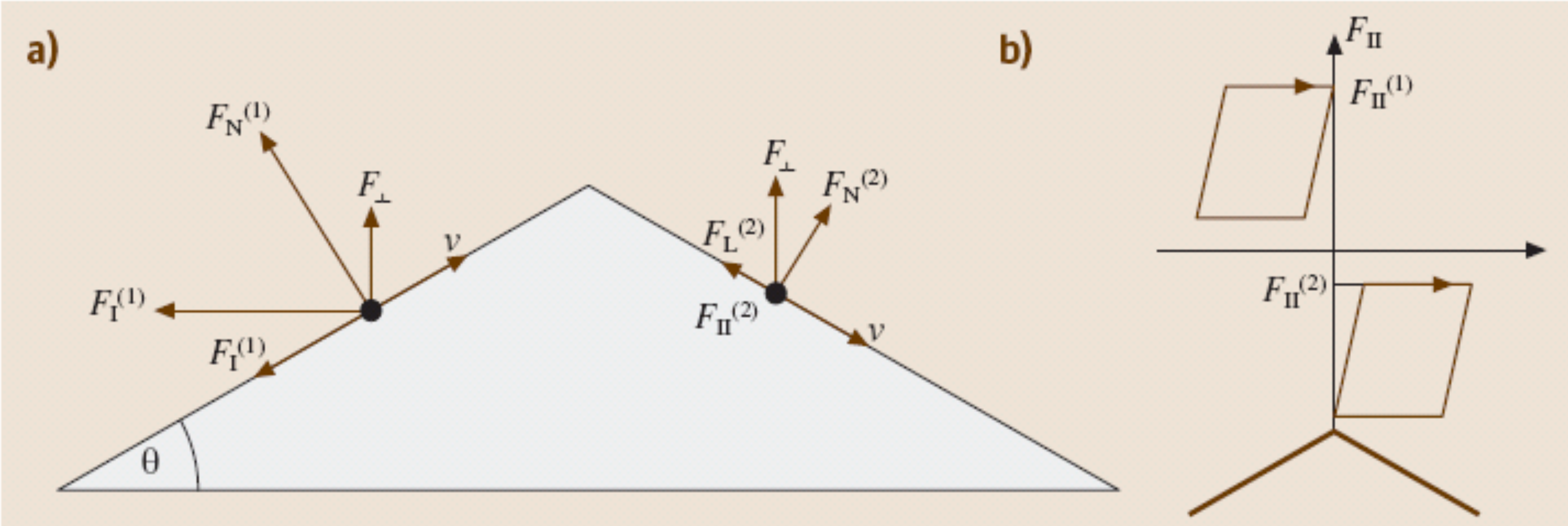

$$F_{//} = \frac{\mu + \tan\theta}{1 - \mu\tan\theta} F_\perp$$

$$F_\perp = \text{const.}$$

$$F_+ \equiv F_{//}^{(1)} + F_{//}^{(2)} = \frac{2\mu(1+\tan^2\theta)}{1-\mu^2\tan^2\theta} F_\perp$$

$$F_- \equiv F_{//}^{(1)} - F_{//}^{(2)} = \frac{2(1+\mu^2)\tan\theta}{1-\mu^2\tan^2\theta} F_\perp$$

(E. Gnecco, PhD Thesis, 2000)